MODULAR FIXTURE DESIGN FOR CNC MACHINING CENTERS

A THESIS SUBMITTED TO
THE GRADUATE SCHOOL OF NATURAL AND APPLIED SCIENCES
OF
MIDDLE EAST TECHNICAL UNIVERSITY

BY

YUSUF KILIÇARSLAN

IN PARTIAL FULFILLMENT OF THE REQUIREMENTS
FOR
THE DEGREE OF MASTER OF SCIENCE
IN
MECHANICAL ENGINEERING

JANUARY 2019

Approval of the thesis:

MODULAR FIXTURE DESIGN FOR CNC MACHINING CENTERS

submitted by **YUSUF KILIÇARSLAN** in partial fulfillment of the requirements for the degree of **Master of Science in Mechanical Engineering Department, Middle East Technical University** by,

Prof. Dr. Halil Kalıpçılar
Dean, Graduate School of **Natural and Applied Sciences** _________________

Prof. Dr. Sahir Arıkan
Head of Department, **Mechanical Engineering** _________________

Assoc. Prof. Dr. Melik Dölen
Supervisor, **Mechanical Engineering, METU** _________________

Examining Committee Members:

Prof. Dr. Mustafa İlhan Gökler
Mechanical Engineering, METU _________________

Assoc. Prof. Dr. Melik Dölen
Mechanical Engineering, METU _________________

Dr. Orkun Özşahin
Mechanical Engineering, METU _________________

Dr. Ulaş Yaman
Mechanical Engineering, METU _________________

Prof. Dr. Sadık Engin Kılıç
Manufacturing Engineering, Atılım University _________________

Date: 18.01.2019

I hereby declare that all information in this document has been obtained and presented in accordance with academic rules and ethical conduct. I also declare that, as required by these rules and conduct, I have fully cited and referenced all material and results that are not original to this work.

Name, Surname: Yusuf Kılıçarslan

Signature:

ABSTRACT

MODULAR FIXTURE DESIGN FOR CNC MACHINING CENTERS

Kılıçarslan, Yusuf
Master of Science, Mechanical Engineering
Supervisor: Assoc. Prof. Dr. Melik Dölen

January 2019, 150 pages

A new modular fixturing system is developed for CNC machining centers in the content of this thesis study. In the proposed fixture, studies are carried on to manufacture precise parts for finish milling operations. Some workpieces are loaded in the proposed fixturing system by using relevant fixture elements. Forces and moments are investigated that are acting during the machining operation. The precision of the machined surfaces is estimated by using Monte-Carlo Simulation. In the experimental section of the thesis, three target pieces are manufactured in a machining center and inspected with CMM. These inspection results are used to evaluate the performance of the developed fixture system. Repeatability of experimental fixture set up is investigated by performing a repeatability test.

Keywords: Modular Fixturing, Kinematic Constraints, Elastic Deformation Analysis, Cutting Force Models, Monte-Carlo Simulation, Fixture Repeatability

ÖZ

CNC İŞLEME MERKEZLERİ İÇİN MODÜLER FİKSTÜR TASARIMI

Kılıçarslan, Yusuf
Yüksek Lisans, Makina Mühendisliği
Tez Danışmanı: Doç. Dr. Melik Dölen

Ocak 2019, 150 sayfa

Bu tez kapsamında CNC işleme merkezlerine yönelik olarak yeni bir modüler fikstür sistemi geliştirilmiştir. Önerilen fikstürde son freze işleminde hassas parça imal edilmesine yönelik olarak çalışmalar yapılmıştır. Örnek iş parçaları önerilen fikstüre ilgili fikstür elemanları kullanılarak yerleştirilmiştir. Freze operasyonu sırasında etki eden kuvvet ve momentler incelenmiştir. İşlenen yüzeylerin hassasiyeti Monte-Carlo simülasyonu kullanılarak tahmin edilmiştir. Tezin deneysel kısmında belirlenen hedef parçadan üç adet işleme merkezinde üretilmiş ve CMM ölçümleri yapılmıştır. Ölçüm sonuçları geliştirilen fiktür sisteminin performansını değerlendirmek için kullanılmıştır. Deneysel işlemler için oluşturulan fikstür düzeneğinin tekrarlanabilirliği yapılan tekrarlanabilirlik testi ile araştırılmıştır.

Anahtar Kelimeler: Modüler Fikstürleme, Kinematik Kısıtlar, Elastik Şekil Değiştirme Analizi, Kesme Kuvveti Modelleri, Monte-Carlo Simülasyonu, Fikstür Tekrarlanabililiği

To My Beloved Family…

ACKNOWLEDGMENTS

I would like to express my very great appreciation to my thesis supervisor Assoc. Prof. Dr. Melik Dölen for his valuable and constructive suggestions all throughout the study. It would not be possible to complete this study without his guidance, assists and mentoring.

I would also like to thank Aselsan A.Ş. for supporting and enabling me to continue my studies.

Finally, I wish to thank my parents for their support and encouragement throughout my study.

TABLE OF CONTENTS

LIST OF TABLES

TABLES

LIST OF FIGURES

FIGURES

CHAPTER 1

INTRODUCTION

1.1. Background

Fundamental information about the basics of the fixtures and their applications is given in this section. The terminology, explained in this section, is used throughout the study.

Fixtures, workpiece holding devices, are used for positioning, fixing and supporting parts securely in the manufacturing processes. To ensure that a manufacturing operation is carried out properly, the workpiece must be properly placed and fastened. The position of a workpiece is determined by locators in the workholding device. Namely, the fixture elements that determine the position of the workpiece accurately in the workholding device are called "*locators*". Locators are placed in predetermined places of workholding devices to accurately locate the workpieces [43]. A symbolic locator, represented by a triangle, is shown in Figure 1.1a. to restrict the movement of the workpiece in one direction. If the locator is not colinear to the center of the rotation, it restricts the motion about that rotation center [42]. This is shown in Figure 1.1b.

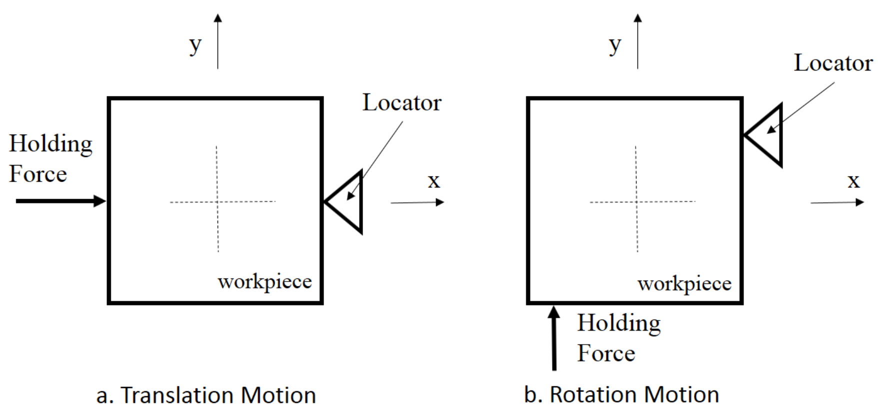

Figure 1.1. Translation and Rotation Motions [42]

Once the workpiece is positioned on locators, “*clamps*” are used to apply holding force. Holding force, applied by the clamps to the workpiece, prevents the translation and the rotation movements of the workpiece to the opposite directions of the locators. Positioning and fastening of a workpiece in a workholding device are illustrated in Figure 1.2. Second holding element is not shown due to clarity.

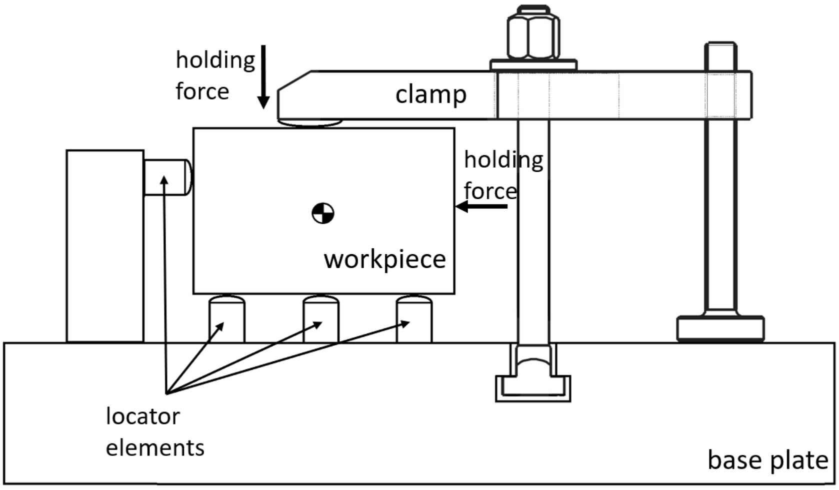

Figure 1.2. Locating of a workpiece

An object has 6 degrees of freedom in space. That is to say, it can make 3 translational and 3 rotational movements. Object can move either positive or negative directions. Consequently, it is free to move in any of twelve directions in space and all of these 12 movements must be restricted to locate a part accurately to perform a manufacturing operation. These 12 movements, 6 translational along X, Y and Z axis and 6 rotational about X, Y and Z axis both negative and positive directions, can be seen in Figure 1.3 [43].

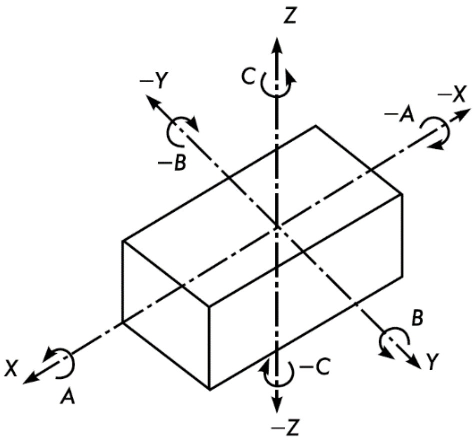

Figure 1.3. Twelve movements in space [43]

Locating pins are used to restrict the movements of a workpiece. Firstly, three locators restrict 4 rotational and 1 axial movements. Secondly, two locators restrict 2 rotational and 1 axial movements. Lastly, one locator restricts 1 axial movement. As a consequence, nine of twelve directions are restricted. This is called “3-2-1 Locating Method” and is also called “Six point locating method”. The restriction of these movements is shown in Figure 1.4. The remaining 3 translational movements are to be restricted by clamping forces. [43]

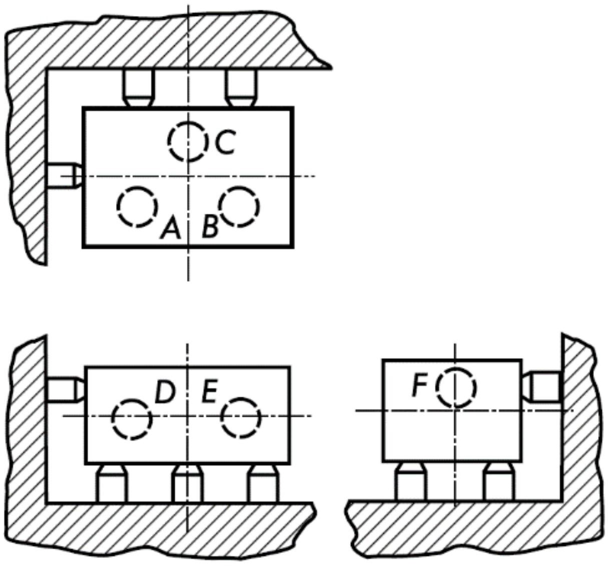

Figure 1.4. Six point locating (3-2-1) method [43]

Basics of the 3-2-1 method can be expressed more properly as below [42].

1. Six locators are required to locate a rigid workpiece accurately. More than six locators cause uncertainty in the position of a workpiece.
2. Three locators define a plane.
3. Locators do not contact with opposite surfaces.
4. There is one locator for each degree of freedom.
5. Locators are placed as far as possible from each other to improve the stability of the workpiece.

As a result, five items presented above establish 3-2-1 methodology all together. Basically, the largest plane of the workpiece contacts with three locators. The surface with the longest edge, orthogonal to this largest surface, is positioned by two locators. The rest locator is placed on the surface perpendicular to both planes [42].

In the locating process of the workpiece, locators must be positioned opposite of the holding forces and tool forces as possible to minimize the deflection and distortion of the workpiece. The holding forces, applied by the clamps must provide continuous contact with all locators. This will ensure the accurate positioning of the workpiece during the machining operation [42].

1.2. Motivation

Fixtures are basic elements used in manufacturing operations. The main function of the fixtures is to fix the workpiece against the forces induced during manufacturing operations. Degree of freedom (DOF) of the workpiece inside the fixture must be completely restrained. In industrial applications, fixtures reduce the DOF of the workpiece by constraining them with a large number of contact points. In other words, the position of the part is not uniquely set. That is, if the part is removed from the fixture and put to the fixture again, it will not be in the former position. This is called undeterministic positioning (leading to reduced repeatability). In other words, the forces acting on the workpiece is statically undetermined. Besides, over-constraining causes undesirable deformations (including the thermo-elastic strains) while machining the product. All and all, the resulting machining accuracy will diminish in such a configuration. On the other hand, if the part is uniquely (i.e. kinematically) fixed, it will attain a deterministic position. Hence, the forces and the corresponding elastic deformations on the fixture elements can be statically determined in this method. Furthermore, since the variation in fixture parameters is significantly reduced in a properly designed fixture, the repeatability of manufacturing operation is in turn improved.

Apart from locator forces, there are three fundamental forces acting on a workpiece during the milling operations: clamping forces, tool forces and weight of the workpiece. All of these forces are shown in Figure 1.5. Under the effect of these forces, the orientation of the workpiece continuously changes during the operation. Therefore, the accuracy of the machined part depends on these forces (and the stiffness of the fixture support elements) during the operation.

Orientation of a workpiece is described with the translational and rotational movements of the workpiece in and about the axes of x, y and z with respect to its initial position in 3D.

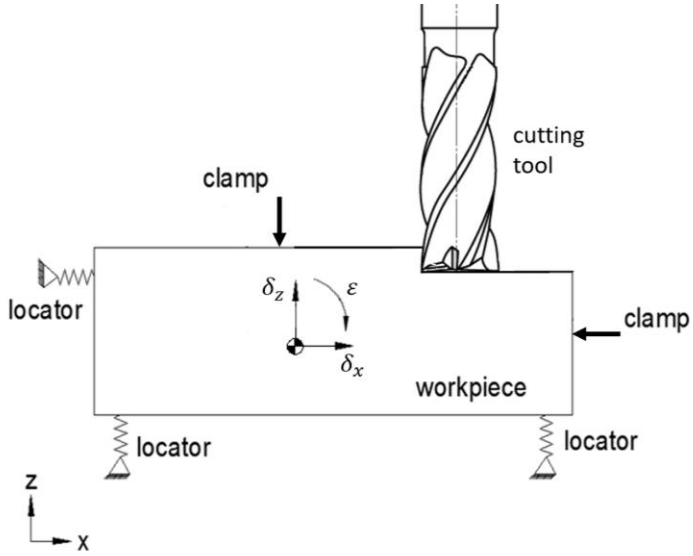

Figure 1.5. Forces acting on workpiece during machining

1.3. Scope of the thesis

Fixtures in manufacturing can be classified into two groups [7].

- Dedicated Fixtures
- Modular Fixtures
- Hybrid (Modular & Dedicated) Fixtures

Dedicated fixtures are used only for the workpiece that can be suitable for that fixture. These fixtures are manufactured generally only for one unique part. On the other hand, modular fixtures have a lot of special fixing elements and it is possible to fix a wide range of different kind of parts in these fixtures during the manufacturing operations.

In the scope of thesis study, a modular fixture system is developed for CNC machining centers. The modular fixture, which is the subject of this thesis, is called *"cubefix"* after this point. Machining of different kind of sample parts are investigated in different aspects such as constraint status of workpiece, manufacturing precision, fixing method, forces & moments, etc. In experimental studies, a target piece is manufactured three times. Manufactured parts are inspected in CMM and compared each other.

1.4. Organization

The thesis consists of 7 chapters. The first topic in the thesis is Introduction. It starts with the background which explains the basic fixture elements and six-point locating method. The motivation to perform this study, scope of this study and the organization of this thesis are presented in Chapter 1.

In second Chapter, review of the state of the art is presented. Fixturing methods and recent developments are mentioned.

Proposed fixture system is presented in Chapter 3. In this chapter fixture elements that are developed in the content of this study are presented. The functions of these fixture elements are introduced and relevant information is given such as material of the elements, development process of the elements and their functionality etc.

In Chapter 4, Locating Status Analysis to define the constraint status of a workpiece is discussed. Determination of locator stiffness functions by using Hertz Theory is presented. Mathematical method to estimate the error during machining operation is developed in this chapter.

In Chapter 5, 6 pieces of different sample parts are fixed to the proposed modular fixture system. Analyses of their Locating Status are performed in this chapter. The estimated precision of the machined surfaces is investigated. Additionally, 6^{th} part, determined as test part, is designed and analyzed.

In Chapter 6, several fixture elements are manufactured and an experimental fixture set up is created by these manufactured elements. Three pieces of workpieces are machined by a CNC machining center by using manufactured fixture elements in different clamping force conditions. Manufactured parts are inspected in CMM and compared with each other. Repeatability of the proposed fixture is investigated.

In Chapter 7, the reached results and concluding remarks obtained in this study are summarized and possible future works are discussed.

CHAPTER 2

REVIEW OF THE STATE OF THE ART

In this section of the thesis, related literature survey will be presented in detail within the scope of designing a modular fixture.

2.1. Fixturing Studies

Zhong and Hu [3] studied modeling of a 4-2-1 fixture and examined the machining geometric variations by using minimum potential energy theory. They claim that 4-2-1 fixture methodology can be a solution to decrease the deformations that resulted from machining operation by using 4-2-1 fixture methodology. They made the kinematic analysis of the over-constrained 4-2-1 fixture methodology by using HTM (homogeneous transformation matrices) and made a comparison with 3-2-1 fixture methodology. In their study they claimed that distortions are higher at 4-2-1 fixture due to over-constrained geometry and contact condition's uncertainty.

Wang et. al. [4] studied the kinematic analysis of locator-workpiece contact. They claimed that fixture must be designed accurately to reduce dimensional variations in the final product. In their study they developed a systematic approach for precise fixture design by using tolerance budgeting. They also took the surface properties of the both locator and the workpiece into account for full kinematics of locator and workpiece contact instead of conventional point kinematic model. They claimed that position and orientation of the workpiece are determined by both locator locations and locator-workpiece contacts.

Walczyk and Longtin [5] developed a mechanical model to locate compliant parts during machining operations. They mentioned that 3-2-1 locating principle is sufficient for rigid bodies but it is insufficient for compliant parts. In their study they developed a computer controlled reconfigurable fixturing device concept for compliant parts by using N-2-1 configuration as an alternative to commercially available expensive devices.

Vukelic et. al. [6] studied the automation of fixture design procedure. They pointed out two important investigation fields: optimization of fixture design and development of fixture design systems. In their study, they worked selection and modification of fixture elements and designing the entire fixture automatically. They classified the fixtures with respect to some features such as machining type, location scheme, clamping scheme, workpiece dimensions, number of simultaneously machined workpieces, clamping force intensity etc. The desired properties of the fixture entered as input information to the program. The program selects the modular parts from the database to design the fixture. It can also make modifications on the fixture elements to approach the optimum fixture design. They performed 969 tests on the various type of parts and they claimed that they got successful results from these tests. However, their method is not effective to design fixtures for extremely complex parts.

Trappey and Liu [7] made a literature survey for fixturing principles, automated fixture design and fixture hardware design subjects in their study. It is mentioned in their study that there are 12 movements both rotational and translational directions both (-) and (+) directions. According to 3-2-1 principle first 3 supporting points restricted 5 movements of the workpiece. The second 2 points restricted 3 movements of the part. Lastly, the last point restricts 1 movement of the part. Rest 3 movements are restricted by clamps. They also classified fixtures into three types: modular, dedicated and hybrid (modular and dedicated). They mentioned that modular fixtures are more flexible than other type of fixtures to manufacture small and medium batch size manufacturing. Besides modular fixtures can be assembled, reassembled and disassembled for different kind of parts.

Grippo et. al. [8] described a procedure and proposed a software tool to design modular fixtures automatically. They mentioned about a software which is capable of manipulating and assembling various modular fixturing applications. They proposed this software to reduce the time to design a fixture.

Wan et. al. [9] developed a method to design the fixture automatically by using smart fixture elements that is appropriate for the required design environment. They used an algorithm that fixture elements adjust their positions in the fixture.

Zheng and Qian [10] developed a fixture shown Figure 2.1 and they examined it systematically by developing a mathematical model. Then they determined the optimal position of fixture elements to precisely fix and clamp the work piece.

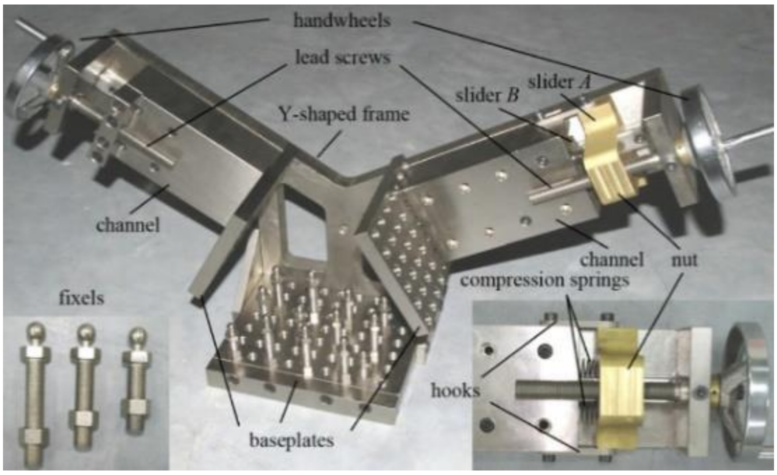

Figure 2.1. A Fixture study [10]

Fan and Kumar [11] investigated the effect of locator and workpiece error on the final product surfaces according to 3-2-1 locating scheme with the help of Taguchi and Monte-Carlo statistical method. Monte-Carlo method was used to determine the contact points of the locators. Taguchi method was used to study the locating effect of the locator’s position at different levels.

Moroni et. al. [12] presented a study regarding the effect of the fixture element error on the geometric tolerances of the workpiece. A drilled hole is investigated on a rectangular workpiece which is located on the 6 locators according to 3-2-1 principle.

They reach some results about the relationship between the position and the height of the locators.

Choudhuri and Meter [13] presented a study regarding the effect of the locator tolerance to the geometric errors on machined surfaces. In their study, they define the effect for each locator to the error on machined surface one by one. They assert that nominal radiuses of locators do not have any effect on the datum establishment error. However, they also mention some researches who propose usage of larger radius to eliminate deformations on part surfaces due to clamping.

Kaya [14] made a study regarding the optimum locator and clamp positions by using genetic algorithms. Genetic algorithm is a random search technique that based on the mechanisms of natural evolution. He stated that genetic algorithm is a powerful technique for locator and clamp position optimization since there is not any analytical relationship between machining error and fixture layout. Ansys finite element program was used to determine the optimum position of the locators and supports by using a correlation between natural environment and fixture layout.

Armilatto et al. [15] investigated the effect of locator position to the accuracy of a hole pattern. In their study they defined the best position of the locators by an analytical approach.

In their study, Chen et al. [16] developed a systematic approach to apply during the conceptual and fundamental design stage of the ultra-precision machine tools. Their system consists of dynamic, thermodynamic, and error budget theories. They listed four main factors that must be considered during the design stage as

- The stiffness budget of the machine tool,
- The dynamic performance,
- The thermal performance,
- The error budget of the machine tool.

In their study they pointed out that stiffness is considerably important in designing a machine tool for rapid machining, because the stiffness has a direct impact on the machining efficiency. The definition of error budged is explained as “potential errors within a machine axis that lead to deviations from the desired motion” in the article. The precision of a machine is affected by the positioning accuracy of the cutting tool with respect to the workpiece surfaces and their relative structural and dynamic loop precisions.

Qin et al. [17] analyzed the clamping sequence of clamps in their study. They developed a mathematical model to decrease the effect of the clamping sequence on the machining quality of the work piece by taking the stiffness of the materials for both work piece and the clamps into account.

Armillotta et. al. [18] developed a systematic approach by using kinematic and tolerance analysis for fixture design. They mentioned in their study that positioning of the workpiece is usually performed by locators before clamping operation. They mentioned that a work holding fixture must ensure a stable and precise positioning of the workpiece with respect to the machine tool and this requirement is more important for the modular fixtures for the efficiency and reconfigurability features. They mentioned in their study that positioning is usually done before clamping by means of highly accurate fixture components called locators in a modular fixture. In their study they mentioned to combine two tests by using some geometric parameters against two main problem sources. Kinematic analysis was used to ensure that there was not any relative motion between the fixture and the workpiece. Tolerance analysis evaluates the robustness of part orientation with respect to manufacturing errors on datum surfaces. In their study they developed a simple calculation procedure by using positioning constraints of screw theory. They developed a locating matrix and decide the constraint status of the workpiece according to rank of the matrix. In their study they state that screw theory provides an effective representation of geometrical constraints on the part due to point contacts with locators.

In the study of Marin and Placid [19] the acceptable violation limit of the locator position was discussed to satisfy required tolerances for the work piece. In other words, they studied the tolerance allocation for the fixture to be in the desired tolerance deviation for the manufactured part.

Fixtures have two main objectives. Firstly, fixtures are used to position the part into the right position relative to the cutting tool. Secondly, they used to hold the workpieces tightly to prevent the displacements during machining operations. In the study of Olaiz et al. [20] a smart and adaptive fixture is presented for the accurate positioning of a planet carrier. They chose electro mechanic actuator in their study instead of hydraulic, pneumatic and piezoelectric actuators, because hydraulic or pneumatic actuators are not suitable for ultra-precision applications. Piezoelectric actuators are extremely accurate but not suitable when large stroke is required. In their work they designed a smart and adaptive fixture that center the planet carrier within .01 mm by using a PLC. Feed drives were used to position the part within required tolerance.

Qin at al. [21] studied the workpiece position error due to fixture locating scheme mathematically. They suggested mathematical relationships for workpiece position errors. These relationships were then used to optimize the positions and dimensions of the locators.

Raghu and Melkote [22] investigated the location error of the workpiece due to fixture geometric errors and the contact between fixture and workpiece. They took elastic deformations due to clamping between fixture and workpiece into consideration in their study.

Tohidi and AlGeddawy [23] developed a mathematical model to determine the location of pins to minimize the preparation time of the fixtures in their study. They tried to minimize the number of the pins that were used in the fixture. They also mentioned about different approaches for flexible fixturing such as sensory-based techniques modular and reconfigurable fixtures, programmable conformable clamps, phase change fixtures and adaptable fixtures.

Tian et. al. [24] studied dynamic performance of a flexure-based mechanism for ultra-precision grinding operation as shown in Figure 2.2. They used a piezoelectric actuator to move the platform. They investigated the flexure-based mechanisms to eliminate the disadvantages of conventional mechanisms such as backlash, stick-slip, friction and larger inertia. They compared the experimental results with the mathematical model.

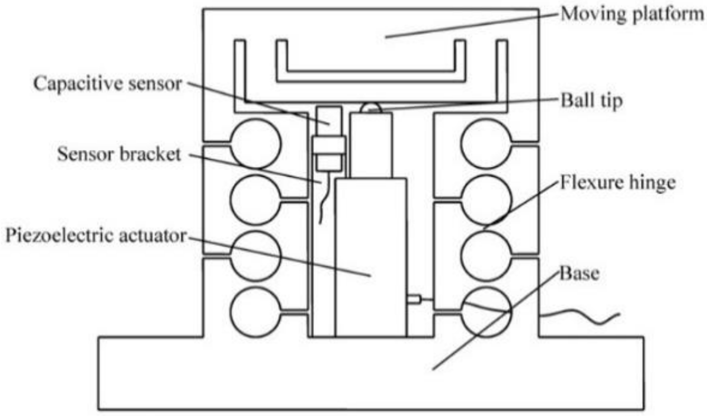

Figure 2.2. Mechanism for an ultraprecise system [24]

A modular fixturing roadmap was developed in Liu's [25] study to change a dedicated fixture to a modular fixture. He classified the functions of a fixture as

- Locating
- Guiding
- Linking
- Clamping
- Supporting

In his study, he mentioned that these five functions complete the modularity of a fixture. He defined the options for every function of the fixture to construct a selection set.

Kakish et. al. [26] examined and listed required design parameters and specifications for **universal modular jigs and fixtures design system** (UMJFS). During this study they documented the definitions of the fixture elements comprehensively.

Chaiprapat and Rujikietgumjorn [29] developed a mathematical model to analyze the geometrical variation of the finished feature by using the tolerance of the datum surface. For 3-2-1 fixturing method there are 3 points to support the part from the bottom of the part. They obtained in their study that to reach more tight tolerances machined features must be located close to the center of the supporting centroid.

In the study of Shirinzadeh [45], programmable clamps to machine different type of turbine blades are mentioned. The pneumatically activated pins support the turbine blade. When the turbine blade is supported by the pins a Kevlar belt holds the part. The system is shown in Figure 2.3.

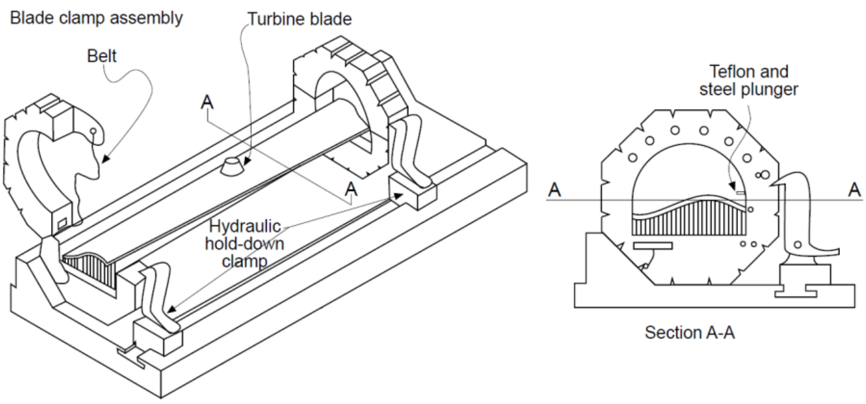

Figure 2.3. A flexible fixture system for turbine blades [45]

2.2. Fixturing Applications for CNC Machining Centers

2.2.1. General-purpose Fixture Elements

There are a variety of fixture elements to hold and position the workpieces during manufacturing operations. Major fixturing elements and methods are mentioned in this part.

2.2.1.1. Vise

Vises, extensively utilized in manufacturing for their ease of use, are possibly the well-known workholders. An example for a vise is shown in Figure 2.4 [49]. Workpiece is squeezed between the vise jaws to perform the manufacturing operations. Despite the fact that jaws are generally driven by a screw mechanism, they can be also actuated hydraulically or pneumatically.

Figure 2.4. A typical vise as a fixturing element [49]

2.2.1.2. Clamps

Clamps are one of the fundamental elements that are used to fix the workpieces. Similar to vises, clamps compress the workpieces to fix them firmly. There are a wide variety of clamp elements. Some of strap clamp types are shown in Figure 2.5 [27].

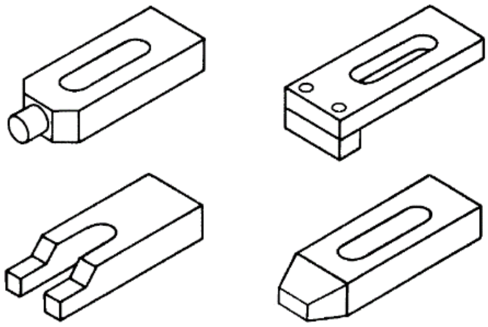

Figure 2.5. Clamps [27]

Additionally, Screw clamps, Cam action clamps, Wedge action clamps, Toggle action clamps and Worm-wheel clamps are the other significant clamps used in workholding applications. An example of a strap clamp application is illustrated in Figure 2.6.

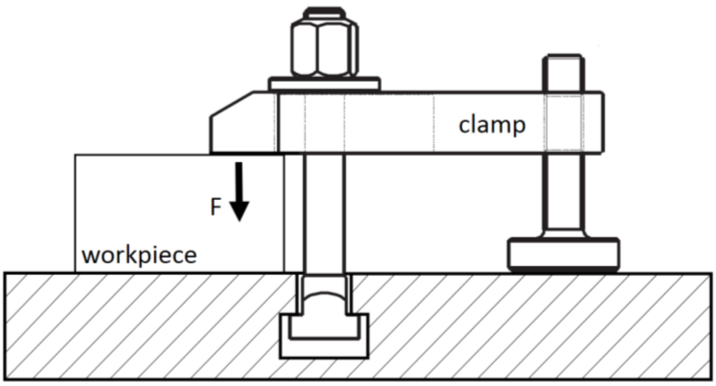

Figure 2.6. Clamp fixing the workpiece

2.2.1.3. Locators

There are several types of locators to position the workpiece. They are divided into two groups according to the contact surface of the workpiece with the locator. External locators position the workpiece by its external surfaces. These locators are classified as integral locators, locating pins, assembled locators, vee locators, locating nests and adjustable locators. Locating pins and adjustable locator are shown in Figure 2.7 and Figure 2.8 respectively [43].

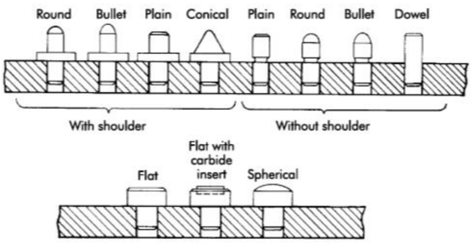

Figure 2.7. Locating Pins [43]

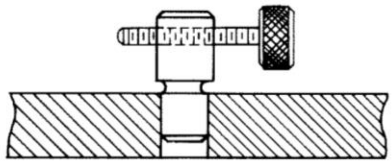

Figure 2.8. Adjustable Locator [43]

It must be ensured that locators are in contact with the workpiece continuously. Several locators such as round, flat, cone, and integral are in contact state shown in Figure 2.9.

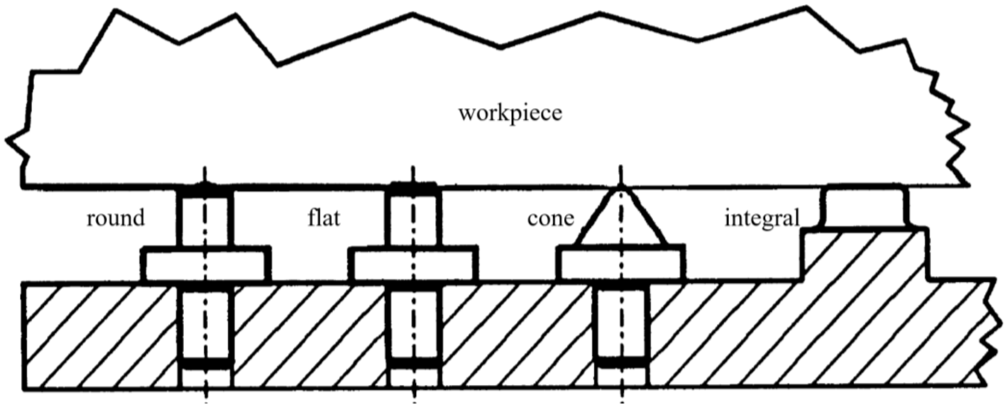

Figure 2.9. Examples for Locators Contacting with Workpiece [42]

Internal locators position the workpiece by its internal surfaces such as holes. These locators are classified as machined locators, commercial pin locators and relieved locators [43].

2.2.1.4. Fasteners

There are several fastening devices used in fixturing applications. These include screws, bolts, nuts, T-nuts, washers, inserts, dowels and pins [43].

2.2.2. Modular Fixturing

Modular fixturing includes a set of modular fixing elements such as plates, bolts, supports, locators, clamps, screws, etc. Main duty of the modular fixtures is fixing different shapes of workpieces by using interchangeable parts in different configurations [27].

2.2.3. Magnetic Fixturing

Magnetic fixturing is mainly focusses on fixing the magnetic materials. There are numerous kinds of magnetic chucks and instruments. Magnetic pulling force can be generated by using electromagnetic or a permanent magnet. Besides, different kind of accessories can be used to fix non-magnetic materials. Basically, non-magnetic material is squeezed between the magnetic fixture and magnetic fixture element [27]. Pull force is at the bottom side of the workpiece. Therefore, rest of the five surfaces except the bottom surface can be machined in magnetic fixturing.

2.2.4. Vacuum Fixturing

Vacuum fixturing is used to apply a uniform force on the workpiece surface. Negative pressure is generated with a vacuum pump and the workpiece is pulled by the fixture. Vacuum fixtures make the fixturing easier especially for the small and thin parts [27]. Every kind of workpieces independent of material type which has a flat surface can be fixed by using a vacuum fixture.

2.2.5. Adhesive Methods

Blumenthal and Raatz [30] investigated the performance of the adhesive systems for micromachining applications. As can be seen in Figure 2.10 workpiece is fixed by using thermoplastic adhesive material and at the end of the operation it can be unloaded by using a heat gun. They claimed that, this is the first time that this method has ever been tried. They asserted that high clamping forces can be prevented by using this method.

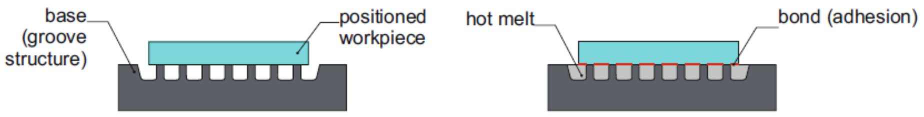

Figure 2.10. An adhesive fixture method [30]

Raffles et. al. [31] investigated the parameters of machining operation of a workpiece by using he **Adhesive Fixturing Systems** (AFS). In their study, AFS provided a gripping force of up to 2800 [N]. Depth of cut value was 3 mm in the AFS fixture. They also compared the dynamic response of the AFS with conventional mechanical gripping system.

Kushendarsyah et. al. [32] investigated the machining of a thin and a thick part separately and compared these two situations experimentally as can be seen in Figure 2.11. They used an adhesive material to glue the part to the table and examined the cutting forces that acts during the machining operation.

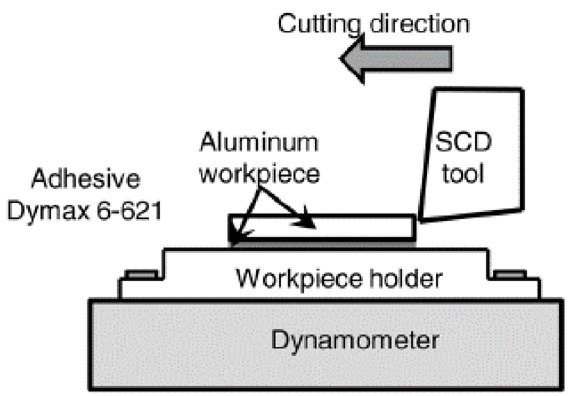

Figure 2.11. Fixturing method [32]

De Meter [33] fixed the part by UV light curable adhesive and examined the performance of the fixturing method experimentally. This method is called **<u>Light Activated Adhesive Gripper</u>** (LAAG). Workpiece is positioned on the adhesive material, then UV light cures the adhesive and workpiece is fixed. More UV light is applied to unbond the adhesive material to unload the part after the operation. Method can be seen in Figure 2.12.

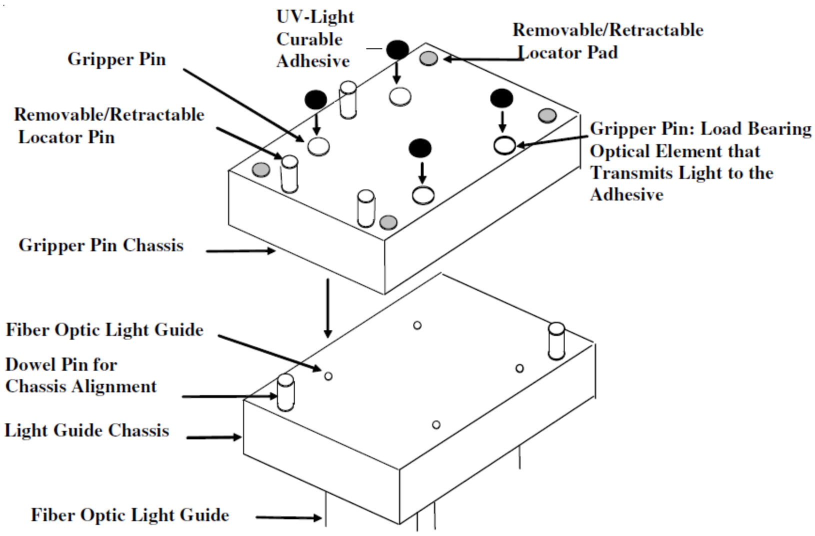

Figure 2.12. Light Activated Adhesive Gripper Method [33]

De Meter and Kumar [34] made a similar study to former paper [33]. In this study, they called the method as **<u>photo-activated work-holding</u>** (PAW). They asserted that part quality, machining time and cost are better than conventional fixturing systems. Bluephoton company sells [35] adhesives and relevant fixture systems. Adhesives can be cured by UV light to fix the workpiece. The method is shown in Figure 2.13.

Figure 2.13. Bluephoton company product [35]

Loctite 480 is a strong adhesive that can be used in manufacturing operations to fix a wide range of materials including metals. After the operations, workpieces can be removed by applying an instant force or heat to the workpiece [51].

Shellac material is used in a similar way to fix the small parts (watch parts etc.) for milling operations. It is a natural thermoplastic material that after the operation heat is applied to the shellac to debond the part [36].

2.3. Advantages & Disadvantages of Modular & Dedicated Fixtures

Modular fixture systems have several advantages over dedicated fixture systems. Firstly, lead time is lesser in modular fixture systems according to dedicated tooling. It is one of the most significant advantage of the modular fixturing. Secondly, modular fixtures are more flexible than dedicated fixtures due to their adaptability to new product implementation. It is easier to make revisions on a modular fixture than dedicated fixtures. Thirdly, elements of the modular fixture systems are reusable and they can be used repeatedly. On the contrary, dedicated fixtures are not reusable and will become useless after manufacturing run. Lastly, modular fixtures can easily replace a dedicated fixture for possible emergency conditions [43]. As far as small batch sizes are concerned, these advantages become more apparent [44].

Despite these advantages, modular fixturing has same disadvantages over dedicated fixturing. Number of elements used in modular fixturing is more than the elements used in dedicated fixturing. Therefore, rigidity of dedicated tooling is better than modular fixturing. Consequently, Modular Fixtures can require more working envelope than dedicated fixtures. Additionally, it can take more time to load a workpiece into the fixture in modular fixturing [44].

2.4. Closure

This section has focused on the review of the state of the art. Examined papers relevant with fixturing studies are summarized and contributions of these studies are emphasized. Fixture design is a subject that has been working on for many years. Therefore, a lot of fixturing elements are developed. In this section of the thesis, general fixture elements are outlined. Different kind of fixturing methods such as adhesive, vacuum, magnetic and modular are summarized. Commercial applications of some adhesive methods are mentioned. In this study, a modular fixture is designed. As a consequence, pros and cons of a modular fixture system over a dedicated fixture system are explained.

CHAPTER 3

PROPOSED MODULAR FIXTURING SYSTEM

This section introduces the elements of the proposed fixturing system (entitled as "Cubefix"). The system is composed of the following components:

- Grid Plate
- Cubic Support Element
    - Index Adjuster
- Locators
    - Risers
    - Shims
- Clamps
    - Screw Clamp
    - Spring Clamp
    - Ratchet Clamp
    - Magnetic Clamp
- Connecting Elements (Screws and Nuts)

The descriptions of the above-mentioned components follow.

3.1. Grid Plate

Grid plate is the fundamental part of the fixture system. All other elements are fastened to grid plate to perform their tasks. Figure 3.1 shows the Grid Plate attached onto the machine table. It is made out of AISI 1045 structural steel due to its accessibility and desirable mechanical properties such as strength and wear resistance.

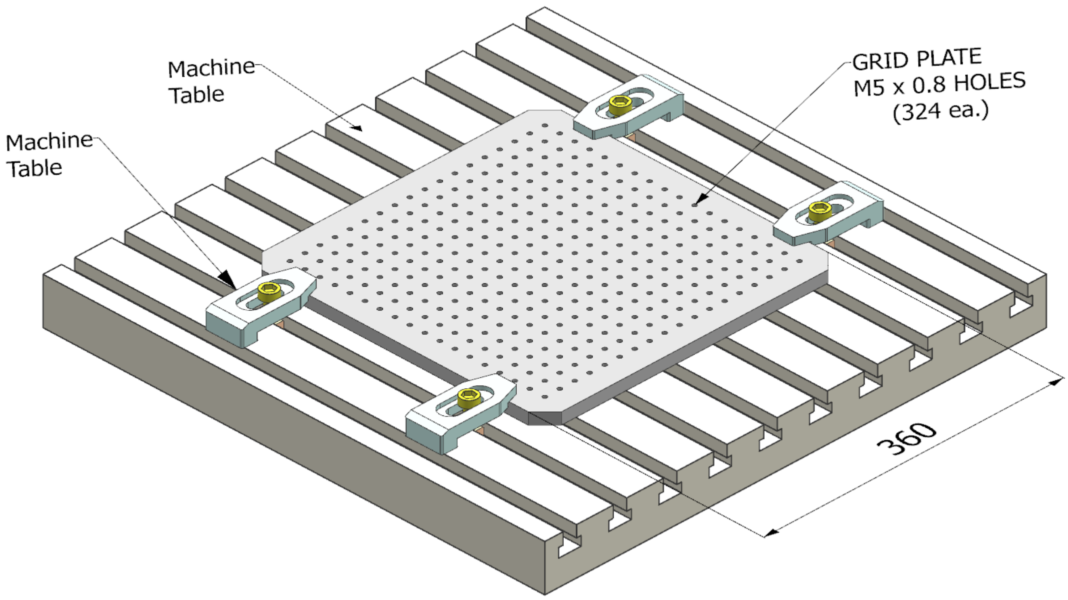

Figure 3.1. Grid Plate Loaded on the Machine Table

There are 324 M5 (Metric 5 mm) threaded holes on the surface of the grid plate to fasten the other elements of the developed fixture system. The distance between M5 holes on the grid plate, which roughly determines the positioning resolution of the device, is selected as 18 mm to house maximum number of the fixture components on the available space. Note that the above-mentioned distance is actually an inherited parameter from Support Element "Cube" mentioned in Section 3.2. However, the finer motions (smaller than 18 mm) can be accommodated by using the holes on the supporting elements.

3.2. Cubic Support Element - Cube

Cubic element ("Cube"), which is illustrated in Figure 3.2, is the main supporting- and connection element of the "Cubefix". Just like the Grid Plate, the material (AISI 1045) for the Cube is determined due to its accessibility, low cost, and suitable mechanical properties such as strength and wear resistance. Note that the Cube have a modular structure so that it can be linked to another cube from any of the six desired surfaces by using bolts.

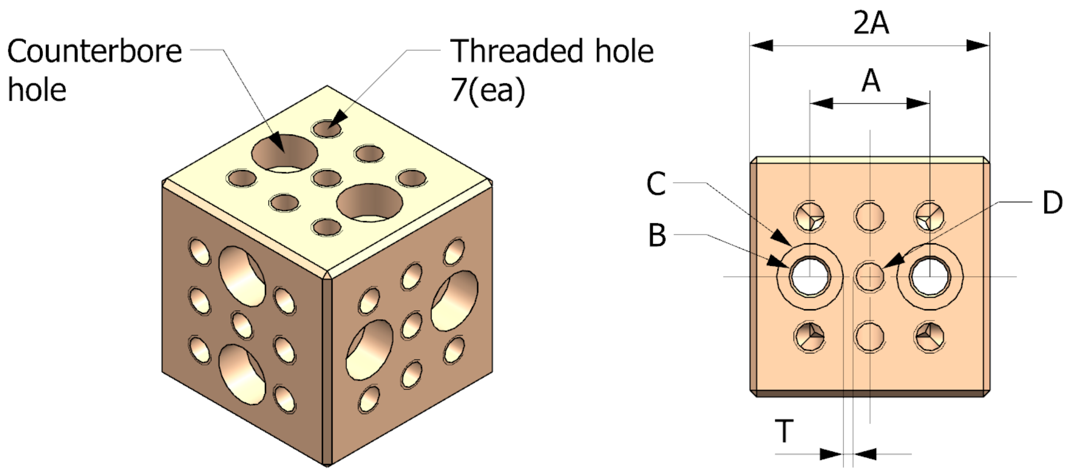

Figure 3.2. Cube element and its parameters

Figure 3.2 also illustrates basic dimensions of a cube element. Each surface of the cube element has 7 threaded holes and 2 counter-bore holes. These counter-bore holes and two of the corresponding threaded holes are used to assemble cube elements to each other. Rest of the threaded holes are employed to fix the other fixture elements to the cube. Note that the distance between two counter-bore holes (A) must be the half size of the cube's outer dimension (2A) to assemble a cube to another on any surface. Additionally, half of the "A" parameter sets the positioning resolution of locators. Once the dimension "A" is calculated, the outer dimensions of the cube element can be specified. Notice that in Figure 3.2, B, C, and D denote the radii of the marked holes. B is clearance hole for D thread size. C is the radius of the counter-bore hole for a hexagonal socket head bolt. "T" denotes the distance between the counter-bore and the threaded hole. There is not any precise relationship between B, C and D. Therefore, an approximation is performed to determine the size "A". The relationship between the above-mentioned parameters can be expressed as

$$A=2(C+T+D) \tag{3.1}$$

Since C is approximately two times of B for standard hexagonal socket bolts and D is approximately equal to B, the dimension "A" can be approximately given as

$$A=6B+2T \tag{3.2}$$

Once the size of the bolt and the "T" parameter are determined, the overall dimensions of the cube element emerge. In this study, M5 hexagonal socket head bolts are selected while "T" is determined as 1.5 [mm]. As a consequence, the remaining dimension of the cube element (2A) is becomes 36 [mm]. It also provides 9 [mm] of resolution in the locator's placement.

A new cube element can be easily fixed onto the grid plate by using two bolts as seen in Figure 3.3. The section view of the assembly is shown in Figure 3.4. Presume that a new cube element is to be attached to the upper surface of the cube in Figure 3.3. New element is placed on the upper surface of the cube in the same orientation. In the second step, new cube element is turned 90° (CW or CCW) and secured by two M5 bolts. These steps are sequentially shown in Figure 3.5, Figure 3.6 and Figure 3.7.

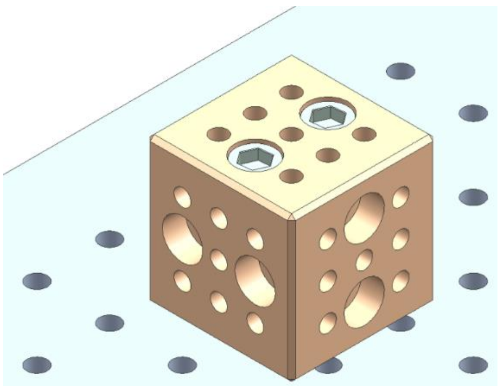

Figure 3.3. Cube connected to Grid Plate

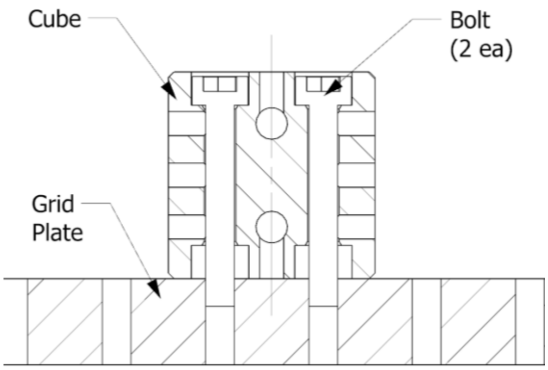

Figure 3.4. Section view of the cube and grid plate

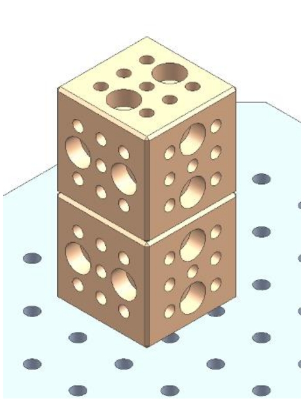

Figure 3.5. Place new cube element in same orientation

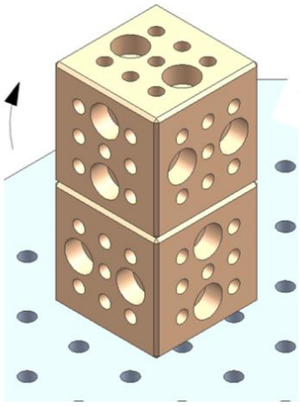

Figure 3.6. New cube element is to be turned 90°

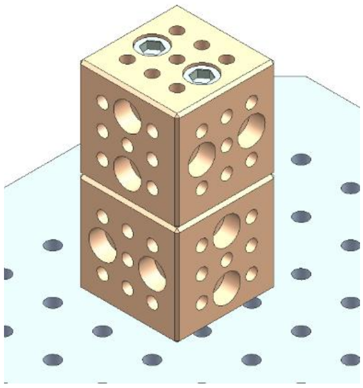

Figure 3.7. Bolts are tightened to fix the cube

Assume that a new cube element is to be added to the cube assembly in Figure 3.8. New cube element is placed onto the Surfaces A, B and C as shown in Figure 3.9. As the final step, the cube is secured by six M5 bolts as illustrated in Figure 3.10. The inner structure of the assembly is displayed in Figure 3.11. As can be seen, none of the bolts intersects with each other. As a consequence, the new element is firmly attached onto these three surfaces and becomes the part of a very rigid structure.

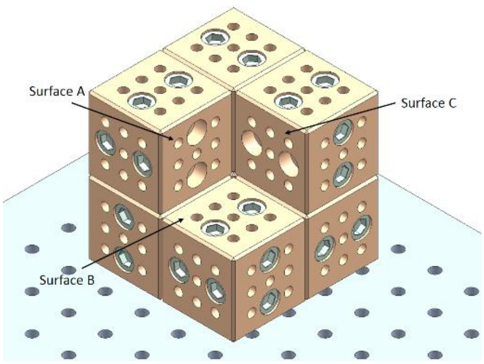

Figure 3.8. Surface A, B and C

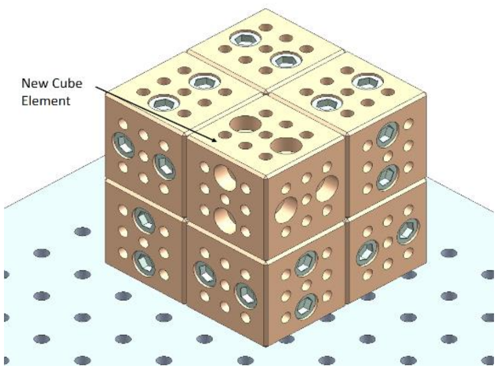

Figure 3.9. Placement of new cube element

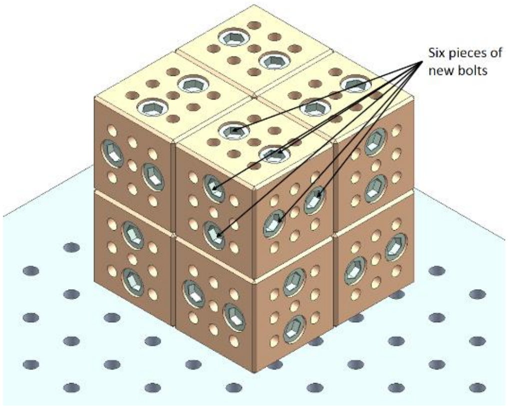

Figure 3.10. New Cube element fixed by 6 bolts

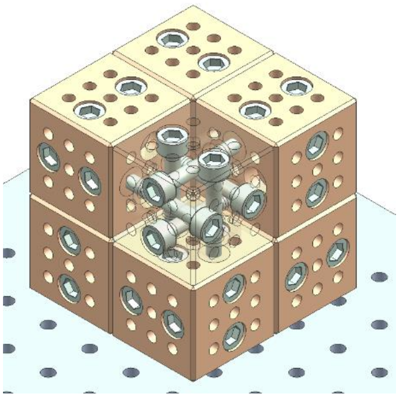

Figure 3.11. Fastening with 6 bolts

Due to its modularity, it is possible to create different fixture configurations with cube elements, very similar to LEGO™ parts. For instance, an intricate configuration is shown in Figure 3.12.

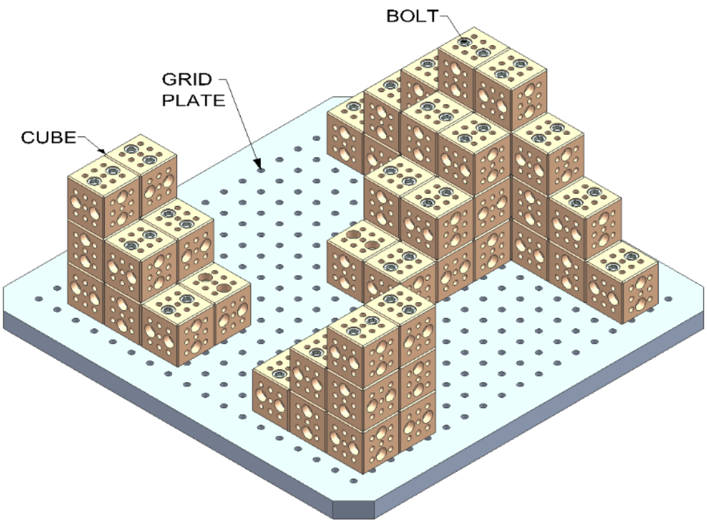

Figure 3.12. A fixture configuration with cubes

Several concepts have been considered during the design phase of the cube element. One of the manufactured prototypes is shown in Figure 3.13. In the first concept, pins are envisioned to locate the interfacing cubes accurately. However, in the final design, these holes are replaced by threaded holes for all practical purposes. Number of threaded holes are increased so that the flexibility of the cube is improved by allowing larger number of Cubefix components to be attached onto its faces. Note that the size of the first prototype was 48 mm. Eventually, the size has been decreased to 36 mm as shown in Figure 3.13. Hence, more cubic elements could be housed on the grid plate.

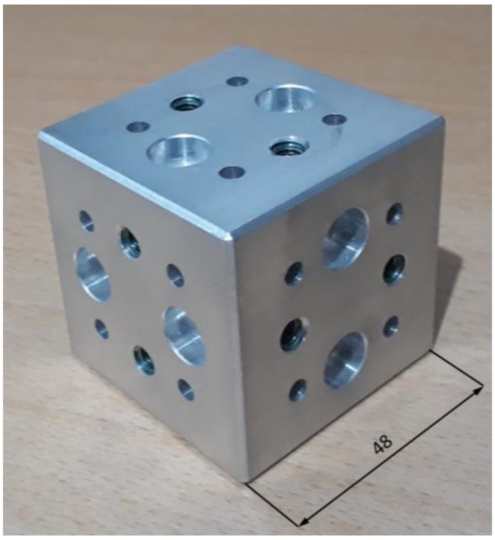

Figure 3.13. First Concept – Manufactured Part

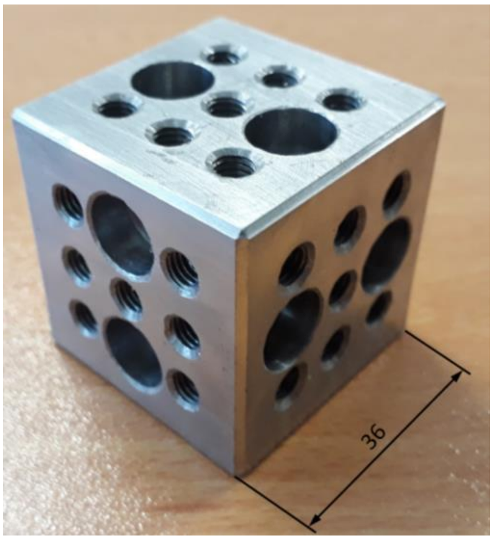

Figure 3.14. Final Design – Manufactured part

3.3. Index Adjuster

Index adjuster is designed to adjust the angular position of cubic support elements. Figure 3.15 illustrates the exploded view of the Index Adjuster. As can be seen from this figure, there is a tooted hub/boss (in the middle of the base) that engages with the conjugate groove inside the index cover. This feature allows the index cover to be rotated at discrete angular intervals of 22.5^{o}. Notice that since both the hub and the groove have sinusoidal tooth patterns, they could be manufactured conveniently through end-milling. Fixing bolt is then used to secure the index cover to index base part. When the cover is fixed at the desired orientation, the support cube could be bolted on the Index Adjuster.

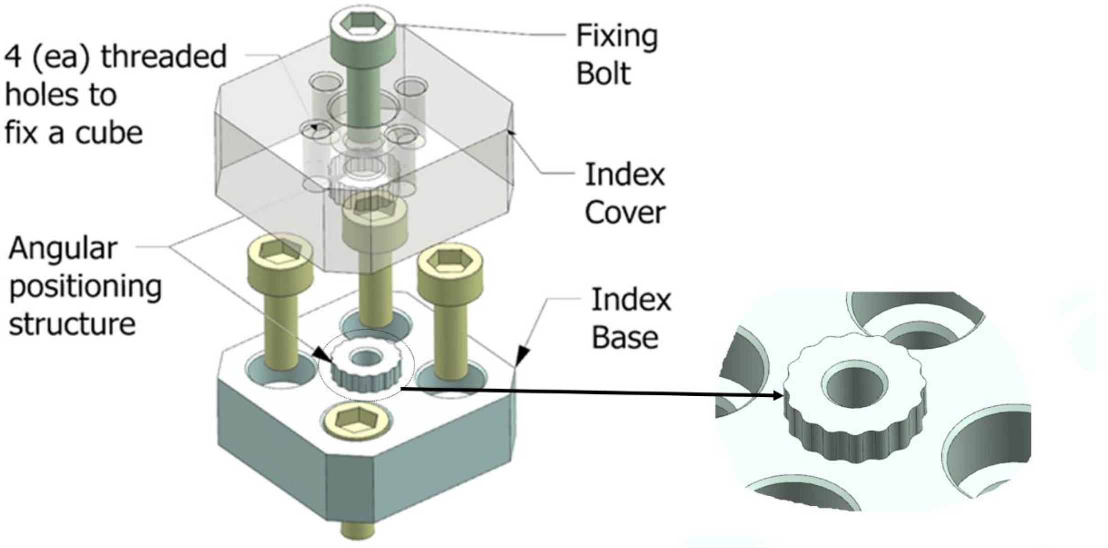

Figure 3.15. Index adjuster exploded view

The mechanism can be positioned between 0° and 360° with a resolution of 22.5°. The several angular positions of the index adjuster are shown in Figure 3.16.

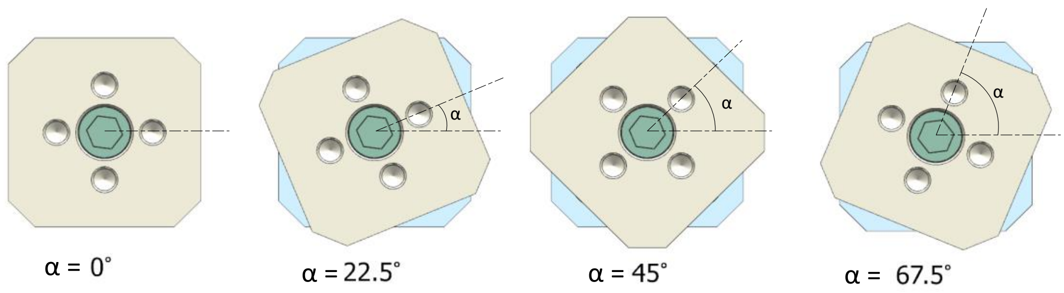

Figure 3.16. Angular positions of Index Adjuster

3.4. Locators

Locators are the key interface elements that position the workpiece accurately (and rigidly). A generic locator is shown in Figure 3.17 where "h" parameter changes from one type of locator to another due to the necessity for different heights. The height of the locators can be chosen from 3 mm to 15 mm with 1 mm of increments (resolution) to increase the flexibility of the fixture system. Locators are mounted on other elements such as Cube, Grid Plate, etc. with the help of its threaded shaft. Note that the planar lateral surfaces on the locator are used as gripping surfaces while bolting. It is made of AISI D3 which is a hardenable tool steel. Note that the surface of the locators must be hardened to increase their elastic limit. A manufactured locator is shown in Figure 3.18.

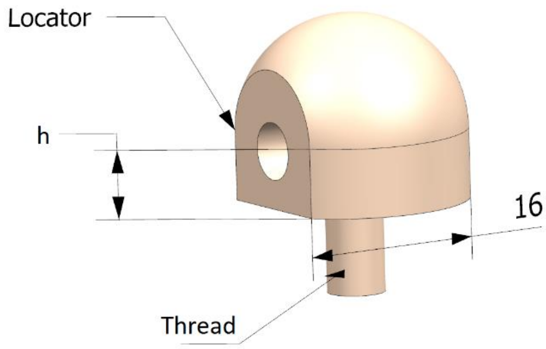

Figure 3.17. Locator

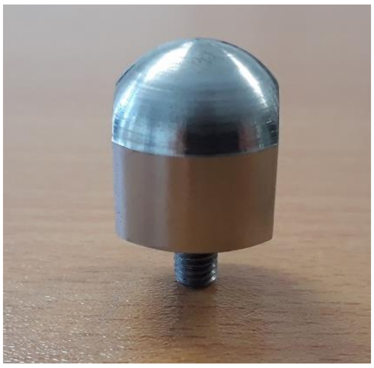

Figure 3.18. Manufactured Locator

3.5. Risers

Risers, as shown in Figure 3.19, are designed to adjust the elevation of the locators accurately. These elements (which are to be made out of AISI D3 tool steel just like the locators) can be mounted on other elements with (integral) threaded shaft at the bottom surface. Usually, the locators are bolted on top of risers by using the threaded hole at the upper surface of the riser. The holes perpendicular to the riser's axis allow them to be tighten via hex key wrenches. Note that a number of different risers (with different H values/heights) is needed to adjust the geometrical position of the locators accurately. Just like cylindrical gauge blocks, a combination of a set of risers may lead to a large number of height options (see also Section 3.6). Notice that the cube in Section 3.2 can also be used as a riser. On the other hand, risers are dimensionally much smaller than cubes and can occupy smaller spaces on the grid plate. Therefore, risers are considered as compact supporting elements for the locator pins to increase the overall flexibility of the Cubefix system.

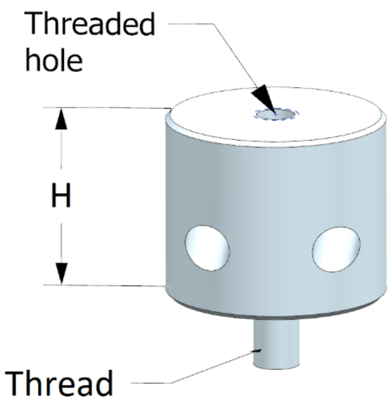

Figure 3.19. Riser

3.6. Shim Set

Locators must firmly contact with workpieces to perform their task. The height of the locator must be accurately adjustable (to the specified level) to accommodate a large number of workpiece topologies. For that purpose, a shim set, which is to be made from AISI D3 tool steel, is designed to fine tune the height of the locators. Just like Johnson gage blocks, the hardened shims are to be ground on both faces to achieve the desired level of parallelism. Isometric view of a shim is shown in Figure 3.20. as illustrated in Figure 3.21, shims can adjust the height by placing them under the locators.

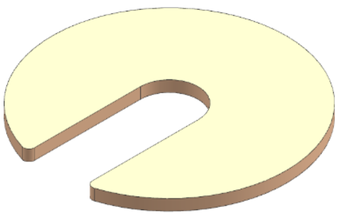

Figure 3.20. Shim

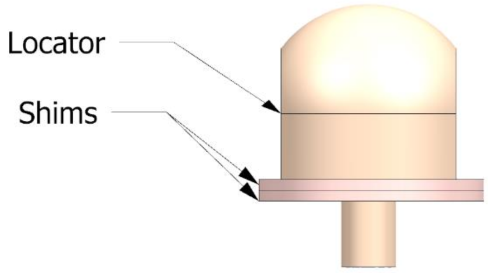

Figure 3.21. Fine tuning the height of the locator

Thicknesses of the shims are shown in Table 3.1. With various combinations of 11 shims listed, it is possible to change the locator heights between 0.05 to 3.05 [mm] with an increment of 0.01 [mm].

Table 3.1. Shim set thicknesses in [mm].

Part name	**Shim thickness**	**Part name**	**Shim thickness**
Shim_1	0.05	Shim_7	0.15
Shim_2	0.06	Shim_8	0.25
Shim_3	0.07	Shim_9	0.50
Shim_4	0.08	Shim_10	0.75
Shim_5	0.09	Shim_11	1.00
Shim_6	0.10		

3.7. Screw Clamp

Screw Clamp is designed to apply the axial force to the workpiece by tightening the screw. This element can be directly connected to the grid plate or cube. The exploded view of screw clamp is shown in Figure 3.22 whereas its prototype, which is made of Al-6063, is displayed in Figure 3.23. The Force Pad, which is made of vulcanized rubber, acts like a spring element while distributing out the clamping force evenly thru the contact surface. This feature is especially useful if that surface has a curvature.

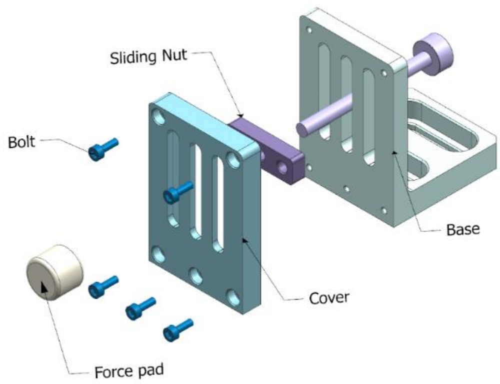

Figure 3.22. Exploded view of Screw Clamp

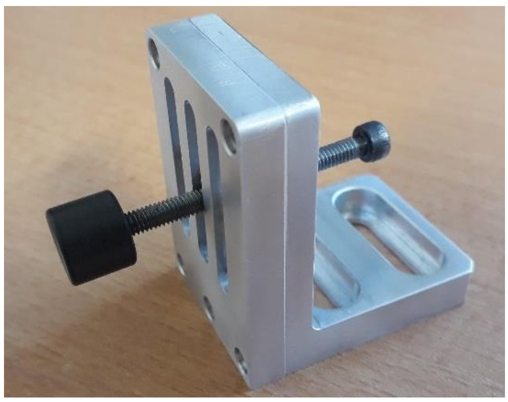
Figure 3.23. Screw Clamp – manufactured

3.8. Spring Clamp

Spring Clamp in Figure 3.24 and Figure 3.25 is developed specifically to apply clamping force along its main (sliding) axis. It can be mounted on the fixture assembly via M5 thread at the end of its guide. The (Clamp) Holder moves along its guide shaft. As the Holder part is pushed down to apply a clamping force on the workpiece, it locks in place via the friction on the shaft. However, as a safety feature, a bolt is added to fix this element in place. Spring Clamp has two configurations: Spring Clamp A incorporates a steel beam acting like a leaf spring (made out of AISI 1090 steel) as shown in Figure 3.24. On the other hand, Spring Clamp B employs the screw plus the Force Pad (used in the Screw Clamp) as illustrated in Figure 3.25. Both configurations utilize the same holder and guide elements.

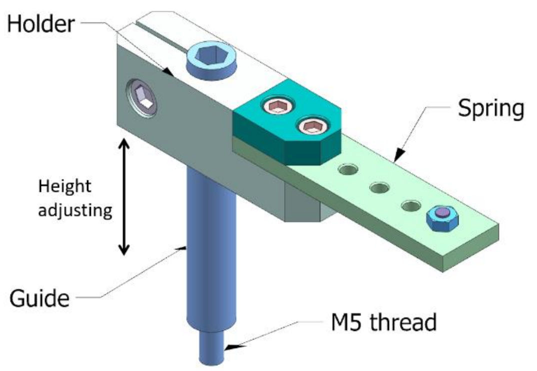

Figure 3.24. Spring Clamp – Config. A

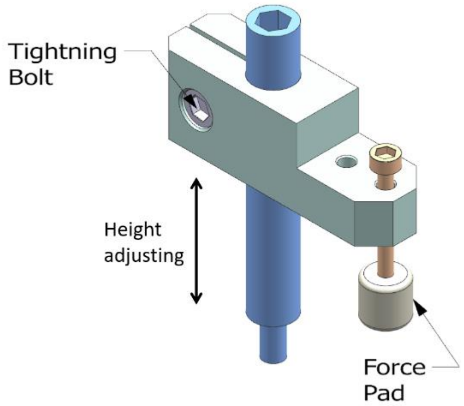

Figure 3.25. Spring Clamp – Config. B

3.9. Ratchet Clamp

Ratchet Clamp, as shown in Figure 3.26, is designed as a modular element to apply clamping force at different angles (-20° to +90°). This element could be mounted on the cube element from the opposite surface via two M5 bolts. Just like Spring Clamp A, this component also utilizes the elastic beam as a leaf spring. Furthermore, since the beam goes inside a groove in the Ratchet body, its position (with respect to the workpiece) could be easily adjusted. As illustrated in Figure 3.27, a ratchet mechanism is employed to lock the rotating arm in place. Here, torque applied by the tension spring provides a permanent contact between the pawl and the ratchet part.

The clamp can be simply wound up through its shaft with a wrench (i.e. Hex key) while the clamping force could be released by pulling out the relief pin on the pawl. However, due to strong friction between the pawl and the ratchet wheel, it is not possible to pull the relief pin directly. Hence, the torque must be first applied by a wrench to the Ratchet body so as to loosen the pin (and the pawl) before pulling. This safety feature prevents abrupt discharging of the clamping spring under tension.

With respect to the materials, the elastic beam serving as a spring is to be made out of AISI 1090 steel due to its high elastic limit and wear resistance. Bushing is planned to be made out of **Ultrahigh Molecular Weight Polyethylene** (UHMW) due to its high wear resistance and low-friction coefficient. Besides, UHMW does not absorb the water when in contact with cutting fluid during machining. The material for remaining sub-parts (Ratchet body, Sphere Pad, Ratched, Relief Pin and Pawl) is selected as AISI 1045 steel due to its accessibility, low cost, and suitable mechanical properties such as strength and wear resistance.

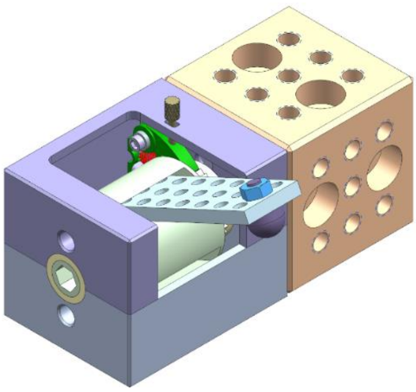

Figure 3.26. Ratchet Clamp attached to a Cube

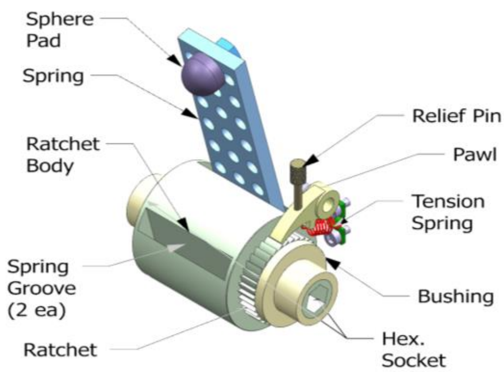

Figure 3.27. Inner structure of the ratchet clamp

3.10. Permanent Magnet based Clamping System

Apart from the clamps discussed in the previous sections, (permanent magnet based) magnetic clamps are also incorporated to the Cubefix system. For this purpose, commercially available permanent magnets (of two different types) are directly utilized as shown Figure 3.28. As can be seen, since the package of Neodymium (Nd) magnets already includes an integral threaded shaft (i.e. screw), they could be readily connected to the Cubefix elements. The magnetic clamping force is adjusted by controlling the distance between the magnet and (ferrous) workpiece.

The major advantages of the magnetic clamps are as follows:

i. Unlike classical clamps, they do not need to be in contact with the workpiece (they are non-tactile);
ii. They could induce huge magnetic forces on metal alloys containing Fe, Ni, Co;
iii. They are compact and can be located in places where classical clamps could not be deployed.

Their disadvantages can be summarized as follows:

i. The magnetic force (i.e. reluctance force) exponentially drops with the increasing airgap;
ii. They do not work with non-ferrous metals.

The following sections concentrates on two critical issues: **i)** Determination of magnetic clamping forces as a function of airgap; **ii)** Application of magnetic clamps to non-ferrous workpieces.

3.10.1. Computation of Magnetic Clamping Force

Magnet manufacturers have classified the magnets with respect to their magnetic and physical properties such as N35, M40 etc. In this representation, letter denotes the maximum working temperature of the magnet: N: 80°C, M: 100°C, H: 120°C etc. Number denotes approximately the maximum energy product of the magnet. Magnetic remanence is related with the magnitude of the magnetic induction. Higher magnetic remanence means stronger magnets. These properties are given in Table 3.2 for several magnets [37].

Table 3.2. Magnet Properties for several magnets [37]

Magnet Code	B_r [Tesla] Magnetic Remanence	Max. Working Temp.[°C]
N40	1.26 – 1.29	80
M50	1.40 – 1.46	100
H44	1.32 – 1.36	120

In this study, Neodymium ($Nd_2Fe_{14}B$) magnets are employed to produce magnetic clamping force on the workpiece. As mentioned before, two different types of magnet are included to the Cubefix system. Cross-sectional view of the magnet is illustrated in Figure 3.28 while one of the magnets used in this study is shown in Figure 3.29. Similarly, the properties of (commercial) magnets considered in this study are presented in Table 3.3 [38].

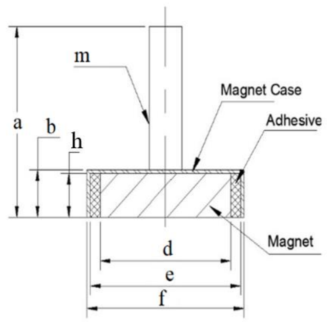

Figure 3.28. Section view of magnets

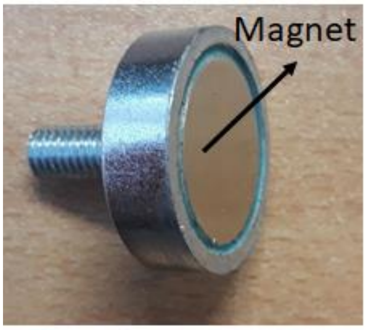

Figure 3.29. Magnet type 2

Table 3.3. Properties of the Magnets used in the study

Type	Class	a [mm]	d [mm]	h [mm]	F [N]	Max. Temp. [ºC]	Residual Magnetism [T]
1	N35	26	24	6	117	80°	1.17/1.21
2	N35	30	32	9	176	80°	1.17/1.21

To compute the reluctance force generated by a magnet, the magnetic flux density of the magnet must be calculated. Note that the magnetic flux density (B) of a disk magnet is dependent on the distance to a ferromagnetic medium (i.e. a plate) [28] and can be expressed as

$$B(x) = \frac{B_r}{2}\left(\frac{h+x}{\sqrt{r^2+(h+x)^2}} - \frac{x}{\sqrt{r^2+x^2}}\right) \tag{3.3}$$

where B_r is the remanence field density [T]; x is the axial distance [mm] from the ferromagnetic material; h is the height of the disk magnet [mm] and r is the radius of the magnet [mm]. In [40], the reluctance force on the ferromagnetic medium (held close to the disc magnet) is given as

$$F = \frac{1}{2}\frac{\mathrm{B}^2 A}{\mu_0} \tag{3.4}$$

where A is the cross-sectional area of the disc magnet; μ_0 is the permeability of air. Hence, substituting Eqn. (3.3) into (3.4) yields

$$\mathrm{F(x)} = \frac{\mathrm{A}B_r^2}{8\mu_0}\left[\frac{\mathrm{h+x}}{\sqrt{\mathrm{r}^2+(\mathrm{h+x})^2}} - \frac{\mathrm{x}}{\sqrt{\mathrm{r}^2+\mathrm{x}^2}}\right]^2 \tag{3.5}$$

The curve in Figure 3.30, which is in good agreement with Eqn. (3.5), shows the change in reluctance force with respect to the above-mentioned distance (i.e. air gap) based on the datasheet provided by the manufacturer.

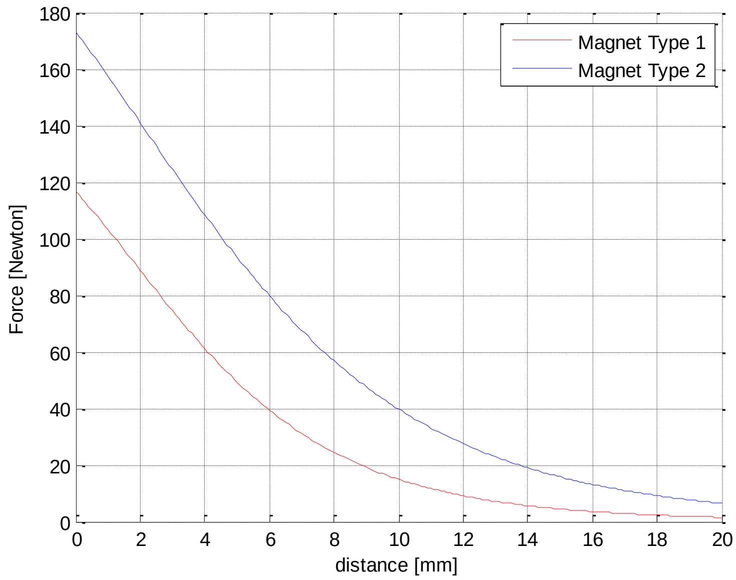

Figure 3.30. Magnetic (reluctance) force variation with respect to the air gap.

3.10.2. Magnetic Clamping Method for Nonmagnetic Materials

In this section, a method allowing nonmagnetic workpieces to be clamped is elaborated. In this technique, ferromagnetic material (i.e. plate) is glued onto the (non-ferrous) part to be clamped by the magnet. Before gluing, masking tape is applied on the relevant surfaces of both plate and workpiece to allow easy separation at the end of the operation. Furthermore, the tape protects the workpiece from glue remnants. A typical cross-section of this clamping system is illustrated in Figure 3.31. The thickness of the tape and the adhesive material is exaggerated to make the illustration more legible.

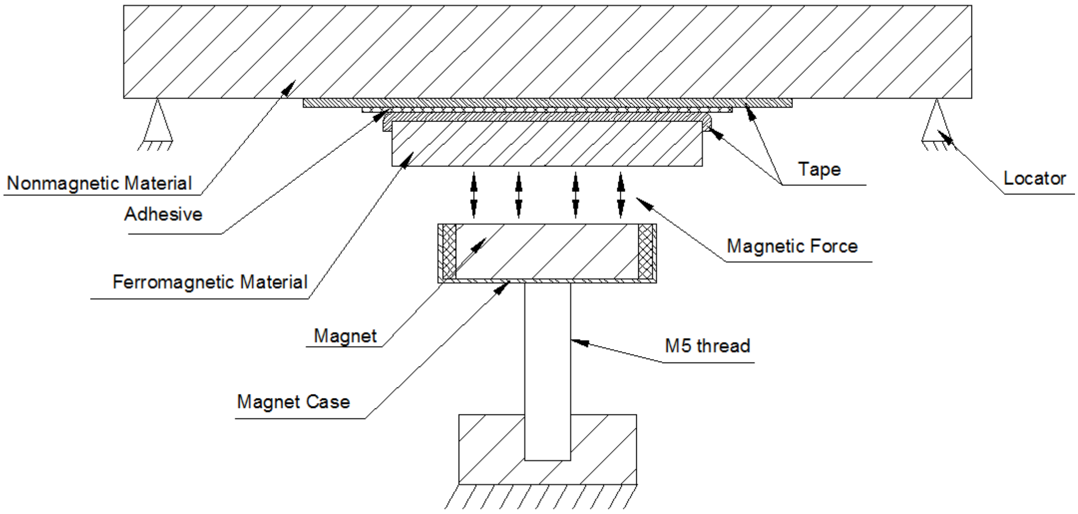

Figure 3.31. Magnetic Clamping Method for Nonmagnetic Materials

The strength of the tape and the adhesive materials are tested experimentally. The strongest magnet that is used in this study can apply 176 [N] of reluctance force on a ferromagnetic material. Hence, the tape and the adhesive tested that they can resist this maximum magnet force without shearing.

Notice that if desired plate can be directly glued onto the surface of the workpiece using strong industrial adhesives like Loctite 406 or 480 (provided that the surface is clean). The glue cures usually within a few minutes. After the machining operation, the application of heat degrades the bond quickly. The glue remnants could be washed off using acetone. Consequently, the above-mentioned preparation could be automated for mass production.

3.11. Bolts, Nuts, T-nuts and Steel Plates

A several kinds of bolts, nuts and T-nuts are included to the Cubefix. M5 bolts are the main connection elements used to attach cube elements to themselves and other fixture components. Likewise, bolts serve as the integral part of the Spring Clamps and Screw Clamps. Nuts are used to fix the magnet parts on the fixture system. They are basically employed as counter nuts to avoid magnet screws getting loose. Consequently, T-nuts are employed to attach the grid plate onto the machine tool table.

Note that steel plates (AISI A283), which will be a part of the magnetic clamps as elaborated in Section 3.10.2, are also incorporated to Cubefix. They will have two sizes: 30×30×4 [mm] and 15×30×4 [mm].

3.12. Closure

Elements of the proposed modular fixturing system are introduced in this section. Within the context of this study, several fixture elements are designed such as Grid Plate, Cube, Index Adjuster, Locator, Riser, Shim Set, Screw Clamp, Spring Clamp and Ratchet Clamp. Key features, area of usage and functions of these elements in the fixture system are discussed. Evolution of the cubic support element and how it is designed are explained in detail.

Different Clamping elements are designed. Additionally, an innovative permanent magnet clamping method is developed. As is known, magnets apply force only magnetic materials. Therefore, an innovative method has been developed to overcome this limitation and is applied to non-magnetic materials.

One of the properties of the magnets is the change of magnetic force with respect to the distance. As a consequence, computation of the magnet force is mentioned to determine the clamping force when the magnet is used as a clamping method.

CHAPTER 4

MODELLING AND QUASI-STATIC ANALYSIS OF PROPOSED MODULAR FIXTURING SYSTEM

The elements of fixture analysis are as follows:

- Selecting the positions of locating- and clamping elements suitable for a given workpiece geometry that enables the easy machining of functional surfaces and features;
- Checking the kinematic constraints imposed on the workpiece to guarantee that the workpiece is in fact well-constrained;
- Determination of the clamping forces that yield the maximum stiffness for the fixture system at hand;
- Estimation of cutting forces in machining operations to be conducted on the workpiece;
- Determination of elastic (and thermo-elastic) deformations in the fixture system (as well as the workpiece) assuming that the machining forces (and resulting torque) acting as external load at a particular location on the workpiece are quasi-static;
- Calculation of deflections on the functional surfaces (on pointwise basis) to make sure that these deviations, which lead to machining inaccuracies, are well within the desired tolerance bands;
- Optimization of locator positions and clamp forces to minimize the elastic deformations in the fixture system for a given set of milling operations.

Due to complicated nature of the analysis, some basic assumptions must be made to simplify the underlying computations:

- Workpiece is rigid;

- Friction between the fixture elements in contact with the workpiece is neglected;
- Elastic deformations at the locating elements are linear and can be modelled as linear spring elements provided that the surfaces are in contact;
- At a particular instant in time, the cutting forces are quasi-static;
- There are no thermo-elastic strains in the fixture/workpiece due to the implicit assumption that coolant is utilized in machining.

These proceeding sections present the analysis methods involved in the afore-mentioned steps.

4.1. Kinematic Constraint Analysis

A fixture is a mechanical device used to hold the workpiece firmly during manufacturing processes. Since every object in 3D space has six degrees of freedom (DOF), all DOF associated with the workpiece must be properly restrained to satisfy required positional and dimensional accuracy.

Asada and By [1] presented a seminal study about automatically configured fixture applications to increase the flexibility of manufacturing system. They designed a fixture layout that could be configured automatically by a robotic manipulator and analyzed the configuration kinematically to obtain deterministic positioning of the workpiece. Furthermore, some mathematical constructs are developed to investigate the accessibility and detachability of the workpiece. In their study, deterministic positioning is defined such that the workpiece contacts with all fixture elements while it is in a unique position. Jacobian matrix of the surface function $\boldsymbol{g}$ with respect to position vector $\mathbf{q}$ is derived as

$$
\boldsymbol{G} = \begin{bmatrix} \frac{\partial g_1}{\partial x_0} & \frac{\partial g_1}{\partial y_0} & \frac{\partial g_1}{\partial z_0} & \frac{\partial g_1}{\partial \theta_0} & \frac{\partial g_1}{\partial \phi_0} & \frac{\partial g_1}{\partial \psi_0} \\ \vdots & \vdots & \vdots & \vdots & \vdots & \vdots \\ \frac{\partial g_i}{\partial x_0} & \frac{\partial g_i}{\partial y_0} & \frac{\partial g_i}{\partial z_0} & \frac{\partial g_i}{\partial \theta_0} & \frac{\partial g_i}{\partial \phi_0} & \frac{\partial g_i}{\partial \psi_0} \\ \vdots & \vdots & \vdots & \vdots & \vdots & \vdots \\ \frac{\partial g_m}{\partial x_0} & \frac{\partial g_m}{\partial y_0} & \frac{\partial g_m}{\partial z_0} & \frac{\partial g_m}{\partial \theta_0} & \frac{\partial g_m}{\partial \phi_0} & \frac{\partial g_m}{\partial \psi_0} \end{bmatrix} \quad (4.1)
$$

where $\boldsymbol{g}(\boldsymbol{q}) = \mathbf{0}$ is the (differentiable) workpiece surface function; *m* is the number of the contact points and $\boldsymbol{q} = [x_0 \quad y_0 \quad z_0 \quad \theta_0 \quad \phi_0 \quad \psi_0]^T$ is the position and orientation vector of the workpiece. They show that the Jacobian matrix of the workpiece must have a rank of 6 to obtain a deterministic position [1]. Constrained status of a workpiece can be one of these categories:

1. Well-Constrained (deterministic)
2. Under-Constrained
3. Over-Constrained

Following [1], Song and Rong [2] developed a mathematical procedure to analyze the fixtures kinematically. They constructed a locating matrix ($\mathbf{W_L}$) [which corresponds to the Jacobian matrix in Eqn. (4.1)] to determine the constraining status of the workpiece. For a well-constrained workpiece, the rank of this locating matrix must be 6 signifying that the workpiece is *statically determinate*. For under-constrained workpieces, the matrix has a rank lower than 6 which in turn indicates that the workpiece is not in static equilibrium. For over-constrained workpieces, the rank is expected to be greater than 6 and thus the system is said to be *hyper-static*. The locating matrix $\boldsymbol{W_L}$ is described in terms of n number of locators as

$$\boldsymbol{W_L} = \begin{bmatrix} a_1 & b_1 & c_1 & c_1y_1 - b_1z_1 & a_1z_1 - c_1x_1 & b_1x_1 - a_1y_1 \\ \cdots & \cdots & \cdots & & & \\ a_i & b_i & c_i & c_iy_i - b_iz_i & a_iz_i - c_ix_i & b_ix_i - a_iy_i \\ \cdots & \cdots & \cdots & & & \\ a_n & b_n & c_n & c_ny_n - b_nz_n & a_nz_n - c_nx_n & b_nx_n - a_ny_n \end{bmatrix} \quad (4.2)$$

where normal vector of the i^{th} locator (with respect the surface of the workpiece at the contact point) is $[a_i, b_i, c_i]$ whereas the point of the contact between the locator and workpiece is given as $[x_i, y_i, z_i]$. Table 4.1 shows the constraint status determination of a workpiece.

Table 4.1. Constraint status respect to rank and number of locators

Rank of W_L	Number of Locators	Status
< 6	-	Under-Constrained
= 6	= 6	Well-Constrained
= 6	> 6	Over-Constrained

4.2. Cutting Force Estimation

Cutting force estimation is of critical importance to assess the elastic deformations taking place in the fixture (and the workpiece). To that end, a simplified end-milling process model, which yields average tangential- and axial forces, is summarized in Appendix A. More elaborate machining process models (such as the ones presented by [53]) could be incorporated to perform more accurate deformation analysis for the fixture.

It is critical to note that the dimensional- and geometric accuracy on the workpiece is attained in finishing operations where the magnitude of the cutting forces is usually less than a few hundred Newtons [52]. Therefore, to perform a preliminary analysis, one can presume that the magnitude of the tangential force is never to exceed 200 [N] while finishing the workpiece held in the modular fixture.

4.3. Elastic Deformation Analysis

Fixtures are used to fix the workpiece properly. During the machining operations a variety of forces are applied on the workpiece:

1. External load (Cutting force/moment)
2. Clamp forces
3. Weight of the workpiece
4. Locator forces

Figure 4.2 shows these forces and moments acting on a generic workpiece. Locator forces are simply the reaction of the locators to the other forces such as clamp forces, cutting forces and part weight.

Workpiece must be located to the fixture in a unique position and orientation. This is the basic goal of the fixture to attain more accurate parts. Therefore, workpiece must be in a state of static equilibrium. Summation of forces and moments that are acting on a workpiece must be zero during the machining operations. That is, force and moment equilibrium for a rigid workpiece can be expressed as

$$\sum_{i=1}^{p} \boldsymbol{F_i} = \boldsymbol{0} \tag{4.3}$$

$$\sum_{j=1}^{r} \boldsymbol{M_j} = \boldsymbol{0} \tag{4.4}$$

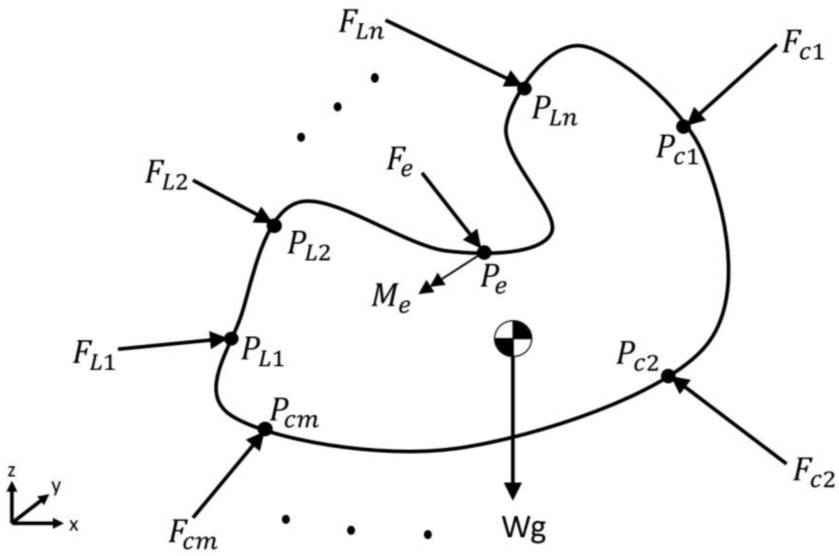

Figure 4.2. Free Body Diagram of a Generic Workpiece.

Assuming that workpiece is constrained by n number of locators and that there are m number of clamps (preloading the locators), Eqns. (4.3) and (4.4) take the following form:

$$\sum_{i=1}^{n} \boldsymbol{F_{Li}} + \sum_{j=1}^{m} \boldsymbol{F_{cj}} + W\boldsymbol{g} + \boldsymbol{F_e} = \boldsymbol{0} \tag{4.5a}$$

$$\sum_{i=1}^{n} \boldsymbol{P_{Li}} \times \boldsymbol{F_{Li}} + \sum_{j=1}^{m} \boldsymbol{P_{cj}} \times \boldsymbol{F_{cj}} + \boldsymbol{P_e} \times \boldsymbol{F_e} + \boldsymbol{M_e} = \boldsymbol{0} \tag{4.5b}$$

where × denotes vectoral multiplication; $\boldsymbol{F_{Li}}$ (3×1) are the locator force vectors [N]; $\boldsymbol{F_{cj}}$ (3×1) refer to the clamping force vectors [N]; W is the mass of the workpiece (i.e. the rigid body) [kg]; $\mathbf{g}$ = [0 0 -9.81]^T is the gravitational acceleration vector [m/s^2]; $\boldsymbol{F_e}$ (3×1) is the cutting force vector acting on the workpiece [N]; $\boldsymbol{P_{Li}}$ (3×1) are the locator contact point vectors [mm]; $\boldsymbol{P_{cj}}$ (3×1) are the clamping point vector [mm]; $\boldsymbol{P_e}$ (3×1) denotes the cutting location vector [N] and $\boldsymbol{M_e}$ (3×1) is the moment generated by the cutting torque vector [N mm]. The moments of the force vectors can be calculated at an arbitrary point in the workspace. However, it is convenient to compute the moments with respect to the **center of gravity** (CG) of the part (especially, when the origin of the Cartesian coordinate system is selected as CG).

4.3.1. Determination of Locator Forces

Since $\boldsymbol{F_{Li}}$ (i ∈ {1, 2, …, n}) are not known in advance, they are to be determined assuming that all locators act like linear spring elements provided that they are in contact with the workpiece. Thus,

$$\boldsymbol{F_{Li}} = -k\ (\boldsymbol{n_{Li}} \cdot \boldsymbol{\delta_i})\boldsymbol{n_{Li}} \tag{4.6a}$$

$$\boldsymbol{\delta_i} \triangleq \boldsymbol{P}'_{Li} - \boldsymbol{P_{Li}} \tag{4.6b}$$

where k is the stiffness of the locator [N/mm]; $\boldsymbol{n_{Li}}$ refers to the surface normal of the locator at the contact point; $\boldsymbol{P}'_{Li}$ refers to the location of the new (locator) contact point after the workpiece reaches a static equilibrium. Notice that the inner (dot) product of $\boldsymbol{n_{Li}}$ and $\boldsymbol{\delta_i}$ in Eqn. (4.6) simply refer to the deflection of the locator in the normal direction and is a scalar quantity. Hence, $-k\ (\boldsymbol{n_{Li}} \cdot \boldsymbol{\delta_i})$ yields the magnitude of the locator's reaction force under compression.

Note that the workpiece must be in contact state with all locators. If the workpiece and the locator are in contact, the distance between the contact point and the center of a particular locator must be smaller than the radius of curvature of the (undeformed) locator as shown in Figure 4.3.

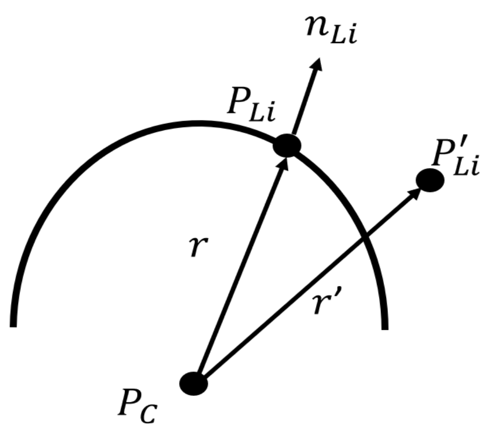

Figure 4.3. Determination of Locator Contact

Thus, the contact condition between a locator and a workpiece can be expressed

$$\boldsymbol{r}' = \|\boldsymbol{P}'_{\boldsymbol{Li}} - \boldsymbol{P}_{\boldsymbol{Ci}}\|_2 = \|\boldsymbol{P}'_{\boldsymbol{Li}} - \boldsymbol{P}_{\boldsymbol{Li}} + r\,\boldsymbol{n}_{\boldsymbol{Li}}\|_2 = \|\boldsymbol{\delta}_{\boldsymbol{i}} + r\,\boldsymbol{n}_{\boldsymbol{Li}}\|_2 < \boldsymbol{r} \tag{4.7}$$

where $\boldsymbol{P}'_{\boldsymbol{Li}}$ is the new contact point after the deformation; $\boldsymbol{P}_{\boldsymbol{Ci}}$ is the center point of the locator and r is the radius of curvature of that locator. It is critical to notice that the condition in Eqn. (4.7) simply boils down to

$$(\boldsymbol{n}_{\boldsymbol{Li}} \cdot \boldsymbol{\delta}_{\boldsymbol{i}}) < 0 \tag{4.8}$$

4.3.2. Locator Stiffness

In (4.6a), the stiffness of the locator (*k*) is needed to determine the magnitude of the corresponding reaction force. For this purpose, Hertz contact theory [46] is to be employed. Figure 4.4 shows two (spherical) elastic bodies in contact and their corresponding parameters.

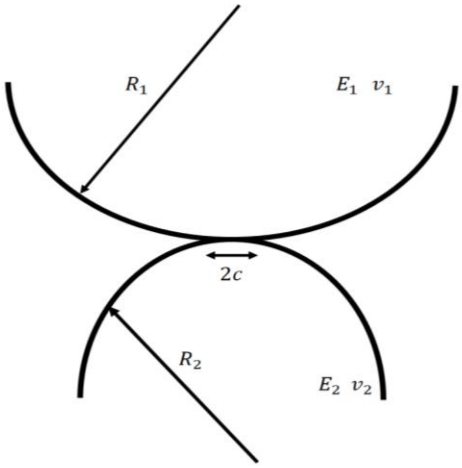

Figure 4.4. Elastic bodies in contact.

Making simplifying assumptions, Hale [47] computes the normal displacement between two contacting bodies:

$$\delta = \frac{c^2}{R_c} \tag{4.9}$$

Here, the contact radius (c), which is a function of the contact force F_L, takes the following form:

$$c = \left(\frac{3F_L R_c}{4E_c}\right)^{1/3} \tag{4.10}$$

where the relative radius (R_c) and the contact modulus (E_c) are defined as

$$\frac{1}{R_c} = \frac{1}{R_1} + \frac{1}{R_2} \tag{4.11a}$$

$$E_c = \left(\frac{1 - v_1^2}{E_1} + \frac{1 - v_2^2}{E_2}\right)^{-1} \tag{4.11b}$$

Hence, combining Eqns. (4.9) and (4.10) yields

$$\delta = \left(\frac{9}{16E_c^2 R_c}\right)^{1/3} F_L^{2/3} \tag{4.12}$$

It is obvious that Eqn. (4.12) is a non-linear function of F_L and cannot be modelled as a simple linear spring element (i.e. $F_L = k\delta$). However, Taylor series expansion of Eqn. (4.12) (with the omission of higher-order terms) leads to a (linear) displacement function defined around an arbitrary operating point (δ_0, F_{L0}). That is,

$$\delta \cong \delta_0 + \left(6R_c E_c^2 F_{L0}\right)^{-1/3}(F_L - F_{L0}) \tag{4.13}$$

where δ_0, by definition, is the displacement when a (pre)load of F_{L0} is applied through to the elastic bodies in contact. Consequently, the normal stiffness at this operating point boils down to

$$\left.\frac{dF_L}{d\delta}\right|_0 \triangleq k \cong \frac{F_L - F_{L0}}{\delta - \delta_0} = \left(6R_c E_c^2 F_{L0}\right)^{1/3} \tag{4.14}$$

It is critical to notice that in this study, the above-mentioned operating point is, by default, the static equilibrium point of the workpiece where no external load (i.e. cutting force) on the part is present.

Figure 4.5 shows the nonlinear relationship between the applied load and the corresponding deflection on a typical (spherical) locator. Note that the slope of this curve (at a certain bias point) leads the normal stiffness k [N/mm] in Eqn. (4.14). In this thesis, since the applied load is expected to be on order of 100 [N], the normal stiffness values can be calculated as 77399 N/mm. However, for the sake of simplicity, the locator stiffness values are assumed to be 70000 [N /mm] in the error simulations conducted in Chapter 5.

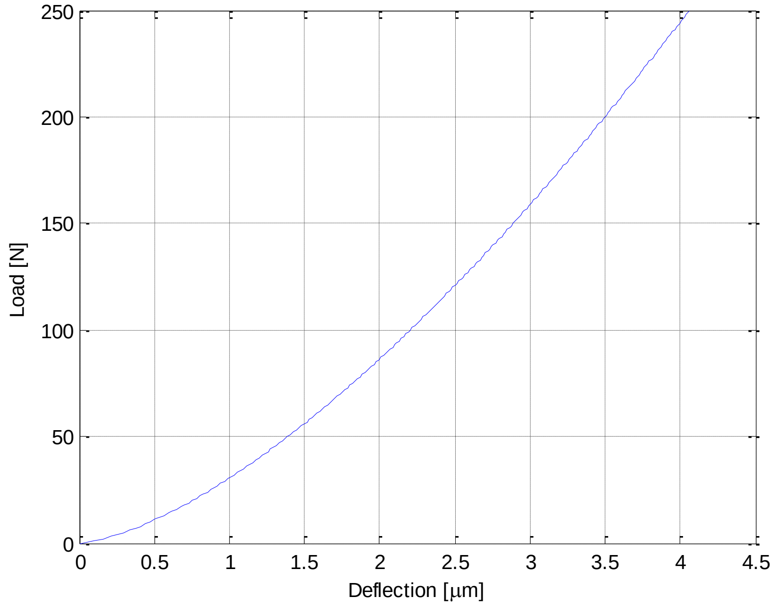

Figure 4.5. Locators deflection with respect to the load.

4.3.3. Quasi-static Motion of the Workpiece

To determine the motion of the rigid workpiece supported by the elastic locators, the *small* motion of the workpiece is first represented by the following motion vector:

$$\boldsymbol{q} = [\delta_x \quad \delta_y \quad \delta_z \quad \varepsilon_x \quad \varepsilon_y \quad \varepsilon_z]^T \tag{4.15}$$

where δ_x, δ_y, and δ_z denote the displacements (on the order of a few micrometers) of the workpiece along the principal axis [mm] while ε_x, ε_y, and ε_z refer to the rotations (on the order of a few arc-seconds) around these axes [rad]. After the static equilibrium is attained, one can simply calculate the new coordinates ($\boldsymbol{P'}$) of any point on the workpiece (including the ones associated with the locators) using homogeneous transformations as

$$\begin{bmatrix} \boldsymbol{P'} \\ 1 \end{bmatrix} = \boldsymbol{T}(\boldsymbol{q}) \begin{bmatrix} \boldsymbol{P} \\ 1 \end{bmatrix} \tag{4.16a}$$

$$\boldsymbol{T}(\boldsymbol{q}) = \begin{bmatrix} 1 & -\varepsilon_z & \varepsilon_y & \delta_x \\ \varepsilon_z & 1 & -\varepsilon_x & \delta_y \\ -\varepsilon_y & \varepsilon_x & 1 & \delta_z \\ 0 & 0 & 0 & 1 \end{bmatrix} \tag{4.16b}$$

Note that since $\mathbf{F_{Li}}$ in Eqn. (4.5) requires $\boldsymbol{P}'_{Li}$, $\mathbf{F_{Li}}$ is actually a function of $\mathbf{q}$. When Eqns. (4.5), (4.6), and (4.16) are combined, a linear equation set can be obtained:

$$\boldsymbol{Aq} + \boldsymbol{B} = \boldsymbol{0} \tag{4.17a}$$

$$\boldsymbol{B} \triangleq \begin{bmatrix} \sum_{j=1}^{m} \boldsymbol{F_{cj}} + W\boldsymbol{g} + \boldsymbol{F_e} \\ \sum_{j=1}^{m} \boldsymbol{P_{cj}} \times \boldsymbol{F_{cj}} + \boldsymbol{P_e} \times \boldsymbol{F_e} + \boldsymbol{M_e} \end{bmatrix} \tag{4.17b}$$

Hence, solving Eqn. (4.17) yields the equilibrium position (and orientation) of the workpiece:

$$\boldsymbol{q} = -\boldsymbol{A}^{-1}\boldsymbol{B} \tag{4.18}$$

It is critical to note that if the workpiece is well-constrained, one can directly solve Eqn. (4.5) for $\boldsymbol{F_{Li}} = F_{Li}\boldsymbol{n_{Li}}$ where only the scalar quantities F_{Li} (i.e. the magnitudes of the reaction forces) need to be determined. In that case,

$$\boldsymbol{R_L} = -(\boldsymbol{W_L^T})^{-1}\boldsymbol{B} \tag{4.19}$$

where $\boldsymbol{R_L} \triangleq [F_{L1} \quad F_{L2} \quad F_{L3} \quad F_{L4} \quad F_{L5} \quad F_{L6}]^T$.

4.3.4. Estimation of Machining Error

Once $\mathbf{q}$ is determined, the deviation vector at the tool contact point ($\mathbf{P_e}$) can be computed as

$$\begin{bmatrix} \boldsymbol{\delta P_e} \\ 0 \end{bmatrix} = \begin{bmatrix} \boldsymbol{T}(\boldsymbol{q})|_{\substack{\boldsymbol{F_e} \neq \boldsymbol{0} \\ \boldsymbol{M_e} \neq \boldsymbol{0}}} - \boldsymbol{T}(\boldsymbol{q_0})|_{\substack{\boldsymbol{F_e} = \boldsymbol{0} \\ \boldsymbol{M_e} = \boldsymbol{0}}} \end{bmatrix} \begin{bmatrix} \boldsymbol{P_e} \\ 1 \end{bmatrix} \tag{4.20}$$

where $\mathbf{q_0}$ refers to the initial position/orientation of the workpiece when no external load is present. The deviation metric, which is presumed to be a good indication about the machining error due to fixture, takes the following form:

$$e = \|\boldsymbol{\delta P_e}\|_2 \tag{4.21}$$

To assess the overall performance of the fixture system, one can perform a Monte Carlo simulation incorporating simplified machining models given in Section 4.2 to obtain a large set of deviations computed at various points on the functional surfaces:

$$\boldsymbol{E} = \{e_1, e_2, \dots, e_M\} \tag{4.22}$$

Thus, $e^* = \max\{\mathbf{E}\}$ could be utilized to evaluate the quality of machining. The procedure is summarized as follows:

1. Given $\{\boldsymbol{n_{L1}}, \boldsymbol{n_{L2}}, \dots, \boldsymbol{n_{Ln}}\}$, $\{\boldsymbol{P_{L1}}, \boldsymbol{P_{L2}}, \dots, \boldsymbol{P_{Ln}}\}$, $\{\boldsymbol{F_{c1}}, \boldsymbol{F_{c2}}, \dots, \boldsymbol{F_{cm}}\}$, $\{\boldsymbol{P_{c1}}, \boldsymbol{P_{c2}}, \dots, \boldsymbol{P_{cm}}\}$, W (mass) and workpiece material; determine the surfaces to be machined on workpiece. If applicable, roughly determine the cutting tool(s) (i.e. tool type/grade, geometry, etc.) and the machining operations to be conducted on the workpiece along with their relevant parameters (i.e. axial depth of cut, radial depth of cut, feed, spindle speed, etc.).

2. Initialize the Monte Carlo simulation: determine maximum sample size (M), *probability density functions* (PDFs) of the random variables in the simulation; set the iteration index (i) to 1.
3. Select a random point on the machined surface ($\mathbf{P_e}$); presuming the machining force is not present (i.e. $\mathbf{F_e} = \mathbf{0}$); calculate the displacement of the workpiece at $\mathbf{P_e}$. with the utilization of the technique highlighted in Section 4.3.2.
4. Using the conditions set in Step 1, generate a tangential force (F_t) (a scalar) acting on the tool. If desired, the simplified model cited in Section 4.1 could be utilized to conduct a more realistic simulation.
5. Generate a random (unity) direction vector ($\mathbf{u}$) (which is chosen orthogonal to the surface normal, $\mathbf{n_e}$) and calculate the force vector: $\boldsymbol{F_e} = F_t\boldsymbol{u}$. If desired, the corresponding spindle torque/moment can be included to the simulation as $\boldsymbol{M_e} \cong \pm F_t(D_c/2)\boldsymbol{n_e}$ where D_c refers to the diameter of the cutting tool; the sign (±) is arbitrarily assigned in the simulation[1].
6. Under the action of $\mathbf{F_e}$ and $\mathbf{M_e}$ at, determine the displacement of workpiece at $\mathbf{P_e}$. Using Eqn. (4.20), estimate the resulting deviation: $\boldsymbol{\delta P_e} = [\delta x \quad \delta y \quad \delta z]^T$.

[1] By definition, $\mathbf{F_e}$ and $\mathbf{M_e}$ are the forces and moments on the **workpiece** as a consequence of the cutting action of the tool. According to the Newton's 3rd law of motion, $-\mathbf{F_e}$ and $-\mathbf{M_e}$ represent the reaction of the workpiece to the tool. In the simulation, the directions of $\mathbf{F_e}$ and $\mathbf{M_e}$ are treated as random process variables owing to the fact that they depend on the actual trajectory of the tool(s) along with the milling types (i.e. up/down-milling). Thus, they **cannot** be properly determined without the presence of a detailed machining plan respective to a specific workpiece.

7. For every locator in the fixture, check whether the contact condition in Eqn. (4.8) is satisfied. If not, issue an alarm signaling that the workpiece is no longer at static equilibrium and go to Step 10.
8. Store the error metric: $e[i] = \sqrt{\delta x^2 + \delta y^2 + \delta z^2}$.
9. Increase the iteration index by 1. If the iteration index is less than M, go to Step 3.
10. End the simulation.

4.4. Closure

This section has concentrated on the elements of fixture analysis. First, a simple method for checking the constraining status of the fixture, is presented. The method essentially constructs a locating matrix with the utilization of the normal- and position vectors of all the locators. The rank of this matrix yields the constraining status. Should the fixture configuration lead to a well-constrained workpiece, the elastic deformation analysis of the workpiece is in order. Two issues are of critical importance in this analysis: **i)** determination of locator stiffness functions; **ii)** computation of cutting forces (acting as an external load on the workpiece). Since the reaction force of a locator pin is a nonlinear function of its deformation, a stiffness function is developed using Hertz contact theory with many simplifying assumptions. With respect to the cutting force, the upper bound of machining forces in finishing operations could be utilized for all practical purposes. Hence, the displacement of a rigid workpiece supported on elastic elements could be simply calculated using the presented technique in this section. Finally, the chapter elaborates a Monte-Carlo simulation procedure in order to compute the deviations on functional surfaces for the sole purpose of predicting (and quantify) the machining quality associated with a particular fixture configuration.

CHAPTER 5

CASE STUDIES

In this section, the feasibility of fixturing six different parts (with various geometric attributes) using Cubefix is investigated. These parts include

- Exhaust Manifold,
- Robot Gripper Arm,
- Suspension Fork,
- Gearbox Casing,
- Throttle Body,
- Test Part (Support Base).

First of all, the solid geometric models of the parts considered for case studies are downloaded from the reference [50]. The relevant information (i.e. material, functional surfaces, manufacturing operations to be conducted, etc.) for these workpieces is gathered to conduct the accompanying analyses.

Using Cubefix elements introduced in Chapter 3, a modular fixture suitable for each part is designed with the utilization of NX CAD software. The constraining status of the designed fixture is then studied using the method presented in Section 4.1.

With the techniques outlined in the Section 4.3, the probable machining errors are estimated by taking into account the required machining operations thru extensive Monte Carlo simulations for each- and every part. The Matlab programs to carry out the relevant computations are given in Appendix B through Appendix F. Details about these case studies follow.

5.1. Part 1 – Exhaust Manifold

Exhaust manifold, which is an old part from automotive industry, is shown in Figure 5.1. The main function of the manifold is to collect the exhaust gases from the cylinders and to direct them into a single pipe for discharge. The element is assumed to be made out of grey cast iron (GG-25) and is to be manufactured by sand casting method. Hence, the surfaces A1 and A2 (shown in red color) is to be face-milled (after casting) employing the proposed fixture system. The perpendicularity of these two surfaces is presumed to be critical.

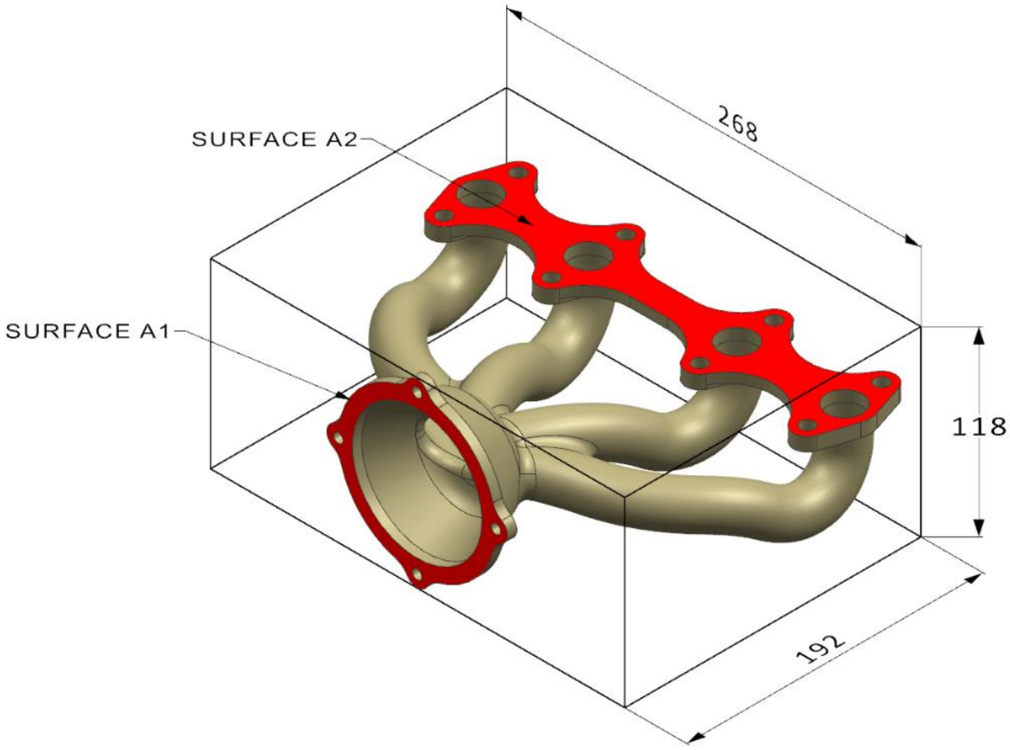

Figure 5.1. Exhaust Manifold

5.1.1. Locating Status Analysis – Part 1

Locator configuration for Part 1 is shown in Figure 5.2. As can be seen, the workpiece is constrained with 6 locators. The normal vectors and the contact points are presented in Table 5.1.

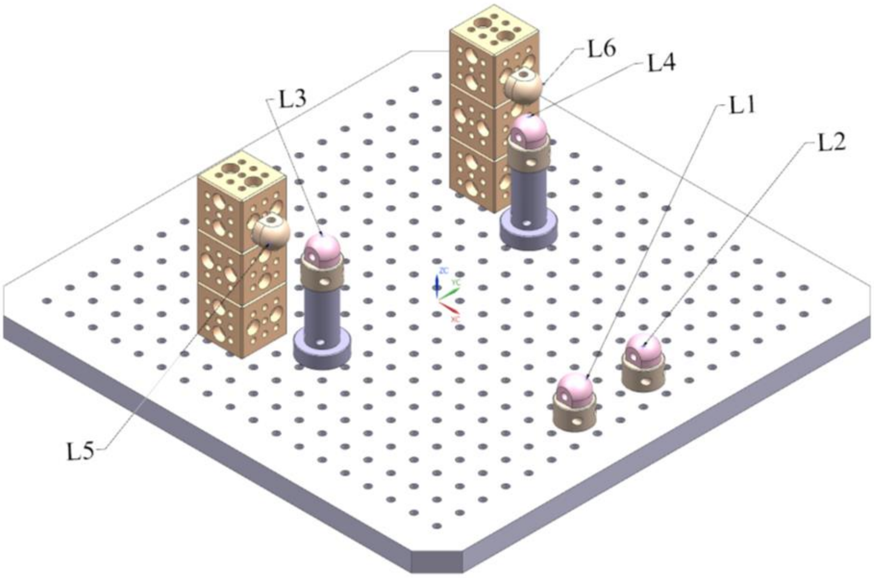

Figure 5.2. Locator Configuration – without Part 1

Table 5.1. Normal Vector and Position of each contact point – Part 1

Locator # i	normal vector $[\boldsymbol{a_i} \quad \boldsymbol{b_i} \quad \boldsymbol{c_i}]$	position of each contact point $[\boldsymbol{x_i} \quad \boldsymbol{y_i} \quad \boldsymbol{z}]$
1	$[0.447 \quad 0.480 \quad 0.754]$	$[139.472 \quad -22.197 \quad 27.545]$
2	$[0.447 \quad -0.480 \quad 0.754]$	$[139.472 \quad 22.197 \quad 27.545]$
3	$[0 \quad 0 \quad 1.000]$	$[-9.000 \quad -81.000 \quad 80.000]$
4	$[0 \quad 0 \quad 1.000]$	$[-9.000 \quad 81.000 \quad 80.000]$
5	$[0.586 \quad -0.810 \quad 0]$	$[-24.212 \quad -107.100 \quad 81.000]$
6	$[0.586 \quad 0.810 \quad 0]$	$[-24.212 \quad 107.100 \quad 81.000]$

Using the data in Table 5.1, the locating matrix in Eqn. (4.2) can be formed as

$$W_L = \begin{bmatrix} 0.447 & 0.480 & 0.7541 & -29.978 & -92.916 & 76.917 \\ 0.447 & -0.480 & 0.7541 & 29.978 & -92.916 & -76.917 \\ 0 & 0 & 1.0000 & -81.000 & 9.000 & 0 \\ 0 & 0 & 1.0000 & 81.000 & 9.000 & 0 \\ 0.586 & -0.810 & 0 & 65.634 & 47.467 & 82.381 \\ 0.586 & 0.810 & 0 & -65.634 & 47.467 & -82.381 \end{bmatrix} \tag{5.1}$$

Note that since the rank of the locator matrix is found as 6, the part in Figure 5.3 is said to be well-constrained in this case. Likewise, Figure 5.4 illustrates the full fixture configuration with two ratchet- and permanent magnet clamps in place while Table 5.2 tabulates the corresponding parameters of these clamps.

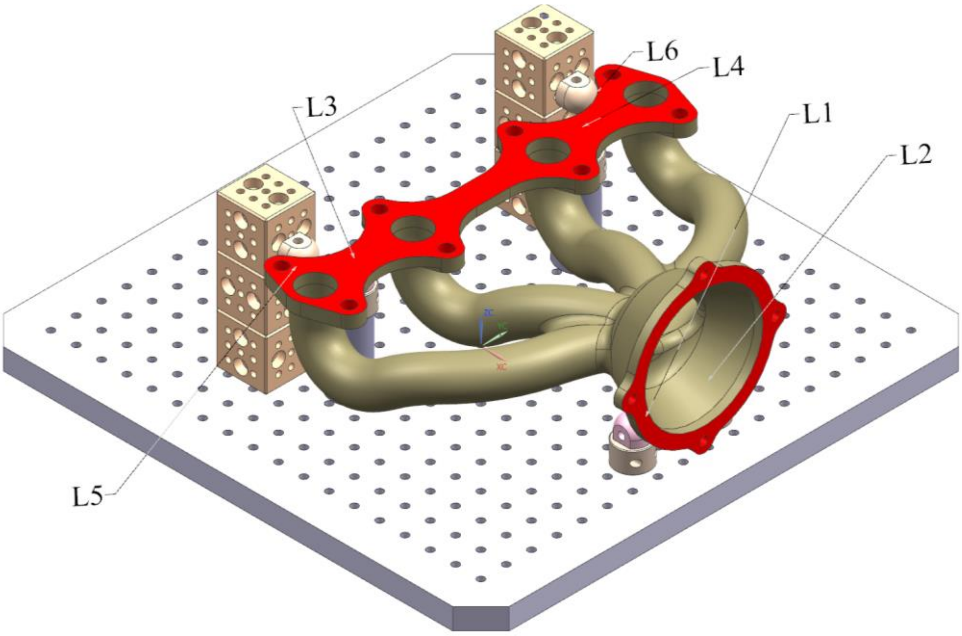

Figure 5.3. Locator configuration for Part 1

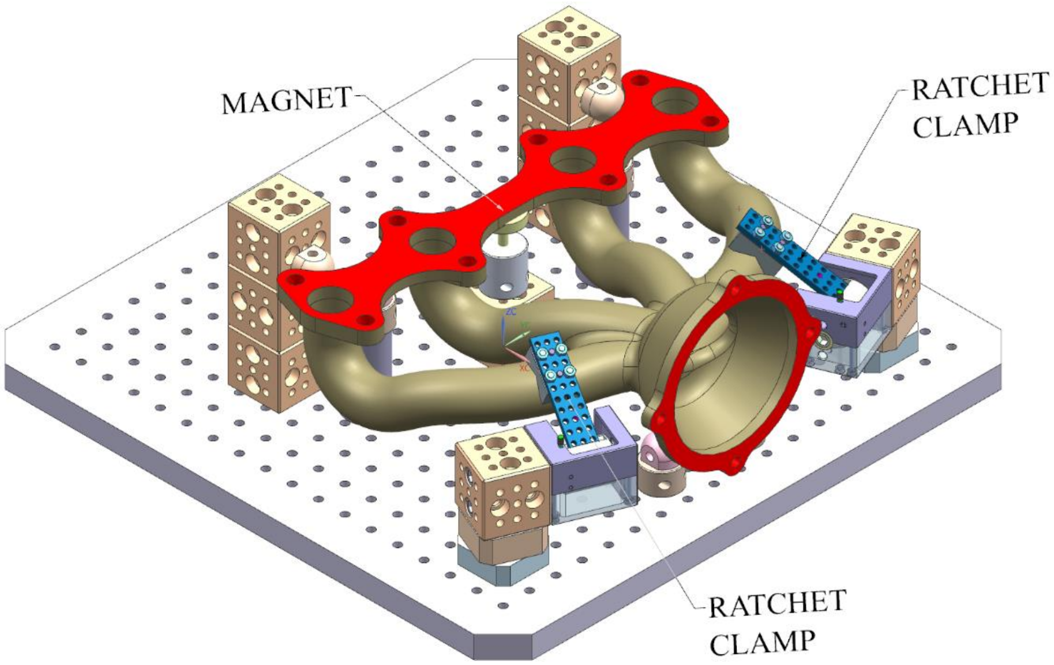

Figure 5.4. Full fixture configuration – Part 1

Table 5.2. Clamping forces on Part 1

Force Application Point	Force Magnitude	Clamping Method
[0 0 90.61]	[0 0 -160]	Magnet
[106.6 -71.9 87.6]	[-50 50 -50]	Ratchet Clamp
[105.0 75.6 87.6]	[-50 -50 -50]	Ratchet Clamp

Notice that under the action of clamping forces, the locator reaction forces along with the accompanying elastic deformations of the spherical locator pins are also computed to guarantee that all locators are properly preloaded (biased). Table 5.3 tabulates these results where "locator's radius of curvature" refers to the radius of a deformed pin (with a nominal size of 10 [mm]). As expected, the locator force vectors ($\mathbf{F}_{Li}$) and their normals ($\mathbf{n}_{Li}$) are collinear. Therefore, it can be concluded that the workpiece is properly in contact with all six locators.

Table 5.3. Locator Forces and Radius of Curvatures – Part 1

Locator #	F_x [N]	F_y [N]	F_z [N]	Locator's Radius of Curvature [mm]
1	121.6	130.9	205.2	9.9961
2	122.5	-131.9	206.8	9.9961
3	0	0	96.8	9.9986
4	0	0	99.2	9.9986
5	232.5	-321.4	0	9.9943
6	233.2	322.4	0	9.9943

5.1.2. Error Simulation – Part 1

Using the data in Table 5.1 and Table 5.2, a Monte-Carlo simulation is conducted to assess the machining quality achievable. Since the material of Part 1 is grey cast iron, the magnitude of the tool force while light machining of this material is computed (and averaged) as 25 [N] using the model in Appendix A. The results of the simulation for the functional surfaces A1 and A2 are shown in Figure 5.5. Simulation Results for Surface A1 - Part 1 and Figure 5.6. As can be seen, the maximum deviation on both surfaces due to the prescribed machining forces is less than 1.6 μm. Hence, the support provided by the fixture can be assumed satisfactory for all intents and purposes.

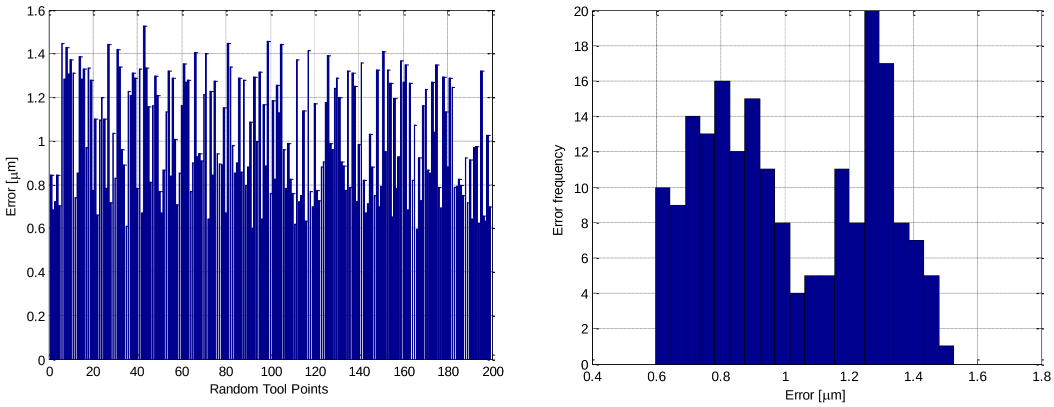

(a) Probable Machining Error **(b)** Error Frequency Chart

Figure 5.5. Simulation Results for Surface A1 - Part 1

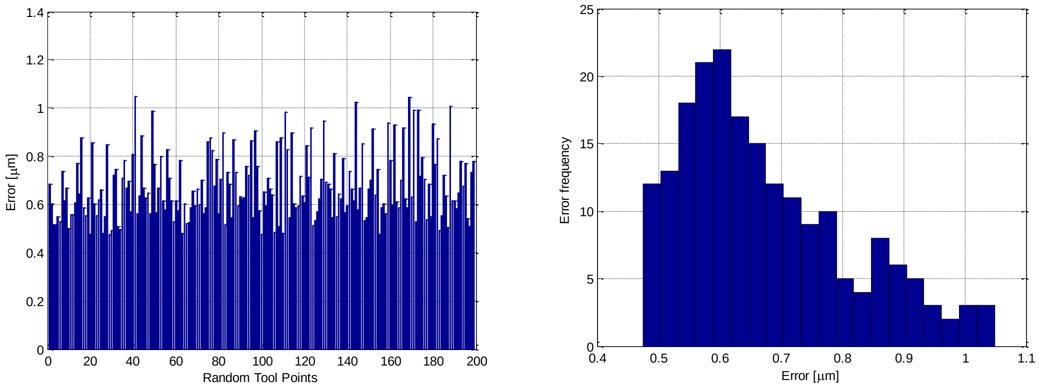

(a) Probable Machining Error **(b)** Error Frequency Chart

Figure 5.6. Simulation Results for Surface A2 - Part 1

5.2. Part 2 – Robot Gripper Arm

Robot Gripper Arm, which is a part from robotic industry, is illustrated in Figure 5.7. It is a structural element for the robotic arms. It is assumed that this element, made from Al-6063, has been rough-machined in a vertical machining center and that there is excess material left on surfaces B1 and B2 (shown in red color) to be finish-machined with the utilization of Cubefix fixture system.

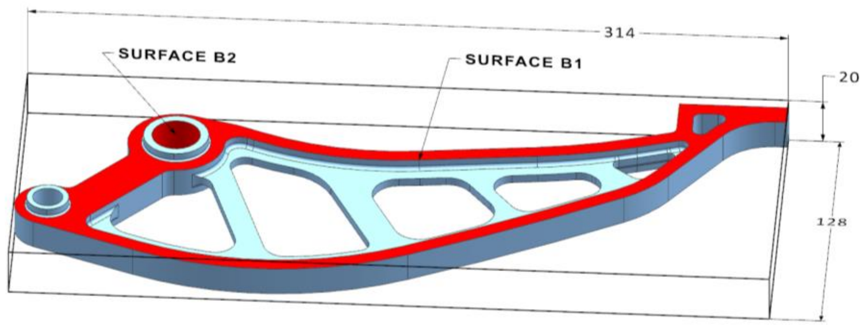

Figure 5.7. Robot Gripper Arm

5.2.1. Locating Status Analysis – Part 2

Locator configuration for Part 2 is displayed in the Figure 5.8. As can be easily seen, the workpiece is again constrained with 6 locators. The normal vectors as well as the contact points are presented in Table 5.4.

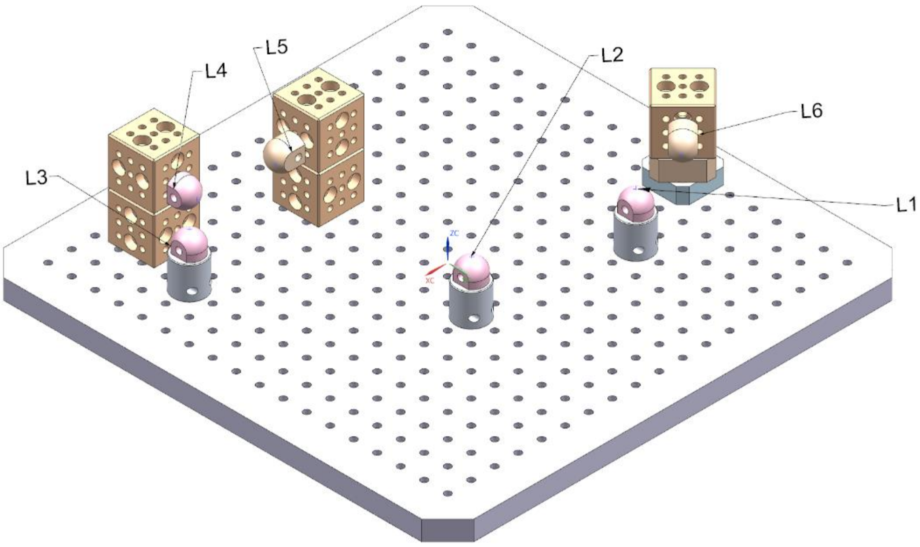

Figure 5.8. Locator Configuration – without Part 2

Table 5.4. Normal vector and Position of each contact point – Part 2

Locator # **i**	**normal vector** $[\boldsymbol{a_i} \quad \boldsymbol{b_i} \quad \boldsymbol{c_i}]$	**position of each contact point** $[\boldsymbol{x_i} \quad \boldsymbol{y_i} \quad \boldsymbol{z}]$
1	$[0 \quad 0 \quad 1.000]$	$[-81.000 \quad 63.000 \quad 40.000]$
2	$[0 \quad 0 \quad 1.000]$	$[27.000 \quad 45.000 \quad 40.000]$
3	$[0 \quad 0 \quad 1.000]$	$[117.000 \quad -81.000 \quad 40.0]$
4	$[0 \quad 1.0000 \quad 0]$	$[-66.2476 \quad 45.3546 \quad 45.0]$
5	$[0.906 \quad 0.422 \quad 0]$	$[32.0671 \quad -49.7590 \quad 45.0]$
6	$[0.749 \quad 0.662 \quad 0]$	$[99.0 \quad -93.0 \quad 45.0]$

Employing the data in Table 5.4, the locating matrix in Eqn. (4.2) can be written as

$$W_L = \begin{bmatrix} 0 & 0 & 1.000 & 63.000 & 81.000 & 0 \\ 0 & 0 & 1.000 & 45.000 & -27.000 & 0 \\ 0 & 0 & 1.000 & -81.000 & -117.000 & 0 \\ 0 & 1.000 & 0 & -45.000 & 0 & 99.000 \\ 0.9064 & 0.422 & 0 & -19.011 & 40.786 & 97.308 \\ 0.7494 & 0.662 & 0 & -29.794 & 33.723 & -124.094 \end{bmatrix} \tag{5.2}$$

Since the rank of the locator matrix is calculated as 6, the part in Figure 5.9 is well-constrained in this case. Similarly, Figure 5.10 shows the full fixture configuration with two spring- and one permanent magnet clamps while Table 5.5 summarizes the corresponding parameters of these clamps.

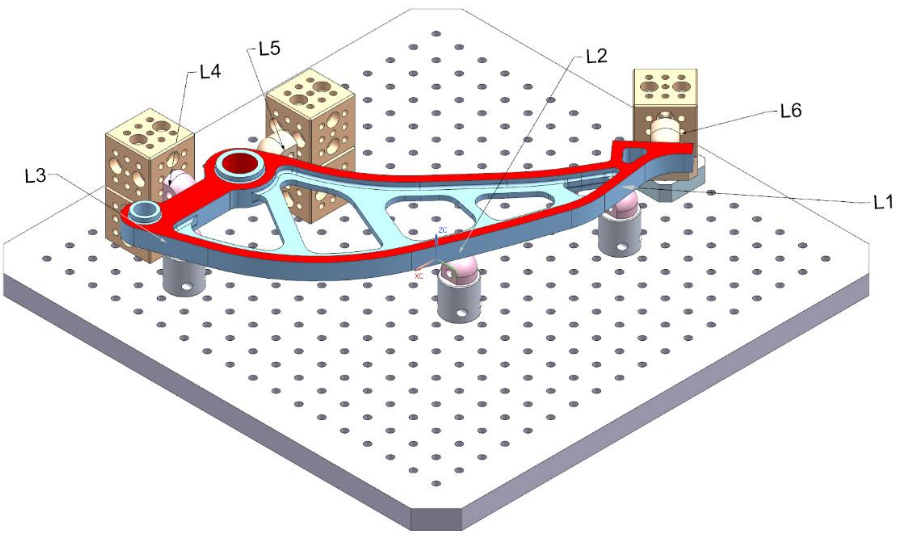

Figure 5.9. Locator Configuration for Part 2

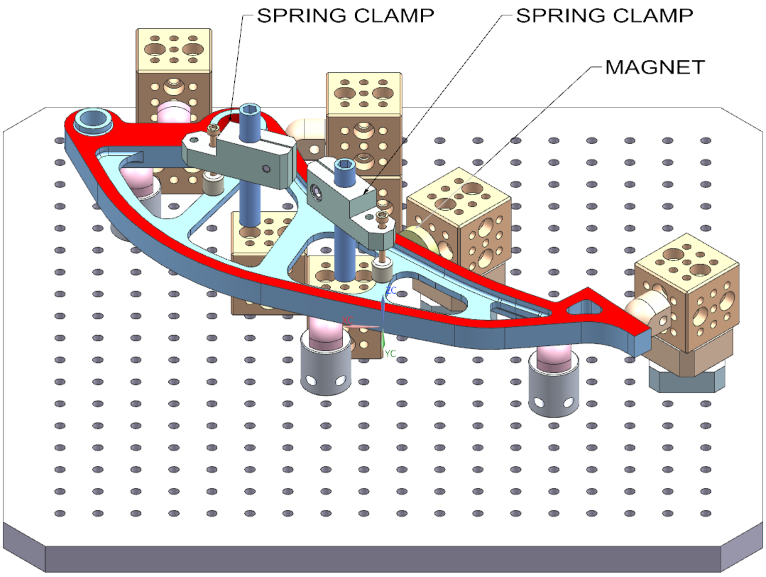

Figure 5.10. Full fixture configuration – Part 2

Table 5.5. Clamping forces on Part 2

Force Application Point	Force Magnitude	Clamping Method
[-14.786 3.213 45.000]	[-120 -120 0]	Magnet
[80.326 -43.714 52.0]	[0 0 -200]	Spring Clamp
[0.315 32.026 52.0]	[0 0 -200]	Spring Clamp

As a cross-check, the locator reaction forces and the corresponding elastic deformations of the locator pins under the action of clamping forces are again computed to see that all locators are properly biased. Table 5.6 tabulates these results. As can be seen, the locator force and their normal vectors are collinear. Thus, the workpiece is properly in contact with all the locators.

Table 5.6. Locator Forces and Radius of Curvatures – Part 2

Locator #	F_x [N]	F_y [N]	F_z [N]	Locator's Radius of Curvature [mm]
1	0	0	99.6	9.9986
2	0	0	130.8	9.9981
3	0	0	179.5	9.9974
4	0	35.6	0	9.9995
5	51.9	24.2	0	9.9992
6	68.0	60.1	0	9.9987

5.2.2. Error Simulation – Part 2

Using the data in Table 5.4 and Table 5.5, a Monte-Carlo simulation is conducted to evaluate the machining quality. Since the material of Part 2 is AL6063, the magnitude of the tool force in light machining of this material is approximated as 15 [N] using the model in Appendix A. The results of the simulation for functional surfaces B1 and B2 are presented in Figure 5.11 and Figure 5.12. As can be seen from these figures, the maximum deviation on both surfaces due to the presence of the machining forces is less than 4.5 μm. Consequently, the support provided by the fixture can be presumed to be acceptable.

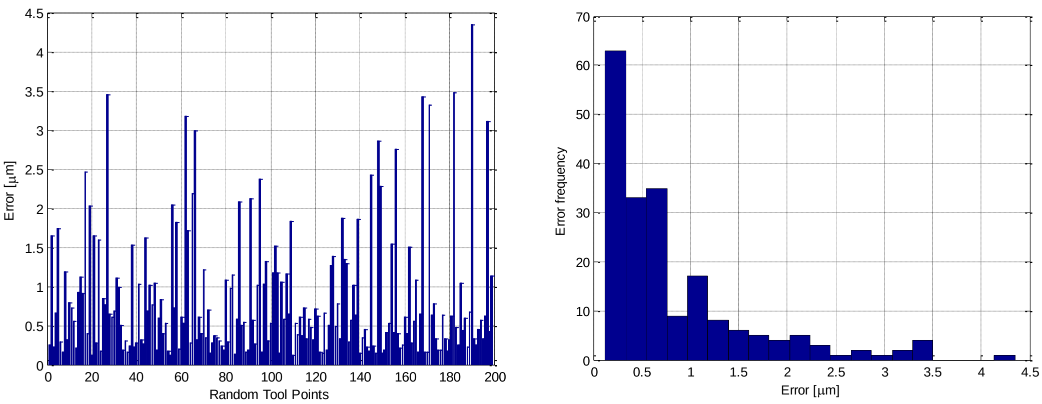

(a) Probable Machining Error **(b)** Error Frequency Chart

Figure 5.11. Simulation Results for Surface B1 - Part 2

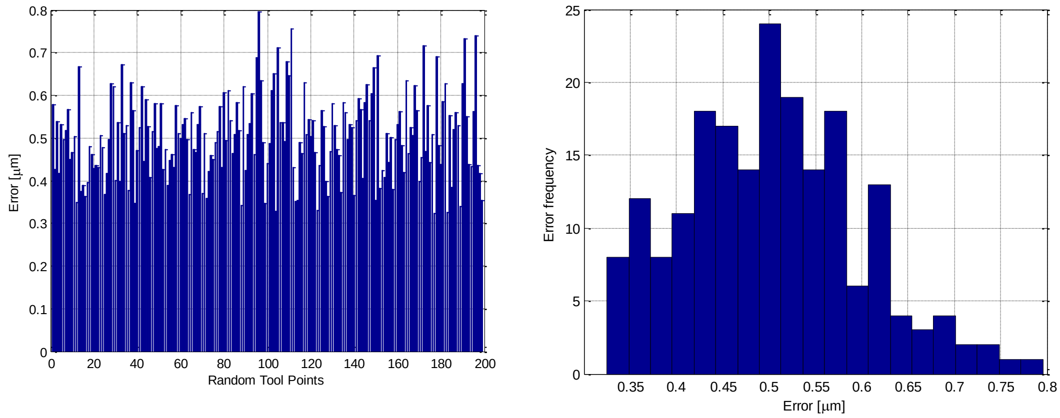

(a) Probable Machining Error **(b)** Error Frequency Chart

Figure 5.12. Simulation Results for Surface B2 - Part 2

5.3. Part 3 – Suspension Fork

Suspension Fork, shown in Figure 5.13, is a part from automotive industry. The element is assumed to be made out of AISI 4140 and is to be manufactured by forging method. Hence, the surfaces C1 and C2 (shown in red color) is to be face-milled with the utilization of the proposed fixture.

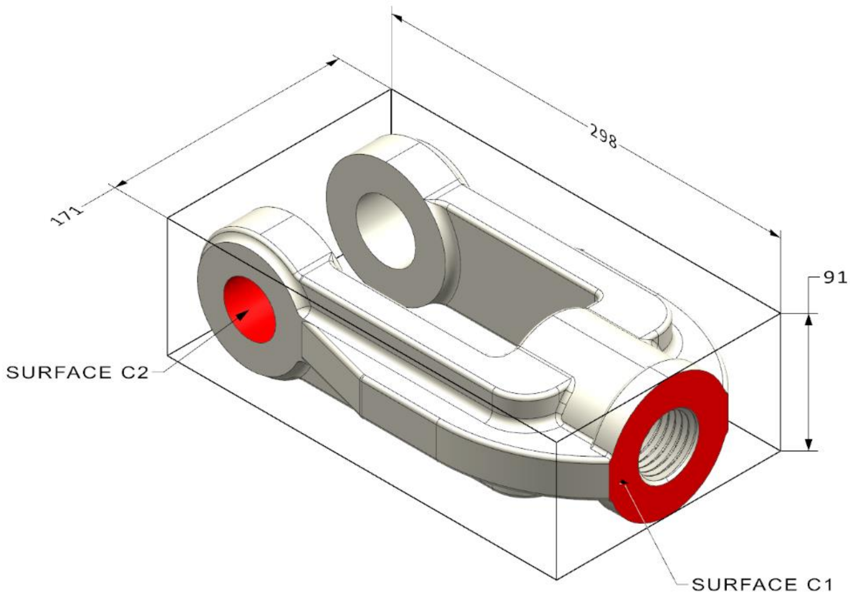

Figure 5.13. Suspension Fork

5.3.1. Locating Status Analysis – Part 3

Locator configuration for Part 3 is shown in Figure 5.14. As can be seen from this figure, the workpiece is restrained with 6 locators. The normal vectors and the contact points are given in Table 5.7.

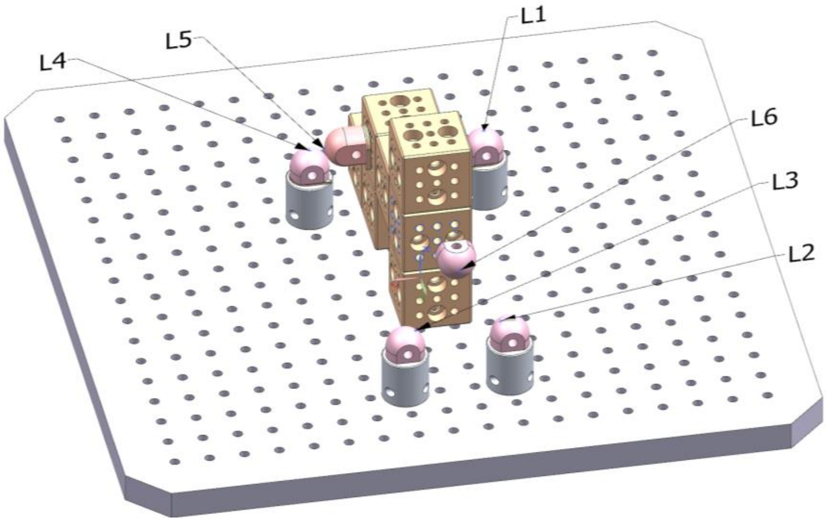

Figure 5.14. Locator Configuration – without Part 3

Table 5.7. Normal vector and Position of each contact point – Part 3

Locator # I	**normal vector** $[a_i \quad b_i \quad c_i]$	**position of each contact point** $[x_i \quad y_i \quad z]$
1	$[0 \quad 0 \quad 1.000]$	$[-45.000 \quad -63.000 \quad 41.157]$
2	$[0.510 \quad 0 \quad 0.859]$	$[-21.892 \quad 99.000 \quad 38.597]$
3	$[-0.510 \quad 0 \quad 0.859]$	$[21.892 \quad 99.000 \quad 38.597]$
4	$[0 \quad 0 \quad 1.000]$	$[45.000 \quad -63.000 \quad 41.157]$
5	$[1.000 \quad 0 \quad 0]$	$[40.713 \quad -45.000 \quad 54.000]$
6	$[0 \quad 1.000 \quad 0]$	$[-9.000 \quad 60.000 \quad 45.000]$

Using the data in Table 5.7, the locating matrix in Eqn. (4.2) can be expressed as follows:

$$W_L = \begin{bmatrix} 0 & 0 & 1.000 & -63.000 & 45.000 & 0 \\ 0.510 & 0 & 0.859 & 85.112 & 38.535 & -50.561 \\ -0.510 & 0 & 0.859 & 85.112 & -38.535 & 50.561 \\ 0 & 0 & 1.000 & -63.000 & -45.000 & 0 \\ 1.000 & 0 & 0 & 0 & 54.000 & 45.000 \\ 0 & 1.000 & 0 & 45.000 & 0 & -9.000 \end{bmatrix} \quad (5.3)$$

Notice that the rank of this locator matrix is again 6 and that the part in Figure 5.15 is well-constrained. Figure 5.16 illustrates the whole fixture configuration with one spring- and two permanent magnet clamps in place. Table 5.8 tabulates the corresponding parameters of the clamps.

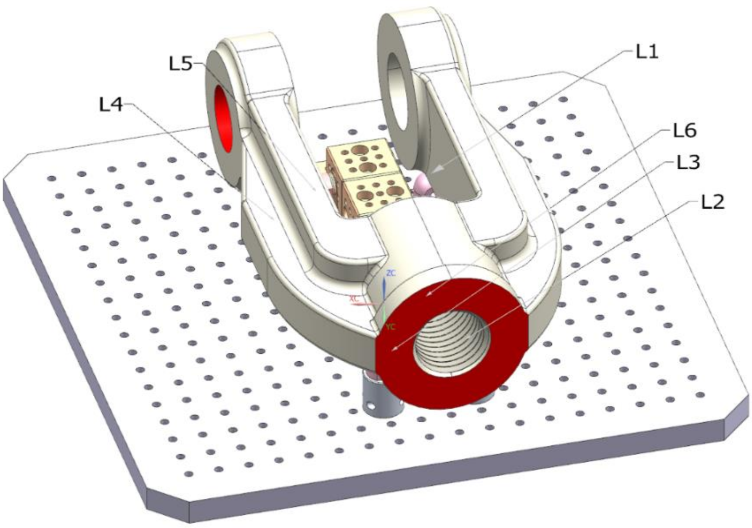

Figure 5.15. Locator Configuration for Part 3

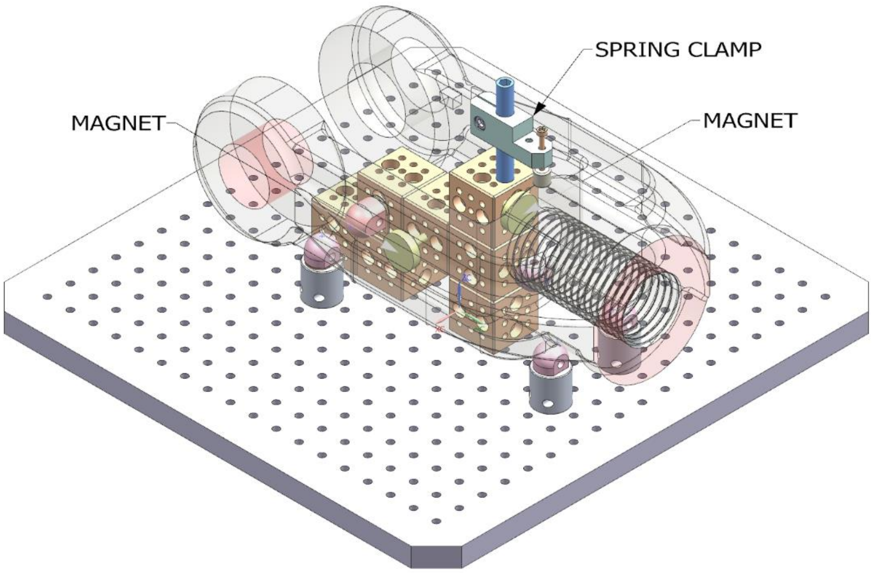

Figure 5.16. Full fixture configuration – Part 3

Table 5.8. Clamping forces on Part 3

Force Application Point	Force Magnitude	Clamping Method
[0 65.034 119.500]	[0 0 -200]	Spring Clamp
[9.000 59.0 99.000]	[0 -100 0]	Magnet
[39.000 -9.000 54.000]	[-100 0 0]	Magnet

To double-check the contact condition, the locator reaction forces and the resulting elastic deformations of the locator (under the action of clamping forces) are again calculated to check whether all locators are adequately preloaded. Table 5.9 summarizes these results. As can be understood, the locator force and their normal vectors are collinear. Therefore, the workpiece is properly in contact with all the locators.

Table 5.9. Locator Forces and Radius of Curvatures – Part 3

Locator #	F_x [N]	F_y [N]	F_z [N]	Locator's Radius of Curvature [mm]
1	0	0	61.6	9.9991
2	61.6	0	103.7	9.9983
3	-49.1	0	82.7	9.9986
4	0	0	68.8	9.9990
5	87.5	0	0	9.9988
6	0	99.9	0	9.9986

5.3.2. Error Simulation – Part 3

Utlizing the data in Table 5.7 and Table 5.8, a Monte-Carlo simulation is performed to predict the machining quality. Since the material of Part 3 is AISI 4140 steel, the magnitude of the cutting force in light machining operation is computed (and averaged) as 40 [N] using the model in Appendix A. The results of the simulation for functional surfaces C1 and C2 are shown in Figure 5.17 and Figure 5.18. As can be clearly seen, the maximum deviation on both surfaces due to the prescribed machining forces is less than 3.1 μm. Hence, the support provided by the fixture can be presumed reasonable for all practical purposes.

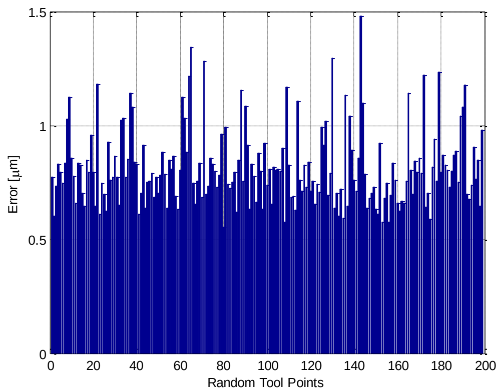

(a) Probable Machining Error

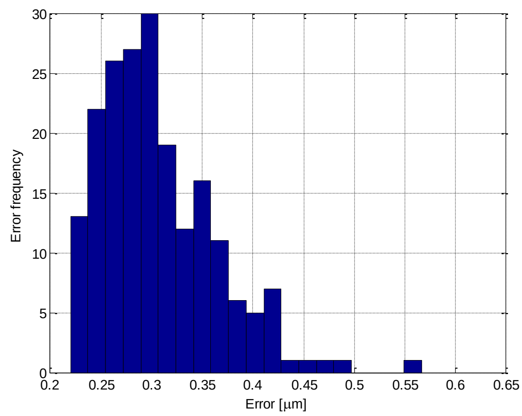

(b) Error Frequency Chart

Figure 5.17. Simulation Results for Surface C1 – Part 3

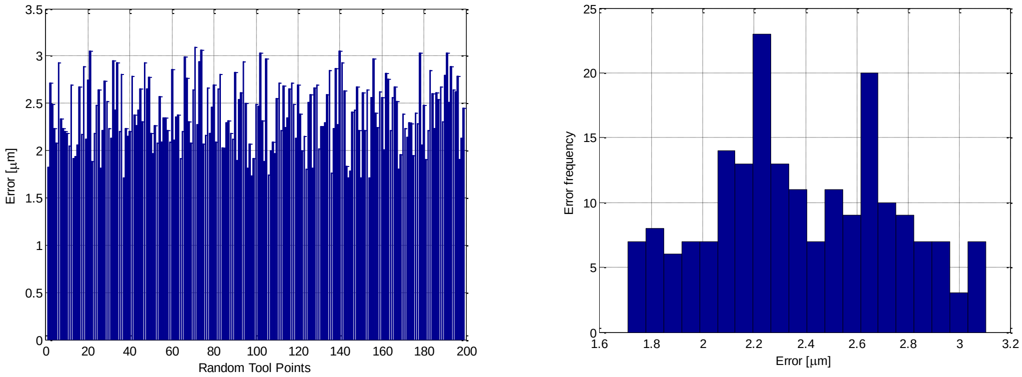

(a) Probable Machining Error **(b)** Error Frequency Chart

Figure 5.18. Simulation Results for Surface C2 – Part 3

5.4. Part 4 - Gearbox Casing

Gearbox Casing, which shown in Figure 5.19, is another part from automotive industry. It protects the gearbox components (i.e. gear shafts, bearings, gears) from external effects. The element is again assumed to be made from grey cast iron (GG-25) and is to be fabricated by sand casting method. Hence, the surfaces D1 and D2 (shown in red color) is to be machined employing Cubefix.

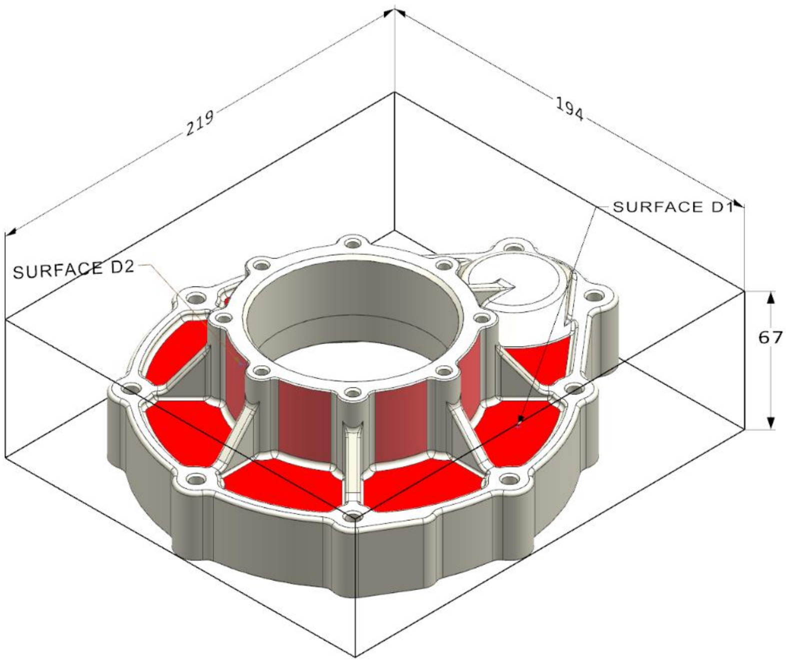

Figure 5.19. Gearbox Casing

5.4.1. Locating Status Analysis – Part 4

Locator configuration for Part 4 is shown in Figure 5.20 where the part is constrained with 6 locators. The normal vectors and the contact points are shown in Table 5.10.

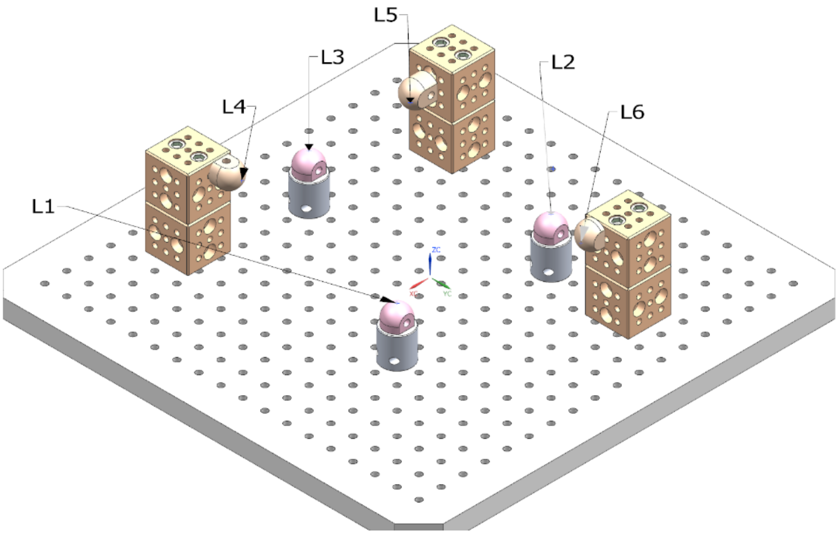

Figure 5.20. Locator Configuration – without Part 4

Table 5.10. Normal vector and Position of each contact point – Part 4

Locator # i	normal vector $[\boldsymbol{a_i} \quad \boldsymbol{b_i} \quad \boldsymbol{c_i}]$	position of each contact point $[\boldsymbol{x_i} \quad \boldsymbol{y_i} \quad \boldsymbol{z}]$
1	$[0 \quad 0 \quad 1.000]$	$[72.000 \quad 45.000 \quad 40.000]$
2	$[0 \quad 0 \quad 1.000]$	$[-54.0 \quad 45.000 \quad 40.000]$
3	$[0 \quad 0 \quad 1.000]$	$[0 \quad -99.000 \quad 40.000]$
4	$[-0.054 \quad 0.998 \quad 0]$	$[71.455 \quad -82.559 \quad 63.000]$
5	$[0.912 \quad 0.409 \quad 0]$	$[-31.5195 \quad -92.0698 \quad 53.000]$
6	$[0.992 \quad 0.125 \quad 0]$	$[-23.020 \quad 100.252 \quad 63.000]$

Using the data in Table 5.10, the locating matrix in Eqn. (4.2) is calculated as

$$W_L = \begin{bmatrix} 0 & 0 & 1.000 & 45.000 & -72.000 & 0 \\ 0 & 0 & 1.000 & 45.000 & 54.000 & 0 \\ 0 & 0 & 1.000 & -99.000 & 0 & 0 \\ -0.054 & 0.998 & 0 & -62.906 & -3.1604 & 66.849 \\ 0.912 & 0.409 & 0 & -21.708 & 48.2163 & 44.881 \\ 0.992 & 0.125 & 0 & -7.887 & 62.2346 & -102.245 \end{bmatrix} \qquad (5.4)$$

Since the rank of the locator matrix is 6, the part in Figure 5.21 is well-constrained. Similarly, Figure 5.22 demonstrates the whole fixture configuration with two screw- and three permanent magnet clamps. Table 5.11 tabulates the relevant parameters of these clamps.

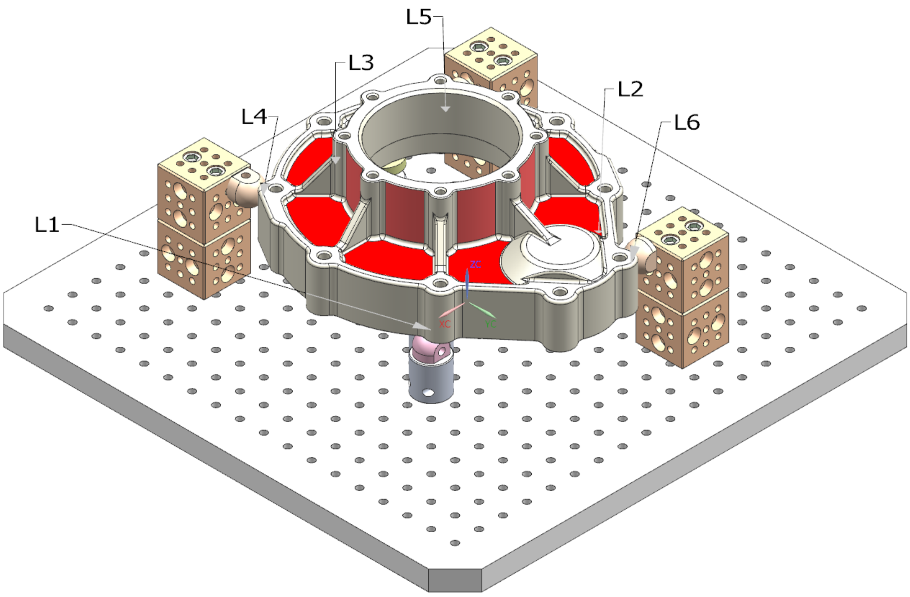

Figure 5.21. Locator Configuration for Part 4

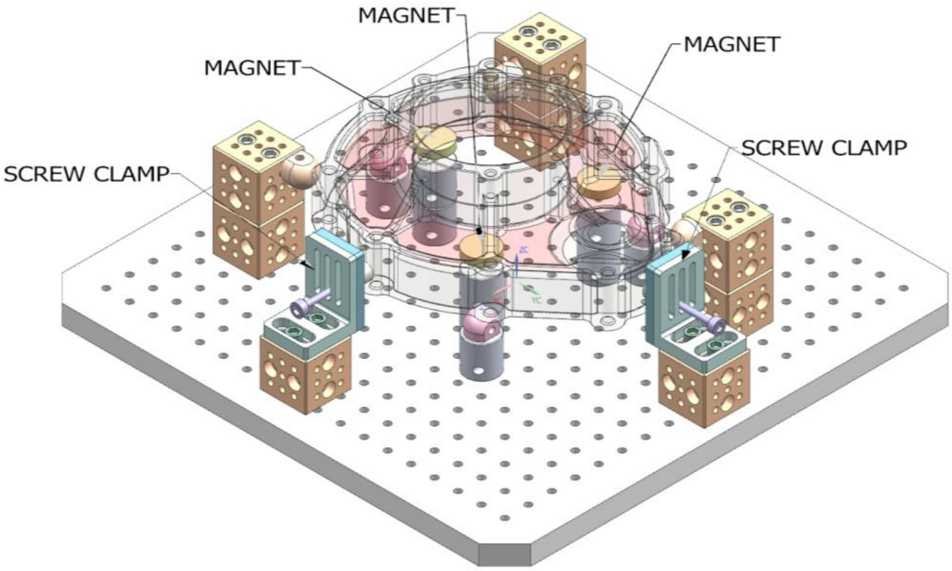

Figure 5.22. Full fixture configuration – Part 4

Table 5.11. Clamping forces on Part 4

Force Application Point	Force Magnitude	Clamping Method
[54.0 27.0 64.0]	[0 0 -100]	Magnet
[-36.0 27.0 64.0]	[0 0 -100]	Magnet
[0.0 -63.0 64.0]	[0 0 -100]	Magnet
[9.0 110.0 54.0]	[0 -100 -0]	Screw Clamp
[106.0 -9.0 54.0]	[-200 0 -0]	Screw Clamp

Table 5.12 specifies the locator reaction forces and the elastic deformations of the locator pins. As expected, the locator force vectors and the normals are found to be collinear. Thus, it can be concluded that the workpiece is properly in contact with all the locators.

Table 5.12. Locator Forces and Radius of Curvatures – Part 4

Locator #	F_x [N]	F_y [N]	F_z [N]	Locator's Radius of Curvature [mm]
1	0	0	115.9	9.9983
2	0	0	101.4	9.9986
3	0	0	92.5	9.9987
4	8.7	154.9	0	9.9977
5	61.8	27.8	0	9.9990
6	148.6	18.0	0	9.9979

5.4.2. Error Simulation – Part 4

With the data in Table 5.10 and Table 5.11, a Monte-Carlo simulation is carried out to predict the resulting machining quality. Since the material of Part 4 is grey cast iron, the magnitude of the tool force in light machining of this material is approximated as 25 [N] using the model in Appendix A. The simulation results for the surfaces D1 and D2 are shown in Figure 5.23 and Figure 5.24. It is obvious from these figures that the maximum deviation on both surfaces is less than 1.7 μm. Hence, the support provided by the fixture can be presumed to be satisfactory.

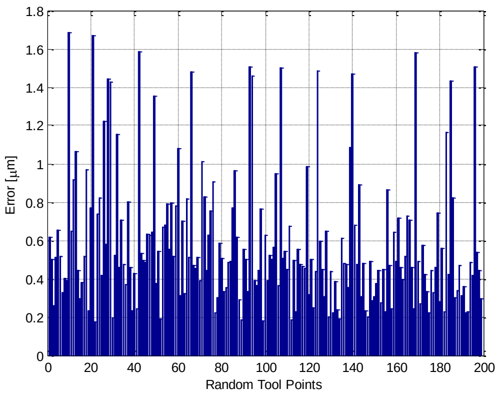

(a) Probable Machining Error

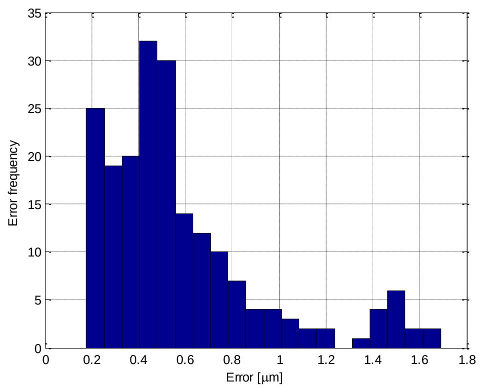

(b) Error Frequency Chart

Figure 5.23. Simulation Results for Surface D1 - Part 4

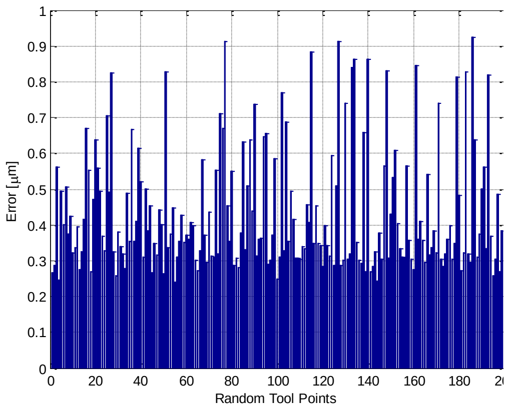

(a) Probable Machining Error

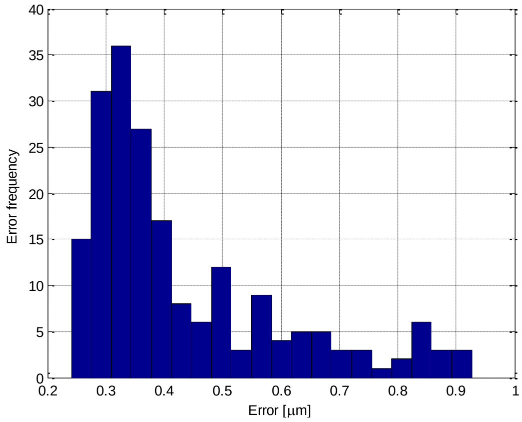

(b) Error Frequency Chart

Figure 5.24. Simulation Results for Surface D2 - Part 4

5.5. Part 5 – Throttle body

Throttle Body, a part from automotive industry, is shown in Figure 5.25. This cast component, which houses the throttle valve (regulating the air intake of an internal combustion engine), is assumed to be made out of G-AlMg5 aluminum. It is further presumed that the rough machining operations have already been completed and that finish machining is to be performed on the surfaces E1 and E2 (as shown in red color).

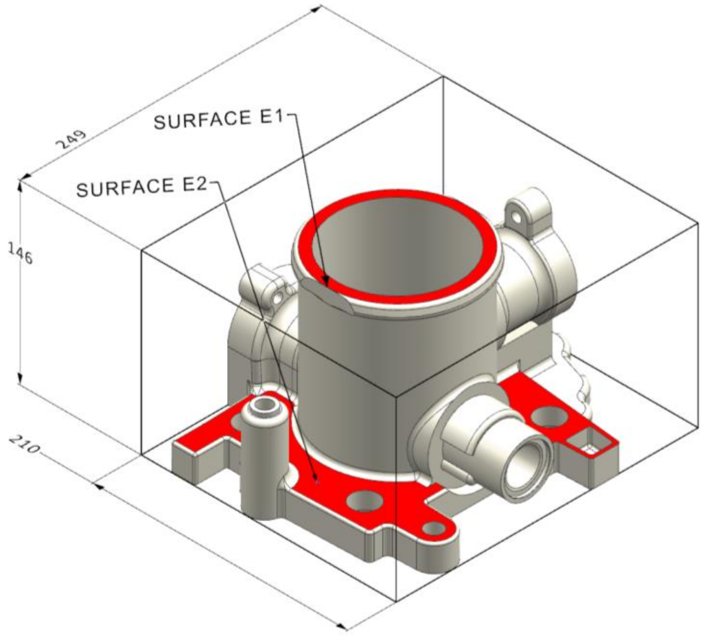

Figure 5.25. Throttle Body

5.5.1. Locating Status Analysis – Part 5

Locator configuration for Part 5 is shown in Figure 5.26. As can be seen, the workpiece is constrained with 6 locators. The normal vectors and the contact points are presented in Table 5.13.

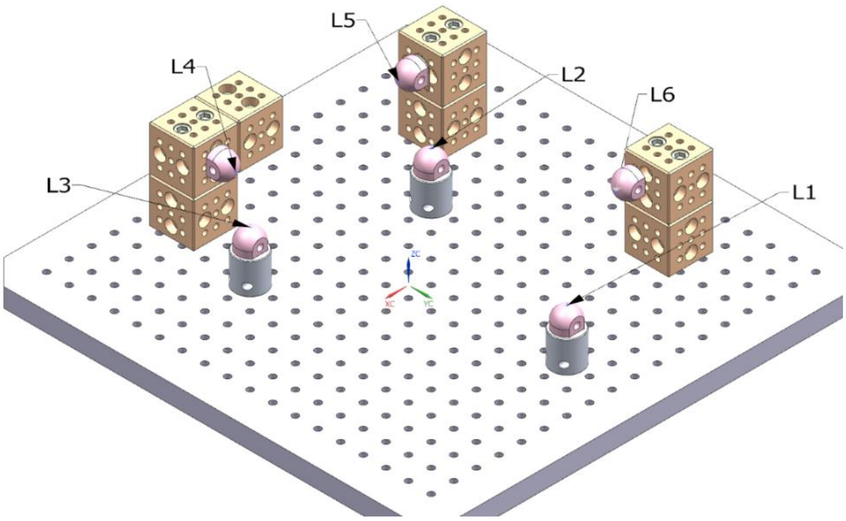

Figure 5.26. Locator Configuration – without Part 5

Table 5.13. Normal vector and Position of each contact point – Part 5

Locator # i	normal vector $[a_i \quad b_i \quad c_i]$	position of each contact point $[x_i \quad y_i \quad z]$
1	$[0 \quad 0 \quad 1.000]$	$[-9.000 \quad 117.000 \quad 40.000]$
2	$[0 \quad 0 \quad 1.000]$	$[-63.000 \quad -45.000 \quad 40.000]$
3	$[0 \quad 0 \quad 1.000]$	$[63.000 \quad -63.000 \quad 40.000]$
4	$[-0.034 \quad 0.999 \quad 0]$	$[44.651 \quad -93.006 \quad 54.000]$
5	$[1.000 \quad 0 \quad 0]$	$[-82.313 \quad -90.000 \quad 54.000]$
6	$[1.000 \quad 0 \quad 0]$	$[-93.000 \quad 72.000 \quad 54.000]$

Using the data in Table 5.13, the locating matrix in Eqn. (4.2) can be formed as

$$W_L = \begin{bmatrix} 0 & 0 & 1.000 & 117.000 & 9.000 & 0 \\ 0 & 0 & 1.000 & -45.000 & 63.000 & 0 \\ 0 & 0 & 1.000 & -63.000 & -63.000 & 0 \\ -0.034 & 0.999 & 0 & -53.967 & -1.884 & 41.377 \\ 1 & 0 & 0 & 0 & 54.000 & 90.000 \\ 1 & 0 & 0 & 0 & 54.000 & -72.000 \end{bmatrix} \tag{5.5}$$

Note that since the rank of the locator matrix is calculated as 6, the part in Figure 5.27 is again well-constrained in this case. Likewise, Figure 5.28 illustrates the complete fixture configuration with one screw- and four permanent magnet clamps in place. Table 5.14 summarizes the corresponding parameters for these clamps.

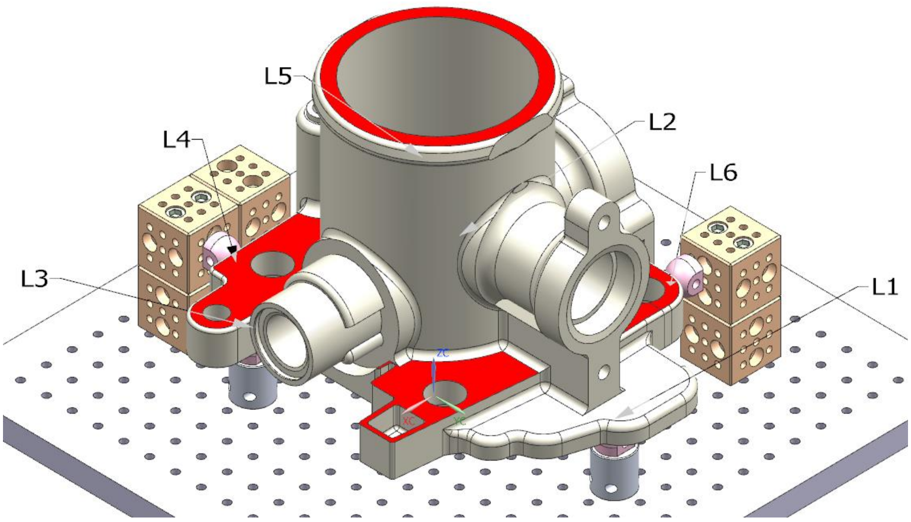

Figure 5.27. Locator Configuration for Part 5

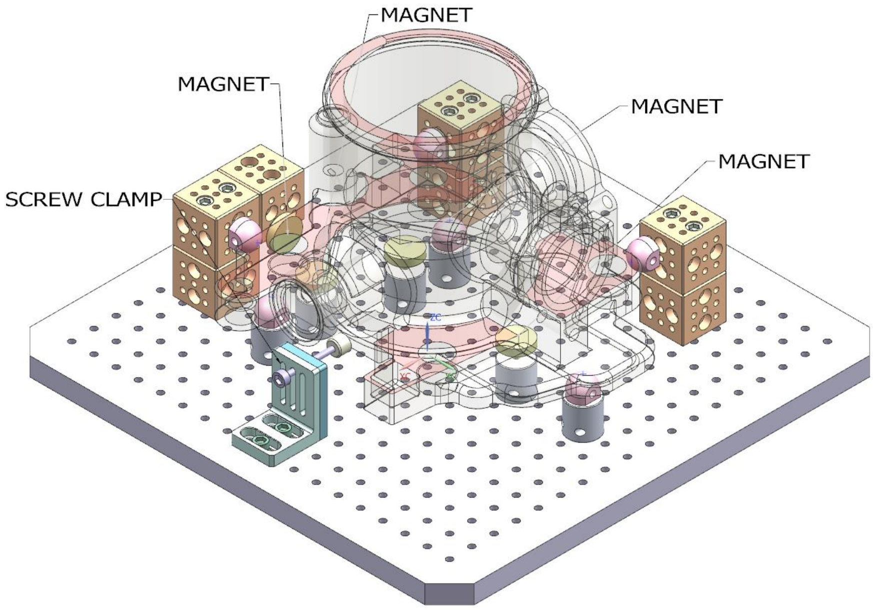

Figure 5.28. Full fixture configuration – Part 5

Table 5.14. Clamping forces on Part 5

Force Application Point	Force Magnitude	Clamping Method
[-9.0 63.0 39.0]	[0 0 -100]	Magnet
[-27.0 -45.0 39.0]	[0 0 -100]	Magnet
[-27.0 -63.0 39.0]	[0 0 -100]	Magnet
[18.0 -95.0 45.0]	[0 -100 0]	Magnet
[66.5 0 41.6]	[-100 0 0]	Screw Clamp

To check the contact condition, the locator reaction forces and the resulting elastic deformations of the locator (under the action of clamping forces) are again calculated to see whether all locators are adequately preloaded. Table 5.15 summarizes these results. As can be seen, the locator force- and the normal vectors are collinear. Thus, the workpiece is properly in contact with all the locators.

Table 5.15. Locator Forces and Radius of Curvatures – Part 5

Locator #	F_x [N]	F_y [N]	F_z [N]	Locator's Radius of Curvature [mm]
1	0	0	81.9	9.9988
2	0	0	161.4	9.9977
3	0	0	88.6	9.9987
4	-3.5	99.9	0	9.9986
5	31.5	0	0	9.9995
6	71..9	0	0	9.9990

5.5.2. Error Simulation – Part 5

Using the data in Table 5.13 and Table 5.14, a Monte-Carlo simulation is conducted to assess the machining quality achievable. Since the material of Part 5 is G-AlMg5 Cast Aluminum, the magnitude of the tool force while light machining of this material is computed (and averaged) as 15 [N] using the model in Appendix A. The results of the simulation for the functional surfaces E1 and E2 are shown in Figure 5.29 and Figure 5.30. As can be seen, the maximum deviation on both surfaces due to the prescribed machining forces is less than 1.0 μm. Hence, the support provided by the fixture can be assumed satisfactory for all intents and purposes.

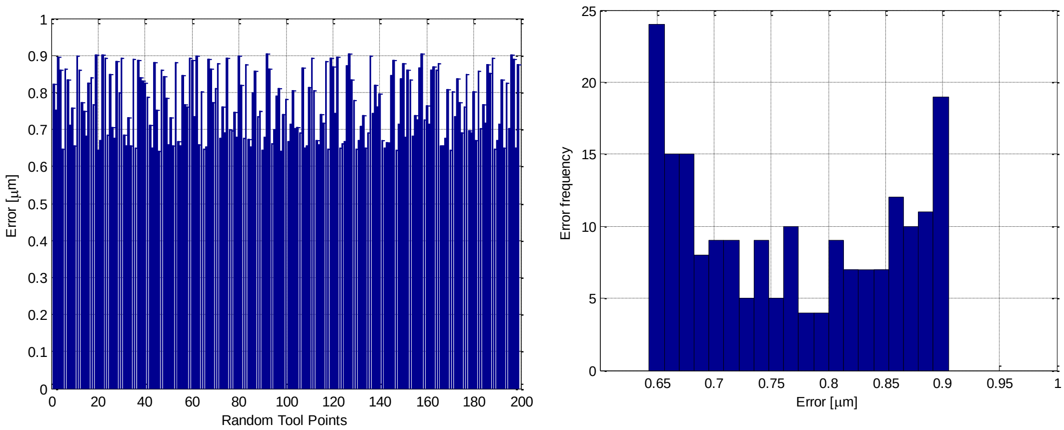

(a) Probable Machining Error **(b)** Error Frequency Chart

Figure 5.29. Simulation Results for Surface E1 - Part 5

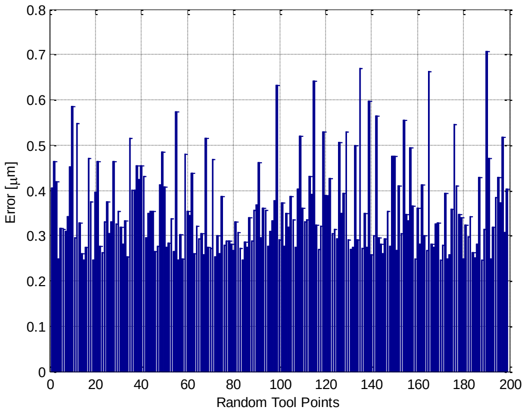

(a) Probable Machining Error

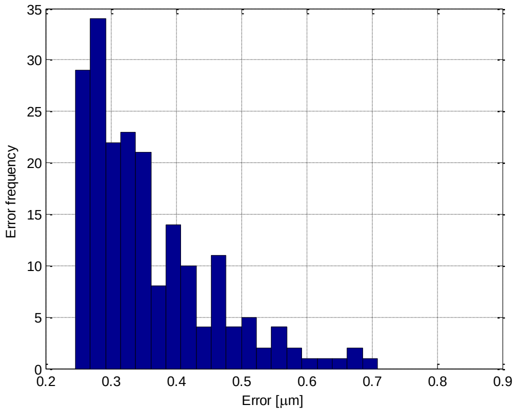

(b) Error Frequency Chart

Figure 5.30. Simulation Results for Surface E2 - Part 5

5.6. Part 6 – Target Piece

Target piece, which is shown in Figure 5.31, is designed specifically to evaluate the performance of the developed fixture system in the scope of thesis. The component, which is to serve as a support base for precision instruments, is used as a test part in experimental studies elaborated in Chapter 6. It is to be made out of Al 6063-T6. All surfaces are to be machined to a finish with the proposed fixture system except for the datum planes D (bottom), E (front), and F (side) that are expected to be in contact with the locators.

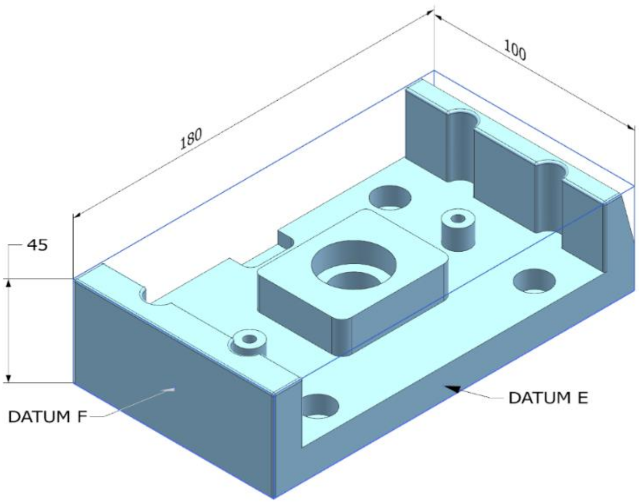

Figure 5.31. Target Piece

5.6.1. Locating Status Analysis – Part 6

Locator configuration for Part 6 is shown in Figure 5.32. As can be seen from this figure, the workpiece is constrained with 6 locators. The normal vectors and the contact points are given in Table 5.16.

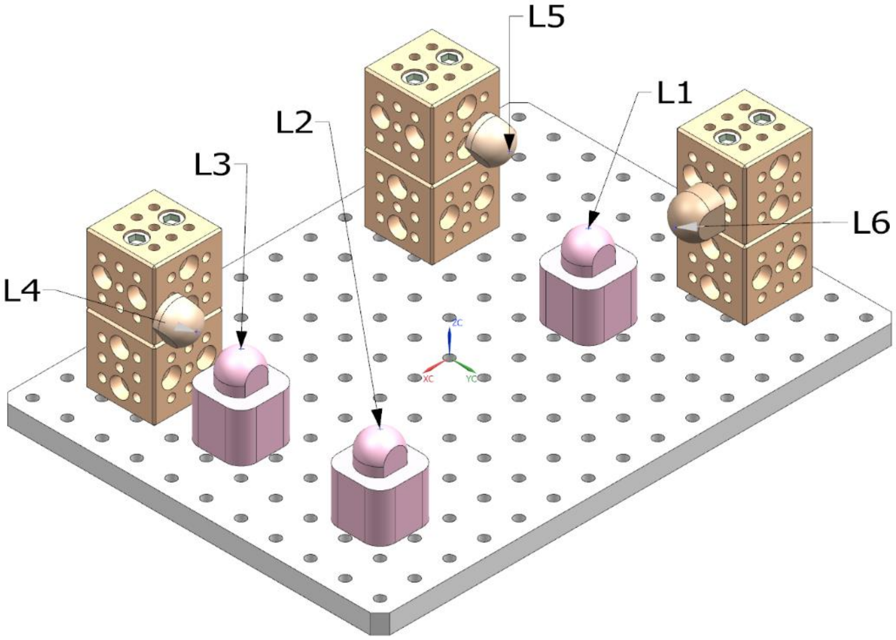

Figure 5.32. Locator Configuration – without Part 6

Table 5.16. Normal vector and Position of each contact point – Part 6

Locator # i	**normal vector** $[\boldsymbol{a_i} \quad \boldsymbol{b_i} \quad \boldsymbol{c_i}]$	**position of each contact point** $[\boldsymbol{x_i} \quad \boldsymbol{y_i} \quad \boldsymbol{z}]$
1	$[0 \quad 0 \quad 1]$	$[-54.000 \quad 18.000 \quad 40.000]$
2	$[0 \quad 0 \quad 1]$	$[90.000 \quad 54.000 \quad 40.000]$
3	$[0 \quad 0 \quad 1]$	$[90.000 \quad -18.000 \quad 40.000]$
4	$[0 \quad 1 \quad 0]$	$[99.000 \quad -32.000 \quad 45.000]$
5	$[0 \quad 1 \quad 0]$	$[-63.000 \quad -32.000 \quad 45.000]$
6	$[1 \quad 0 \quad 0]$	$[-72.000 \quad 45.000 \quad 45.000]$

With the data in Table 5.16, the locating matrix in Eqn. (4.2) can be expressed as

$$W_L = \begin{bmatrix} 0 & 0 & 1 & 18.0 & 54.0 & 0 \\ 0 & 0 & 1 & 54.0 & -90.0 & 0 \\ 0 & 0 & 1 & -18.0 & -90.0 & 0 \\ 0 & 1 & 0 & -45.0 & 0 & 99 \\ 0 & 1 & 0 & -45.0 & 0 & -63 \\ 1 & 0 & 0 & 0.0 & 45 & -45 \end{bmatrix} \tag{5.6}$$

The rank of the locator matrix is 6 and thus the part in Figure 5.33 is well-constrained in this case. Similarly, Figure 5.34 illustrates the overall fixture configuration with four permanent magnet clamps. Table 5.17 tabulates the relevant parameters of these clamps.

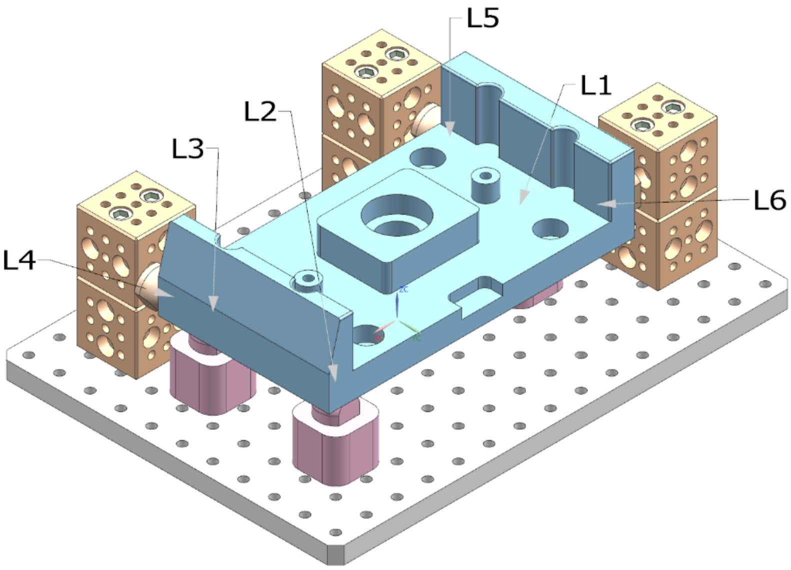

Figure 5.33. Locator Configuration for Part 6

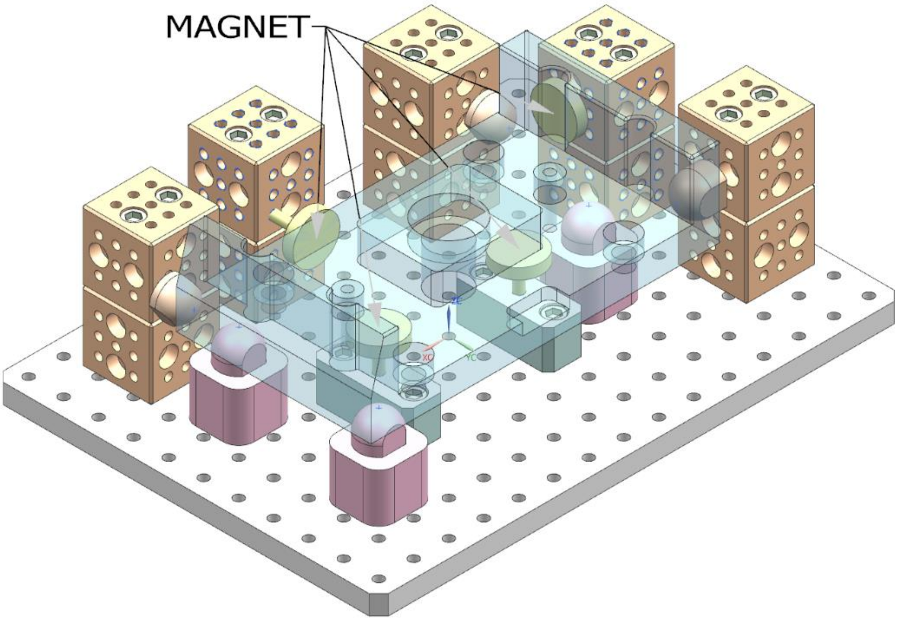

Figure 5.34. Full fixture configuration – Part 6

Table 5.17. Clamping forces on Part 6

Force Application Point	Force Magnitude	Clamping Method
[-18.000 18.000 40.000]	[0 0 -100]	Magnet
[54.000 18.000 40.000]	[0 0 -100]	Magnet
[36.000 -32.000 45.000]	[0 -100 0]	Magnet
[-72.000 -18.000 54.000]	[-100 0 0]	Magnet

To cross-check the contact condition, the locator reaction forces and the accompanying elastic deformations of the locator (under the action of clamping forces) are again computed to perceive whether all locators are adequately loaded. Table 5.18 summarizes these results. As can be seen, the locator force- and the normal vectors are once again collinear. Consequently, the workpiece is properly in contact with all the locators.

Table 5.18. Locator Forces and Radius of Curvatures – Part 6

Locator #	F_x [N]	F_y [N]	F_z [N]	Locator's Radius of Curvature [mm]
1	0	0	105.136	9.9985
2	0	0	52.398	9.9993
3	0	0	52.444	9.9993
4	0	84.436	0	9.9988
5	0	15.541	0	9.9998
6	99.999	0	0	9.9991

5.6.2. Error Simulation – Part 6

With the utilization of the data in Table 5.16 and Table 5.17, a Monte-Carlo simulation is performed to evaluate the machining quality attainable. Since the material of Part 1 is Al 6063, the magnitude of the cutting force in light machining of this material is determined as 15 [N] using the model in Appendix A. The simulation results containing all the functional surfaces are presented in Figure 5.35. As can be seen, the maximum deviation on all surfaces due to the prescribed machining forces is less than 1.4 μm. Hence, one can infer that the support of the fixture is quite satisfactory for all practical purposes.

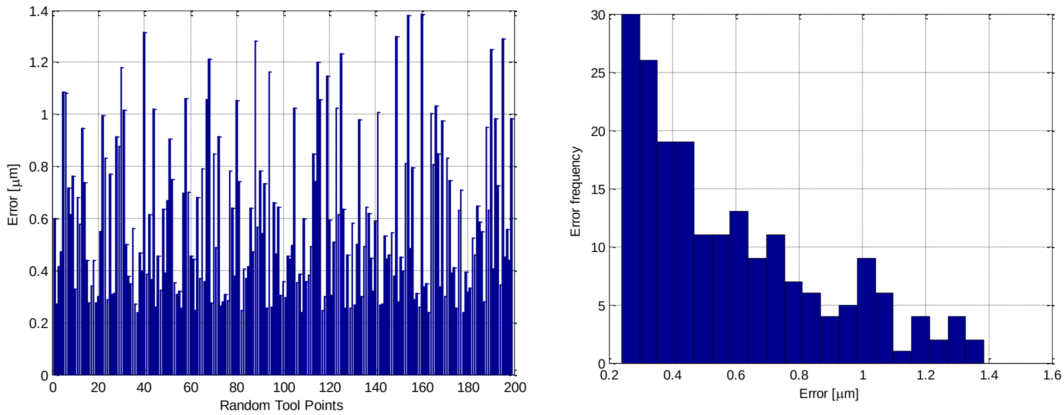

(a) Probable Machining Error **(b)** Error Frequency Chart

Figure 5.35. Simulation Results for Part 6

5.7. Under-Constrained & Over-Constrained Cases

All the parts considered so far are found to be well-constrained owing to the fact that the accompanying fixtures are specifically configured (or designed) to yield such constraining states via some trial-and-error. This section takes into consideration of under-constrained- and over-constrained cases using Part 6 as the example.

5.7.1. Under-Constrained Case

Figure 5.36 and Figure 5.37 illustrate an under-constrained ("text-book") case where Locators 1, 2, and 3 are in line. The normal vectors and contact points of the locators are shown in Table 5.19.

.

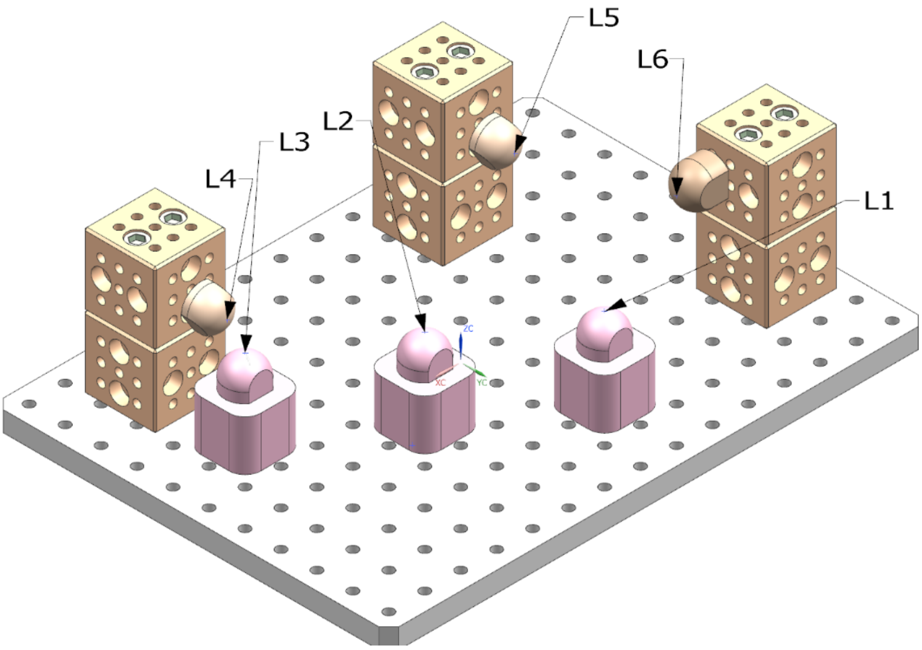

Figure 5.36.Locator configuration for under-constrained case

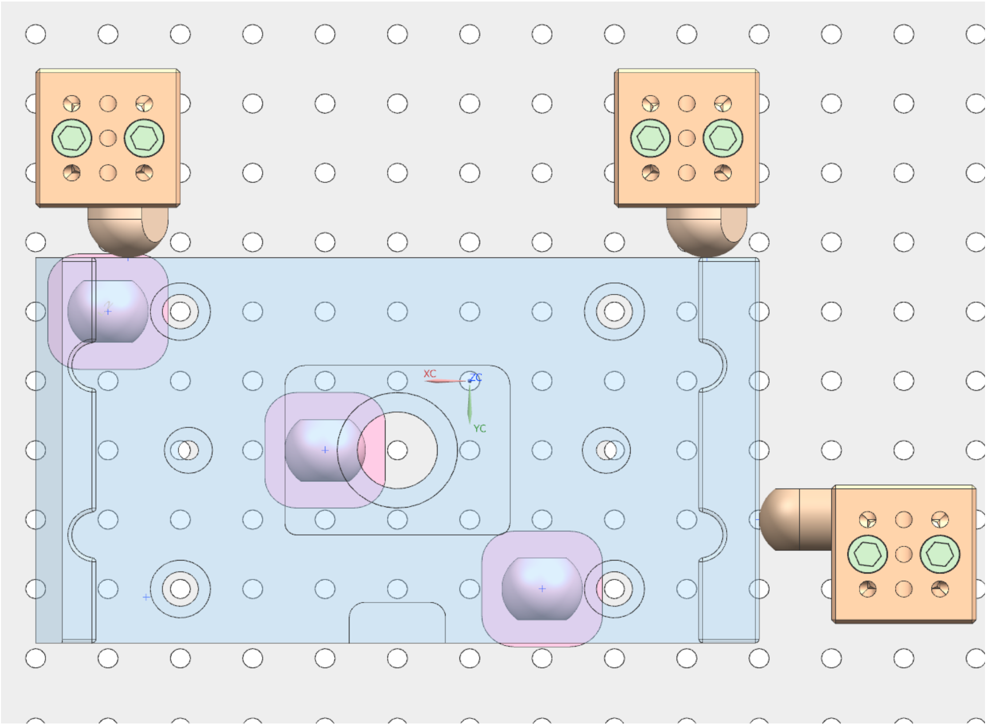

Figure 5.37. Under-Constraint locator configuration for Part 6 - Top view

Table 5.19. Normal vector and Position of contact point for under-constraint case

Locator # **i**	**normal vector** $[\boldsymbol{a_i} \quad \boldsymbol{b_i} \quad \boldsymbol{c_i}]$	**position of each contact point** $[\boldsymbol{x_i} \quad \boldsymbol{y_i} \quad \boldsymbol{z}]$
1	$[0 \quad 0 \quad 1]$	$[-18.0 \quad 54.0 \quad 40.0]$
2	$[0 \quad 0 \quad 1]$	$[36.0 \quad 18.0 \quad 40.0]$
3	$[0 \quad 0 \quad 1]$	$[90.0 \quad -18.0 \quad 40.0]$
4	$[0 \quad 1 \quad 0]$	$[85.0 \quad -32.0 \quad 45.0]$
5	$[0 \quad 1 \quad 0]$	$[-59.0 \quad -32.0 \quad 45.0]$
6	$[1 \quad 0 \quad 0]$	$[-72.0 \quad 36.0 \quad 54.0]$

With the data in Table 5.19, the locating matrix in Eqn. (4.2) can be formed as

$$
W_L = \begin{bmatrix} 0 & 0 & 1 & 54.0 & 18.0 & 40.0 \\ 0 & 0 & 1 & 18.0 & -36.0 & 0 \\ 0 & 0 & 1 & -18.0 & -90.0 & 0 \\ 0 & 1 & 0 & -45.0 & 0 & 85.0 \\ 0 & 1 & 0 & -45.0 & 0 & -59.0 \\ 1 & 0 & 0 & 0 & 54.0 & -36.0 \end{bmatrix} \tag{5.7}
$$

This time, the rank of the locator matrix is found as 5. Consequently, one of the locators at the bottom must be moved to a *unique* position where it is not aligned with the remaining locators.

5.7.2. Over-Constrained Case

As for the case, there are 4 locators at the bottom of the part as shown in Figure 5.38. Top view of the locator configuration is illustrated in Figure 5.39. The normal vector and position vector for each contact point is given in the Table 5.20.

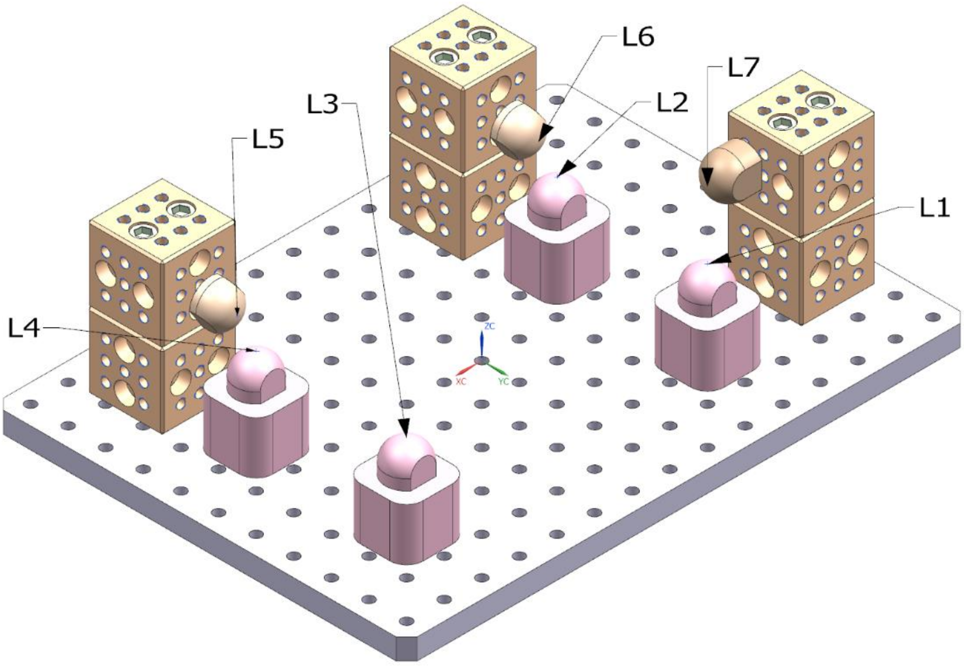

Figure 5.38. Locator configuration for over-constrained case

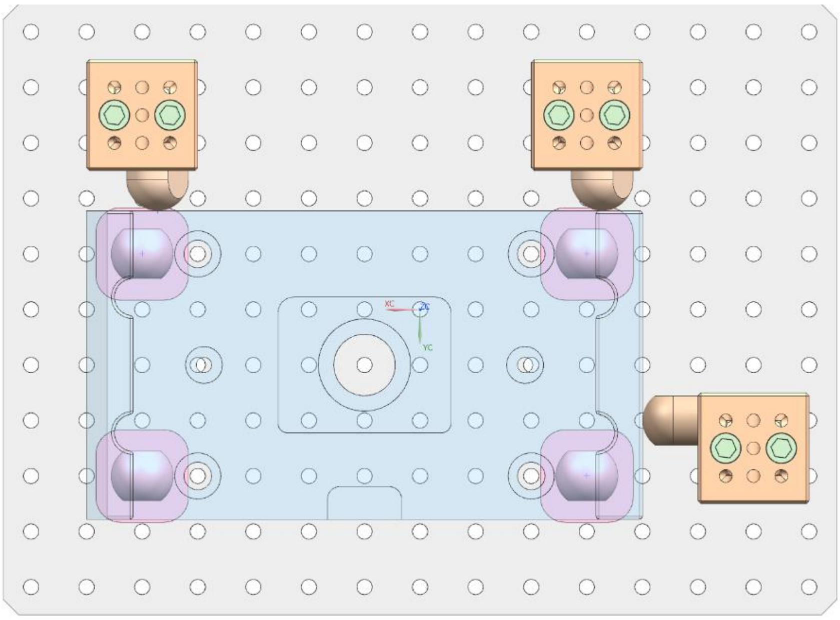

Figure 5.39. Over-Constrained locator configuration for Part 6 – Top view

Table 5.20. Normal vector and Position of contact point for over-constrained case

Locator # **i**	**normal vector** $[a_i \quad b_i \quad c_i]$	**position of each contact point** $[x_i \quad y_i \quad z]$
1	$[0 \quad 0 \quad 1]$	$[-54.0 \quad -54.0 \quad 40.0]$
2	$[0 \quad 0 \quad 1]$	$[-54.0 \quad -18.0 \quad 40.0]$
3	$[0 \quad 0 \quad 1]$	$[\ 90.0 \quad 54.0 \quad 40.0]$
4	$[0 \quad 0 \quad 1]$	$[\ 90.0 \quad -18.0 \quad 40.0]$
5	$[0 \quad 1 \quad 0]$	$[\ 85.0 \quad -32.0 \quad 45.0]$
6	$[0 \quad 1 \quad 0]$	$[-59.0 \quad -32.0 \quad 45.0]$
7	$[1 \quad 0 \quad 0]$	$[-72.0 \quad 36.0 \quad 54.0]$

Using the data in Table 5.20, the locating matrix in Eqn. (4.2) becomes

$$W_L = \begin{bmatrix} 0 & 0 & 1 & -45.0 & 63 & 0 \\ 0 & 0 & 1 & 27.0 & 63 & 0 \\ 0 & 0 & 1 & 27.0 & -81 & 0 \\ 0 & 0 & 1 & -45.0 & -81 & 0 \\ 0 & 1 & 0 & -45.0 & 0 & 76.0 \\ 0 & 1 & 0 & -45.0 & 0 & -68.0 \\ 1 & 0 & 0 & 0 & 54 & -9.0 \end{bmatrix} \tag{5.8}$$

The rank of locating matrix is 6 while the number of locators contacting with workpiece is 7. Hence, according to Table 4.1, the part is over-constrained. Notice that the rank of the locating matrix will be still 6 even after one of the locators at the bottom is removed. Consequently, the part will become well-constrained under that circumstance.

It is critical to notice that (as mentioned in Chapter 4), even though the workpiece is found to be well-constrained, the locators might still lose contact under the action of the cutting forces. This is especially true when the clamping forces are insufficient. Hence, the workpiece will eventually become under-constrained. As a rule of thumb, each- and every clamp must exert a force greater (at least two folds) than the magnitude of the largest (resultant) cutting force in machining operations. However, this condition alone does not guarantee the static equilibrium of workpiece at all times (even though the magnitude of the cutting force is less than those of the clamps) since moments created by the cutting force components might reduce some of the locator reaction forces to zero. Consequently, to assure that all locators are in contact with the workpiece, the static equilibrium must be succinctly checked under the worst machining scenario. In Appendix C, the relevant Matlab programs developed to this end are presented.

5.8. Closure

In this section, six different workpieces, which are mostly adapted from automotive industry, are introduced. These dissimilar parts include Exhaust Manifold, Robot Gripper Arm, Suspension Fork, Gearbox Casing, Throttle Body, and Support Base. Constraint analysis as well as machining error analysis on different surfaces of the parts are performed. This section essentially shows that all of these parts could be successfully attached on the table of a machining center using the modular fixture elements elaborated in Chapter 3.

CHAPTER 6

EXPERIMENTAL STUDIES

In this section, the performance of the proposed modular fixture is to be evaluated through a number of machining tests. Furthermore, the repeatability of the fixture is assessed by checking the position of the workpiece in five successive loading/unloading attempts. The details of the experimental study will follow.

6.1. Manufacturing Experiments

Using the modular fixture elaborated in the previous chapter, the target piece (Part 6) which is explained in the previous chapter, is to be machined. Due to the topology of the functional surfaces on this test part; magnetic clamps, which could be placed in close proximity to the locators (side by side), are required to avoid interference with the cutting tool. Unfortunately, since the test piece is made out of a non-ferrous metal (Al-6063-T6), a number of steel plates must be attached onto the workpiece to generate the desired clamping (i.e. reluctance) force. To investigate the effect of magnetic clamping forces comparatively, three test pieces (titled A, B, C) are manufactured. Note that as the main variable in this setup, the magnetic clamping forces are changed by adjusting the distance between the permanent magnet and the steel plate. The following sections elaborate the experiments.

6.1.1. Test-Piece Preparation

In this study, roughing operations of all parts are to be performed using a conventional mechanical vise in case the *prototype* fixture fails to secure the part under the action of relatively large machining forces. Figure 6.1 illustrates the initial block in the vise while Figure 6.2 shows the semi-finished part which constitutes 0.1 mm of finishing allowance on all surfaces (except for datum planes).

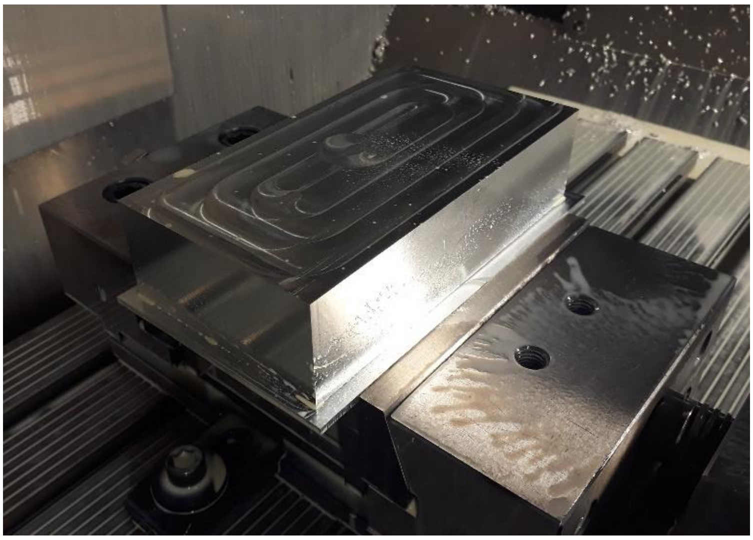

Figure 6.1. Initial block metal before machining

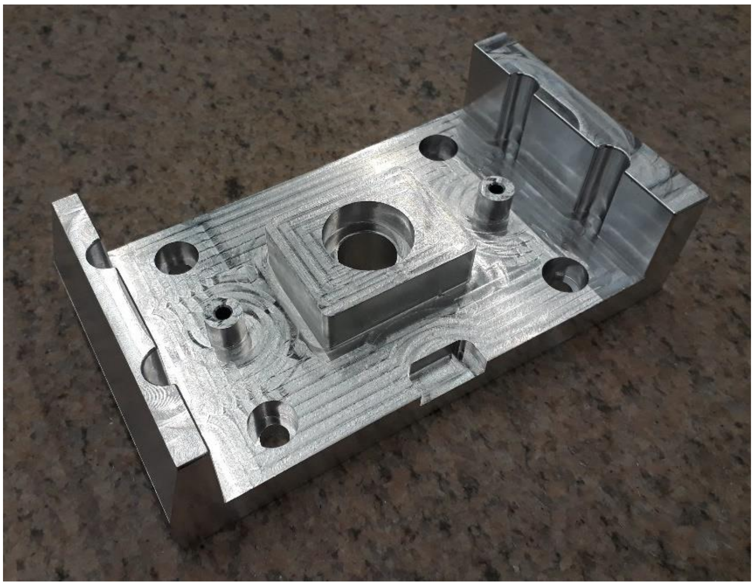

Figure 6.2. Semi-finished part

Next, the steel plates are attached onto the target piece using the technique elaborated in Section 3.10.2. Figure 6.3 illustrates the taped workpiece. Here, the industrial adhesive Loctite 406 [39] is employed to glue the steel plate onto the (taped) aluminum workpiece as shown in Figure 6.4.

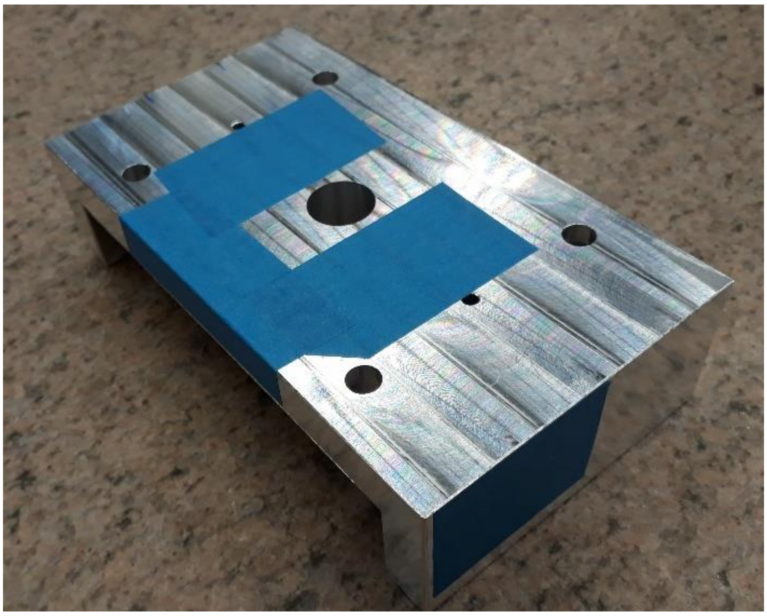

Figure 6.3. Taped workpiece

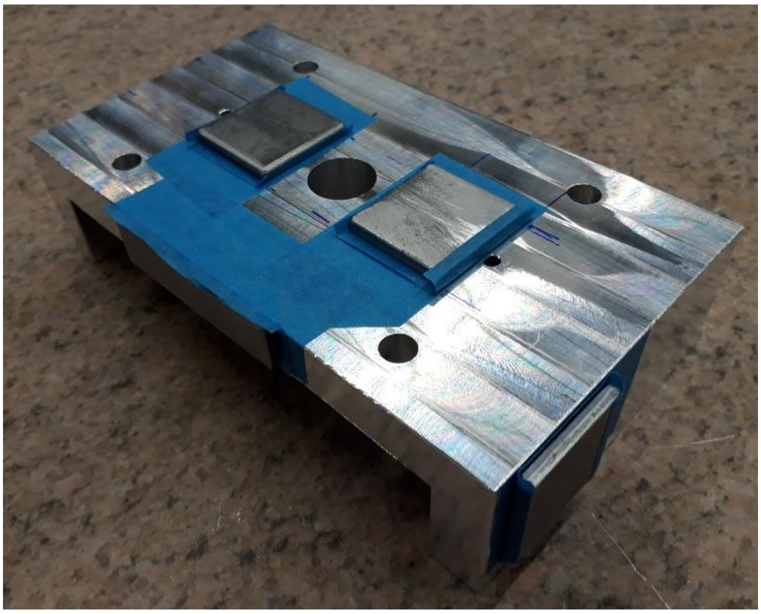

Figure 6.4. Prepared workpiece for finishing operations

Figure 6.5 illustrates the manufactured Cubefix elements and their corresponding (3-2-1) fixture arrangement. In this configuration, Neodymium (Nd) magnets (a total of 4) provide the prescribed clamping forces. The fixture elements used in this arrangement are as follows:

- 1 Grid Plate,
- 10 Cubes,
- 6 Locators (h = 5 [mm]),
- 4 Magnetic Clamps (Type 1),
- 3 Risers (H = 25 [mm]),
- 3 Special abutments for magnetic clamps,
- 20 bolts (for mounting cubes to each other and onto the grid plate).

Please note that some minor modifications have been performed on the fixture elements discussed in Chapter 3:

- Grid plate used in experimental studies are manufactured smaller than the designed fixture element in Section 3.1 due to budget restrictions.
- Since a set of risers (as prescribed in Chapter 3) has not been manufactured due to time and budget restrictions of the project, 3 special abutments for magnetic clamps are manufactured in place of these risers to decrease the overall cost (and manufacturing time) of the project.
- Risers and locators at the bottom of the workpiece are manufactured as integrated pieces due to above-mentioned reasons.

Similarly, the loaded part onto the fixture is shown in Figure 6.6.

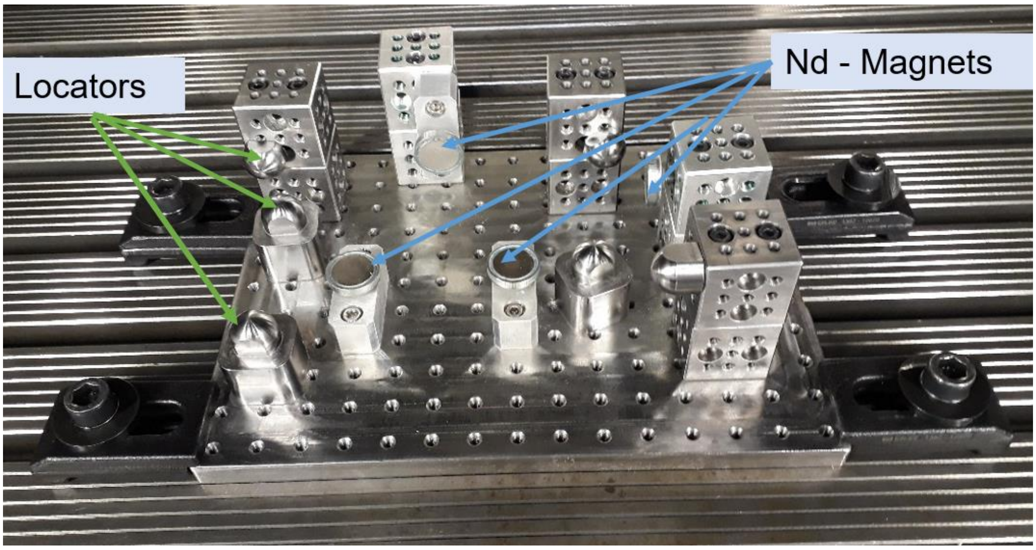

Figure 6.5. Cubefix arrangement

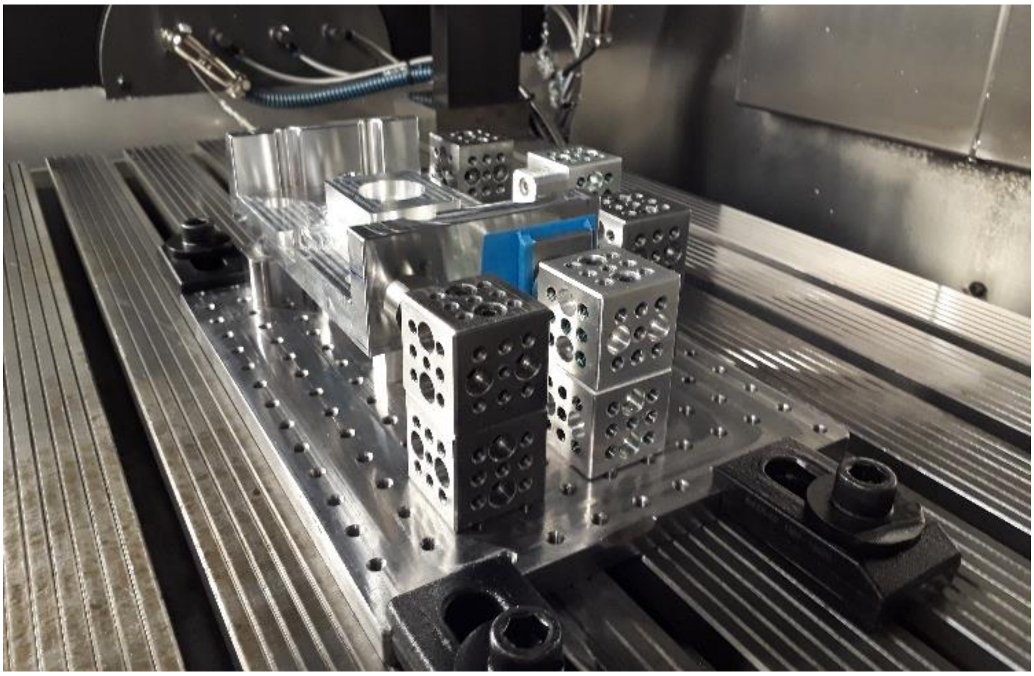

Figure 6.6. Loaded (semi-finished) workpiece to the Cubefix

6.1.2. Machining

For machining tests along with manufacturing of the fixture elements, a five-axis vertical machining center (DMG HSC 105) is used. This machining center, which is shown in the Figure 6.7, has a workspace of 1110×800×600 [mm] with a maximum spindle speed of 18000 [rpm] while its positioning accuracy is 5 [μm] at each axis.

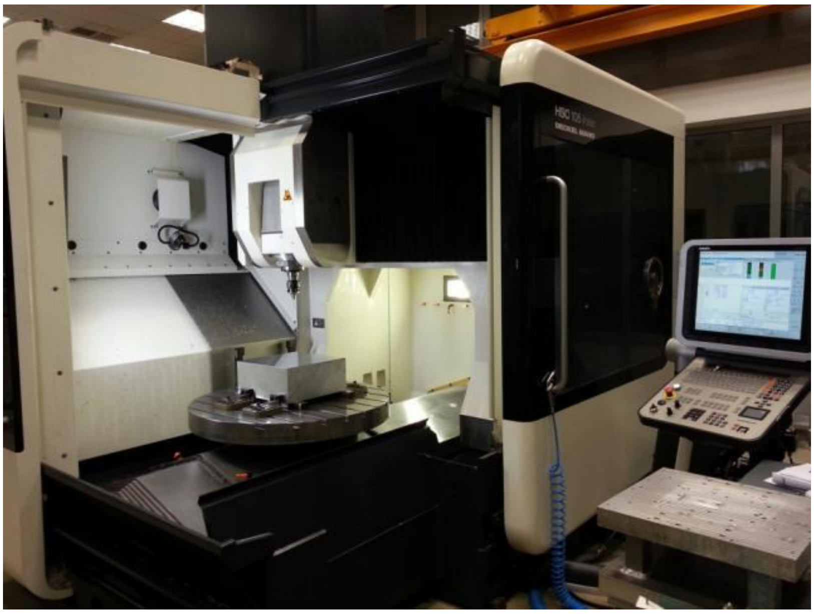

Figure 6.7. DMG HSC 105 Vertical Machining Center

An NC program (i.e. “G-code”) for finishing operations (for three test parts) is created with the utilization of NX-CAM software package. The properties of the tools used in the finishing operations are summarized in Table 6.1.

Table 6.1. Tools that are used for the experimental studies

Tool Name	Tool Material	Spindle Speed [rpm]	Feedrate [mm/min]	Usage
Ø 8 end mill	S. Carbide	8000	800	Wall and Floor operations
Ø 4 end mill	S. Carbide	12000	1000	Boring operations
Ø 4 ball mill	S. Carbide	12000	1000	Angular surfaces

Three test parts are then to be machined when subjected to different clamping forces. The distance between the parts and the magnets (i.e. the resulting clamping forces) are set differently for each part. The distance (e.g. air gap) is set as 0.5, 1.0, and 0.1 mm for Part A, B, and C respectively. For Part C, the air gap shown in Figure 6.8 is adjusted using a piece of paper (which roughly has a thickness of 100 microns) as illustrated in Figure 6.9. Finally, Figure 6.10 shows all the finished test pieces.

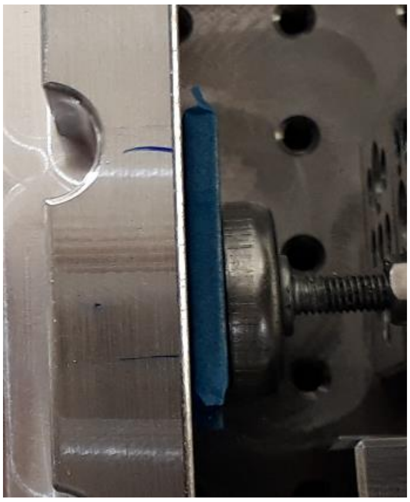

Figure 6.8. Distance- Magnet and Part C

Figure 6.9. Adjusting Magnet Distance -Part C

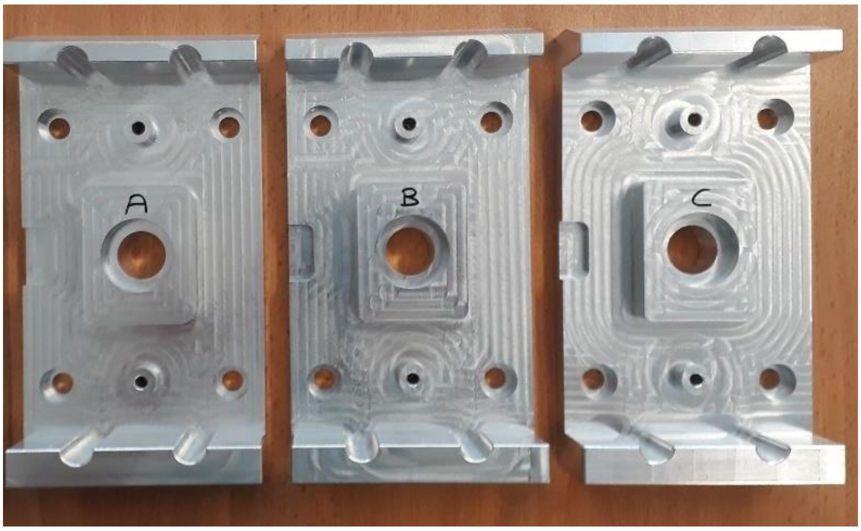

Figure 6.10. Manufactured test parts using Cubefix

6.1.3. CMM Measurements

To evaluate the quality of machining for all test parts, a DEA Advantage CMM, shown in Figure 5.33, is utilized. This CMM with a workspace of 1200×2200×1000 [mm] has an overall accuracy of A = 2.2 + L/333 [μm] where L refers to the characteristic measurement length in [mm].

Figure 6.11. DEA Advantage CMM

Figure 6.12 illustrates the CMM measurements on a test part. Figure 6.12 shows the technical drawing of the part which constitutes 32 different dimensional- and geometric tolerances to be evaluated by the CMM.

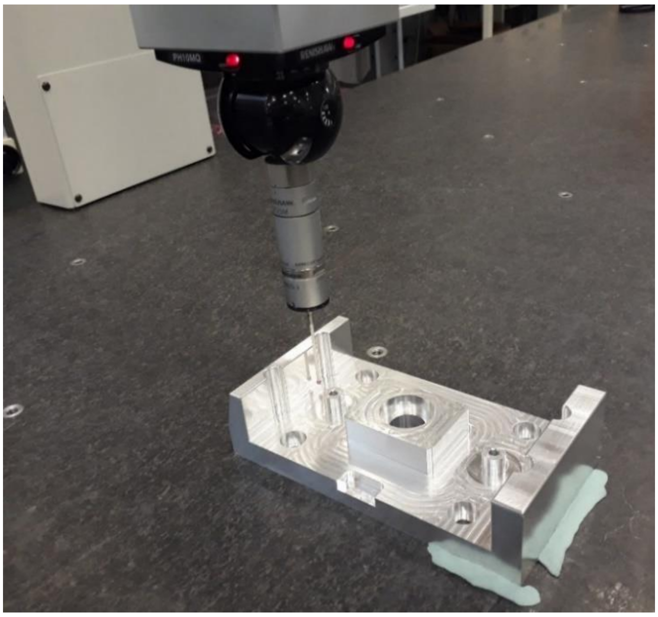

Figure 6.12. Measurement of a test part

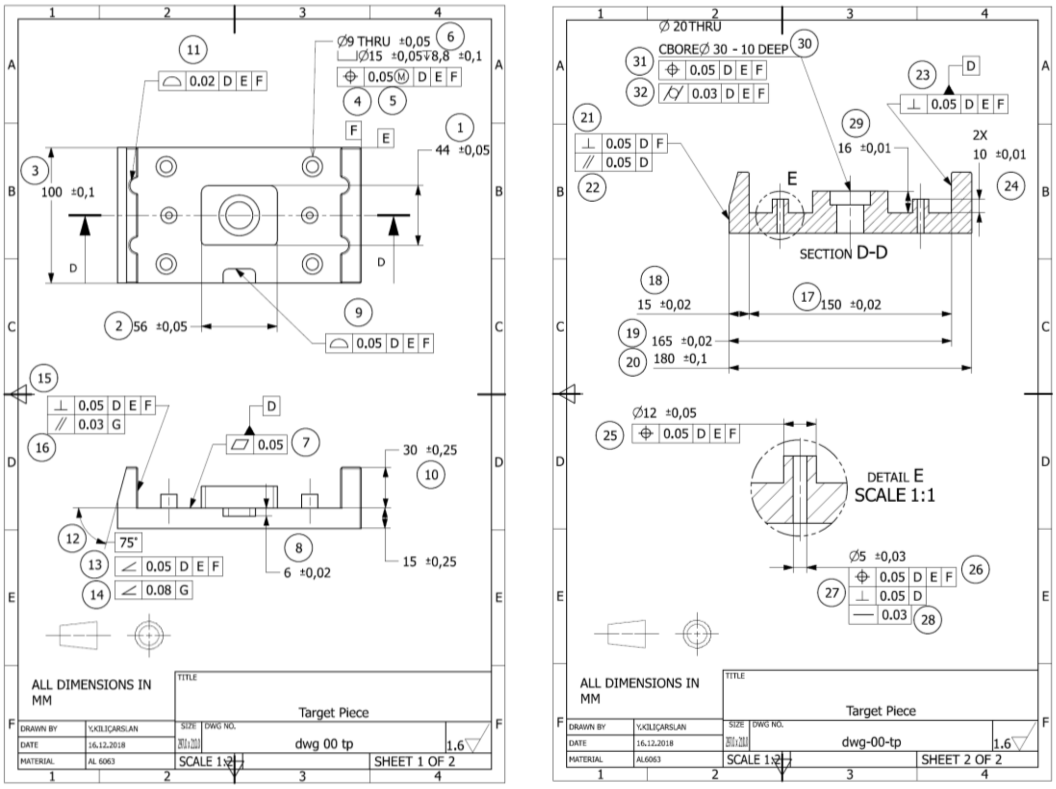

Figure 6.13. Dimensional and geometric tolerances on the test pieces

6.1.4. Results and Discussions

The CMM results are summarized in Table 6.2. Deviation from the nominal values are shown in the left portion of Table 6.2. Furthermore, the best part on a certain geometric feature is marked by "x" sign in the table columns labelled as "Best GD&T Entity." Similarly, Figure 6.14 presents the deviations from the nominal values using histograms.

As can be clearly seen from Table 6.2, Part C, which has a superiority in 15 geometric items (out of 32), is apparently the best "quality" part among all test pieces according to CMM results. Part A and Part B have advantage on 12 and 7 items respectively. To elaborate, Part C has the lowest deviation on the geometric features between 1 and 6 (except for the 4^{th} and 5^{th}). However, all parts are close contenders on flatness (7^{th} feature): Part A, B, and C have flatness values of 0.002, 0.002 and 0.005 [mm] respectively. As a consequence, Cubefix seems to be better alternative to attain tight flatness tolerances.

Part B is the worst part with respect to the 9^{th}, 11^{th}, 22^{nd}, 23^{rd}, 25^{th} and 31^{st} features. Inspection results for the features 12 and 16 are, in fact, close to each other on all parts. Part C is the better on some geometrical attributes such as angularity, profile and perpendicularity. These include the 9^{th}, 13^{th}, 14^{th} and 15^{th} features.

Features 22 and 23 are the perpendicularity and parallelism form tolerances with respect to datum A and datum D respectively while feature 24 is the height of the bosses from datum A. Part C has again yields the best inspection results on these features.

Part C yields the best results for the 29^{th} feature (i.e. middle boss height from the datum A) and the 32^{nd} feature (i.e. cylindricity of the middle boss hole).

To sum up, the clamping force has a significant effect on the accuracy of the parts as expected. This effect is seen clearly on the results for the Part B which was subjected to the lowest clamping force.

Table 6.2. Dimensional Comparison of the Manufactured Parts

	Deviation From Nominal Dimension [mm]			**Best GD&T Entity**			**Explanation**
#	**Part A**	**Part B**	**Part C**	**Part A**	**Part B**	**Part C**	
1	-0.010	-0.101	0.000			x	Dimensional Tolerance
2	-0.008	-0.020	0.002			x	Dimensional Tolerance
3	0.183	0.144	0.032			x	Dimensional Tolerance
4	0.052	0.051	0.202		x		True Pos. (Hole Center)
5	0.052	0.113	0.204	x			True Pos. (Hole Center)
6	-0.007	-0.004	0.000			x	Dimensional Tolerance
7	0.002	0.002	0.005	x	x		Flatness (Datum D)
8	-0.004	-0.002	-0.006		x		Dimensional Tolerance
9	0.064	0.151	0.059			x	Surface Profile
10	0.008	0.012	0.007			x	Dimensional Tolerance
11	0.038	0.350	0.150	x			Surface Profile
12	-0.003	-0.015	0.008	x			Angularity
13	0.036	0.036	0.019			x	Angularity
14	0.044	0.044	0.007			x	Angularity
15	0.026	0.026	0.003			x	Perpendicularity
16	0.055	0.055	0.058	x	x		Parallelism
17	-0.002	-0.007	-0.041	x			Dimensional Tolerance
18	-0.020	-0.109	-0.098	x			Dimensional Tolerance
19	-0.032	-0.084	0.012			x	Dimensional Tolerance
20	-0.031	-0.011	-0.079		x		Dimensional Tolerance
21	0.011	0.068	0.040	x			Perpendicularity
22	0.014	0.098	0.003			x	Parallelism
23	0.028	0.163	0.019			x	Perpendicularity
24	-0.004	-0.005	0.001			x	Dimensional Tolerance
25	0.046	0.435	0.163	x			True Pos. (Hole Center)
26	0.035	0.024	0.113		x		True Pos. (Hole Center)
27	0.004	0.013	0.062	x			Perpendicularity
28	0.018	0.025	0.032	x			Straightness
29	-0.006	-0.004	0.003			x	Dimensional Tolerance
30	-0.004	-0.002	0.003		x		Dimensional Tolerance
31	0.027	0.178	0.107	x			True Pos. (Hole Center)
32	0.017	0.074	0.015			x	Cylindricity
				12	**7**	**15**	

[*] Part which has lowest deviation is marked with “x” for the related dimension.

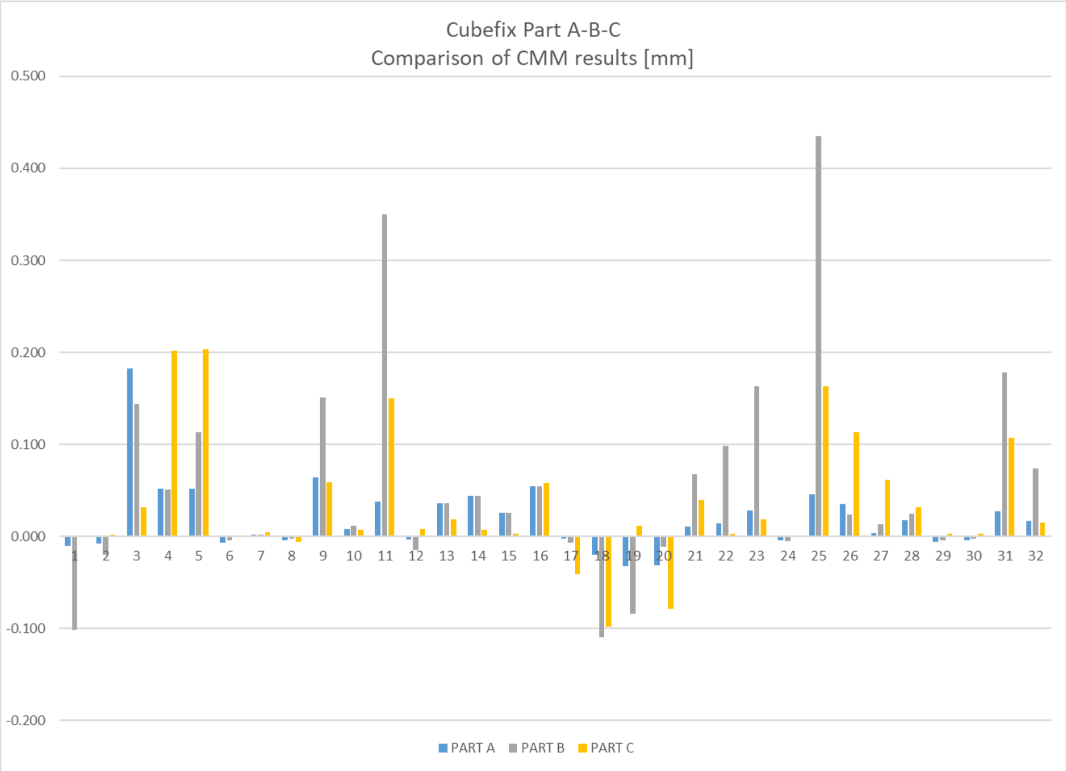

Figure 6.14. CMM results for all the test parts

6.2. Repeatability Tests

It is obvious that a fixture must put a workpiece in the same position after each every loading. Small variation in positioning of part indicates that the fixture is more repeatable. As the last step, the repeatability of the developed fixture is investigated using a CMM.

In these tests, the fixture is first attached onto CMM plate/table and is fixed by the clamps so as to avoid the motion of the plate during the inspecton- and workpiece loading/unloading operations. After loading the fixture, a point on grid plate is selected as a reference (i.e. “set zero”) point for CMM inspection. Afterwards, the part is loaded onto the fixture and six points on target piece are selected for inspection to determine the repeatability of the developed modular fixture. Note that the part is unloaded after each inspection and is loaded once again for the next inspection. Zero point of the CMM program along with the inspected points are shown in Figure 6.15. Similarly, locators and their corresponding numbers are illustrated in Figure 6.16.

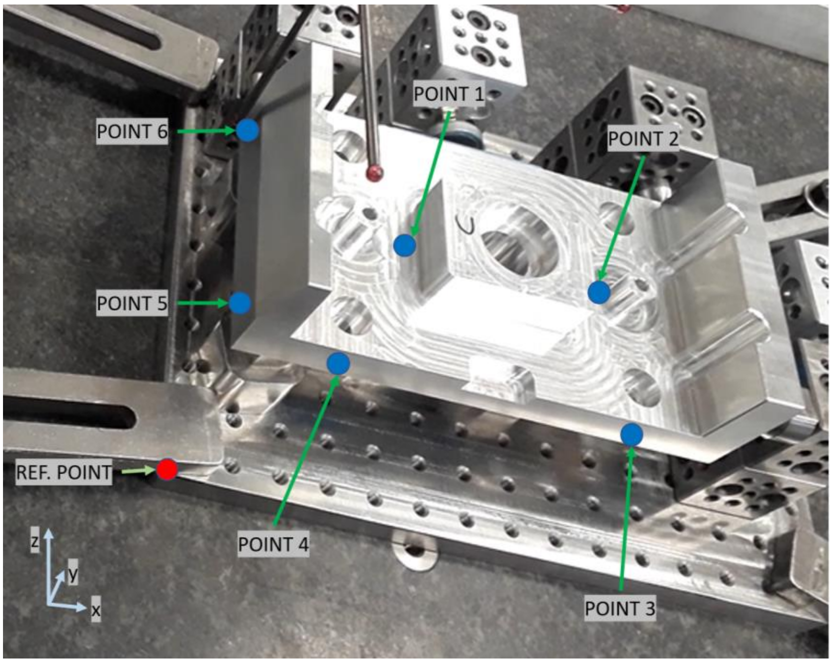

Figure 6.15. Inspected Points at CMM

With respect to the loading procedure, the slightly tilted part (pivoted at L3) is placed onto 1st and 2nd locators gradually while it is leaning against the 4th, 5th and 6th locators. The contact between the locators and part is visually checked after each loading. Note that in this configuration, the part is secured by magnetic clamps at each plane (as described in Sections 5.6 and 6.1). In the repeatability test, the magnet distance is set as 1.0 mm to ease the loading/unloading procedure.

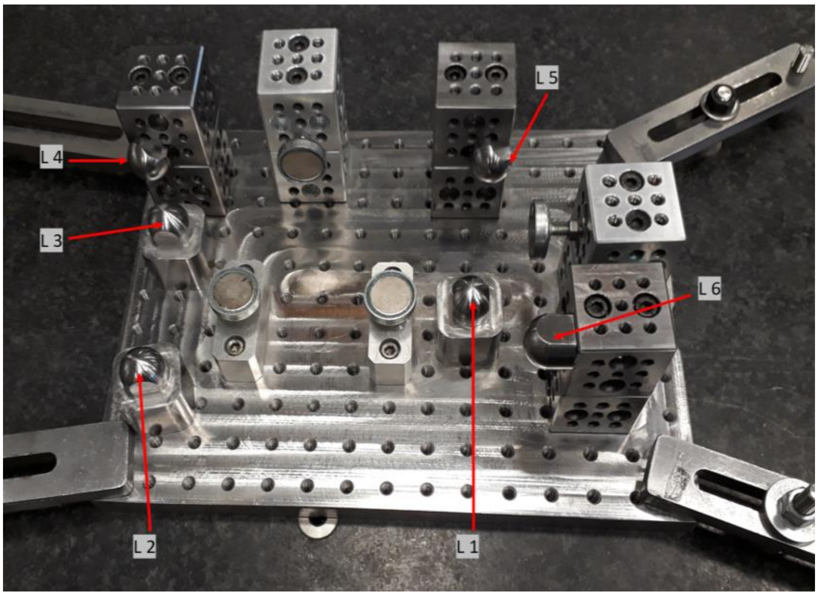

Figure 6.16. Locator numbers

The repeatability test is performed on Leitz CMM (Model PMM-C 24.16.10) which has a volumetric measurement error of 1.6 + L/600 [µm] (where L refers to the characteristic measurement length in mm) and a volumetric probing error of 1.3 µm. The temperature of the hall (where the CMM is located) is highly regulated at 21^{o}C.

Inspection results for the points shown in Figure 6.15 are presented in Table 6.3. In this table, $i \in \{1,2,3,4,5,6\}$ denotes the index of measured points on test piece while $j \in \{1,2,3,4,5\}$ refers to the measurement number. Note that at inspection points 1 and 2, the CMM takes measurements only along Z axis at ***predefined*** (i.e. programmed) (x,y) coordinates. Similarly, for inspection points 3 and 4, their Y-coordinates are recorded at the preselected (x,z) coordinates while only X-axis measurements are performed for the remaining points. Therefore, the inspection results are presented for the measured *"axis (i,j)"* (where axis $\in$ {X,Y,Z}) in the "*CMM inspection*" portion of the Table 6.3.

Table 6.3. Inspection results for repeatability tests

Point	**Measurement Point [mm]**			**CMM inspection (j) [mm]**				
(i)	**X**	**Y**	**Z**	**1**	**2**	**3**	**4**	**5**
1	61.990	80.831	Z (1,j)	54.947	54.947	54.947	54.948	54.947
2	135.908	81.374	Z (2,j)	54.952	54.952	54.951	54.952	54.951
3	152.614	Y (3,j)	48.999	31.333	31.332	31.333	31.335	31.333
4	47.629	Y (4,j)	48.999	31.205	31.205	31.204	31.205	31.203
5	X (5,j)	48.416	48.999	9.201	9.203	9.205	9.205	9.205
6	X (6,j)	121.635	48.999	9.066	9.070	9.070	9.070	9.069

Figure 6.17, Figure 6.18 and Figure 6.19 illustrate the registered errors (i.e. deviations from the mean) for each and every test points. Similarly, the statistical data (i.e. standard deviations, max/min/mean values, maximum deviations) derived from Table 6.3 is presented in Table 6.4. As a measure for positioning repeatability of the Cubefix, 3σ (i.e. three times the standard deviation) is utilized since 99.7% of the positioning errors is expected to fit into the 3σ band in the worst case. Finally, the repeatability for each axis is shown in Table 6.5. According to these results (as expected), the Z axis has the highest repeatability (i.e. smallest deviation) followed by the Y- and X axes respectively.

Table 6.4. Statistical data derived from CMM inspection results

Point	**Maximum**	**Minimum**	**Max. Deviation**	**Mean**	**Std. Dev.**	
(i)	**[mm]**	**[mm]**	**(Max – Min) [mm]**	**[mm]**	**σ [µm]**	**3σ [µm]**
1	54.948	54.947	0.001	54.947	0.447	1.342
2	54.952	54.951	0.001	54.952	0.548	1.643
3	31.335	31.332	0.003	31.333	1.095	3.286
4	31.205	31.203	0.002	31.204	0.894	2.683
5	9.205	9.201	0.004	9.204	1.789	5.367
6	9.070	9.066	0.004	9.069	1.732	5.196

Table 6.5. Repeatability for each axis

Axis	Repeatability (3σ) [μm]
X	± 5.367
Y	± 3.286
Z	± 1.643

As can be seen from Table 6.5, the positioning repeatability apparently improves along the axis where the workpiece is supported on a higher number of locators owing to the fact that the rigidity of the fixture is higher along such a direction. Hence, one can infer that increasing the rigidity of the locators may yield improved repeatability (and eventually accuracy) of the modular fixture. Notice that the magnitudes of the clamping forces have direct effects on the ***bias*** (or operating) points of the locators (See Section 4.3.2). In the repeatability tests, the magnetic clamping forces have been set to relatively low magnitudes for the sake of convenience. Hence, one might speculate that the repeatability of the fixture might improve significantly by increasing these clamping forces.

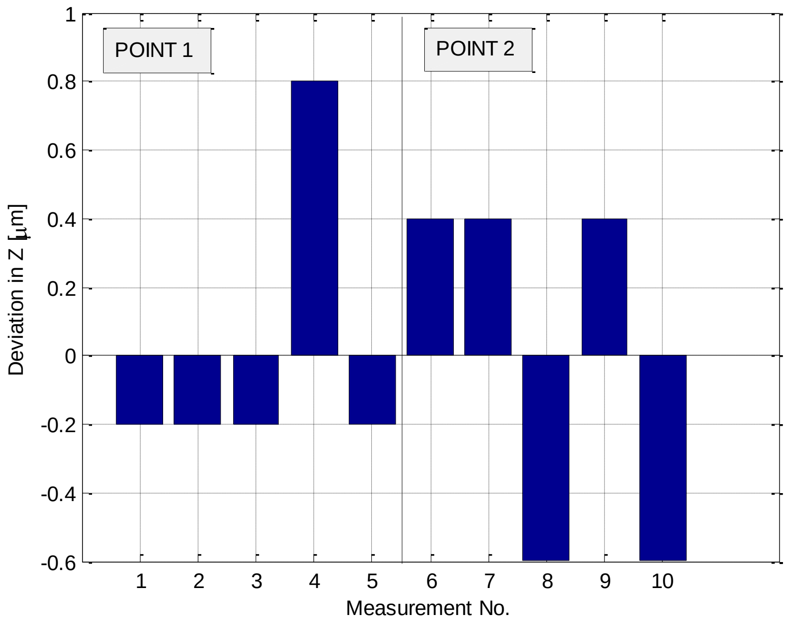

Figure 6.17. Deviation in Z axis.

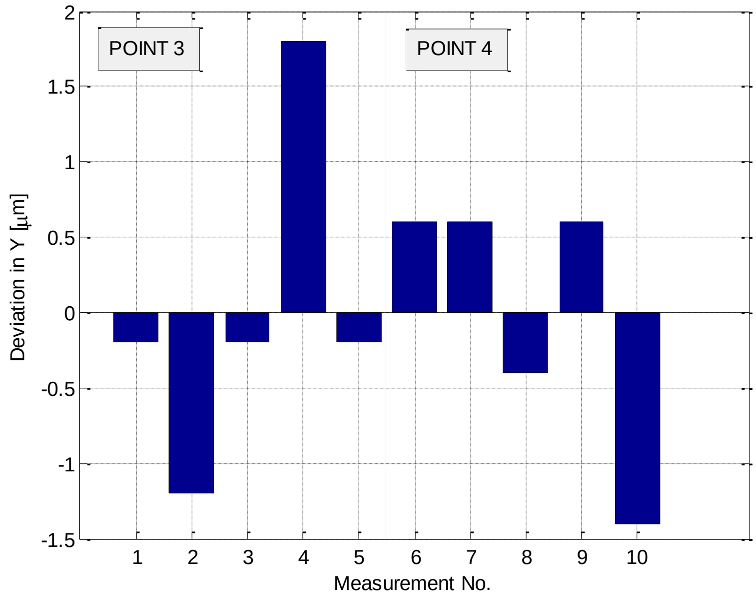

Figure 6.18. Deviation in Y axis.

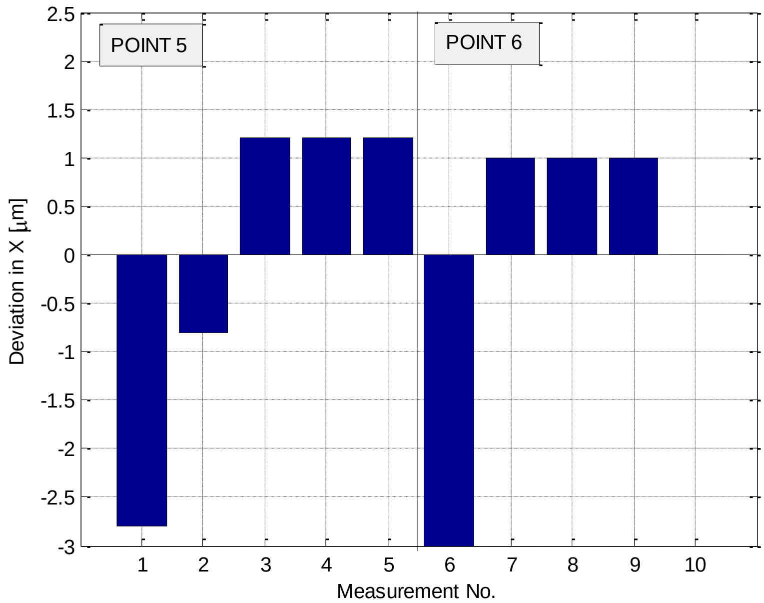

Figure 6.19. Deviation in X axis.

6.3. Closure

Machines, used for manufacturing and inspection purposes during the study, are presented. Fixture elements, used in experimental studies, are manufactured and presented in this section.

Manufacturing of the target pieces and manufacturing steps are explained in detail. After the manufacturing, target pieces are inspected in CMM. Inspection results of the manufactured parts are presented and compared.

The repeatability of the fixture system is investigated. Six points are inspected five times to determine the repeatability of the fixture system. In the repeatability test, it is determined that Z axis has the best repeatability. However, X axis is the worst repeatable axis compared to Y and Z axes.

CHAPTER 7

CONCLUSIONS & FUTURE WORKS

In this thesis, a modular fixture system that allows workpieces to be kinematically constrained is designed and realized. The key features and contributions of this study are as follows:

- As demonstrated in Chapter 5, due to modular nature of the proposed fixturing system (Cubefix), a large number of workpieces with different geometric attributes can be easily connected to the tables of CNC machining centers.
- By adding new components, the Cubefix system is expandable and is upward scalable.
- Experimental machining studies on test pieces (as discussed in Chapter 6) show that the performance of Cubefix system is satisfactory.
- A novel magnetic clamp (incorporating a strong permanent magnet) is designed and implemented within the scope of this thesis. Unlike conventional ones, this magnetic clamp is extremely useful in securing odd shaped pieces without obstructing the functional surfaces. The clamp has been successfully deployed to pull down the non-ferrous (i.e. Al-6063) test part with the utilization of an iron plate fastened to the workpiece via a strong double-sided tape. Experimental investigations indicate that this clamping scheme has worked well in securing the workpieces.
- A number of Matlab programs/tools (as discussed in Chapter 4 and in Appendix) has been developed to analyze the elastic deformations in a modular fixturing system like Cubefix. The tools are capable of estimating the machining accuracy to a certain degree utilizing simple cutting force models. Experimental studies indicate that these estimates are generally in good

agreement with the CMM measurements done on the test parts. Hence, the predictions of programs can be successfully employed as a guideline for modular fixture design and configuration analysis.

- Repeatability of the developed fixture has been determined for each axes by performing CMM inspection of the target piece in the experimental fixture set-up. Inspections are performed for six points. Each point is inspected five times.

The research as entirety is not fully complete by any means. In addition to studies performed in the content of this thesis, there exists a number of improvement opportunities in this work:

- Due to time- and budget restrictions, the major components (e.g. cube, locator, base plate) of Cubefix, which are made from alloy/tool steel, have not been core-hardened. Hence, all elements used in the study were susceptible to plastic deformations at their contacting surfaces. Hence, the next version should take into consideration the case/core hardening of the above-mentioned components so as to increase their surface hardness (i.e. resistance to plastic deformations) along with their dimensional stability.
- The magnetic clamp system (as is) uses screws to adjust the height and airgap between the workpiece and magnet. This is obviously not a very efficient mechanism to control the reluctance force developing in between two media. Hence, a flux path regulation/diversion mechanism (as used in the magnetic stands of dial gauges) could be incorporated to the clamp design as a future improvement.
- Active magnetic clamp systems, which induce Eddy currents in the metals, could be developed in the near future so as to attract (hold down) non-ferrous workpieces without the use of iron plates.
- The elastic deformation models developed in this study do not take into account the static friction between the contacting surfaces. Despite the fact that the inclusion of the friction process leads to the analysis of quasi-kinematic

constraints, the estimation results would be much more realistic and accurate than the present state.

- In the current study, no attempt was made to determine the optimal locations for the locators and the clamps. Hence, an optimization method can be included to the fixture analysis programs developed.
- Similarly, to improve the quality of fixture analysis, cutting process simulators (like CutPro) and FEA packages (like ANSYS) computing the deformations of the workpieces/locators can be incorporated to the loop. Apart from static analysis, dynamic deformation analysis could be developed as for future study.
- Different experimental parts must be manufactured in the proposed fixture to understand the overall performance of the fixture. Besides, number of the experimental parts should be increased.
- Finally, with new and improved Cubefix components, much more detailed experimental studies could be conducted to assess fully the potential of the proposed fixture system.

REFERENCES

[1] H. Asada and A. B. By, “Kinematic Analysis of Workpart Fixturing for Flexible Assembly with Automatically Reconfigurable Fixtures”, *IEEE Journal of Robotics and Automation*, vol. 1, no. 2, pp. 86-94, 1985.

[2] H. Song and Y. Rong, “Locating completeness evaluation and revision in fixture plan”, *Robotics and Computer-Integrated Manufacturing*, vol. 21, no. 4-5, pp. 368-378, 2005.

[3] W. Zhong and S. J. Hu, “Modeling Machining Geometric Variation in a N-2-1 Fixturing Scheme”, *Journal of Manufacturing Science and Engineering*, vol. 128, no. 1, pp. 213-219, 2006.

[4] M. Y. Wang, T. Liu and D. M. Pelinescu, “Fixture Kinematic Analysis Based on the Full Contact Model of Rigid Bodies”, *Transactions of the ASME*, vol. 125, no. 2, pp. 316-324, 2003.

[5] D. F. Walczyk and R. S. Longtin, “Fixturing of Compliant Parts Using a Matrix of Reconfigurable Pins” *Transactions of the ASME*, vol. 122, no. 4, pp. 766-772, 2000.

[6] D. Vukelic, U. Zuperl and J. Hodolic, “Complex system for fixture selection, modification, and design”, *Int. J Adv. Manuf. Technol.*, vol. 45. no. 7-8, pp. 731–748, 2009.

[7] J. C. Trappey and C. R. Liu, “A Literature Survey of Fixture Design-Automation”, *Int. J Adv. Manuf. Technol.*, vol. 5, no. 3, pp. 240-255, 1990.

[8] P. M. Grippo, B. S. Gandhi and M. V. Thompson, “The Computer-Aided Design of Modular Fixturing Systems”, *The International Journal of Advanced Manufacturing Technology*, vol. 2, no. 2, pp. 75-88, 1987.

[9] N. Wan, Z. Wang and R. Mo, “An intelligent fixture design method based on smart modular fixture unit”, *Int. J. Adv. Manuf. Technol.,* vol. 69, no. 9-12, pp. 2629–2649, 2013.

[10] Y. Zheng and W. H. Qian, “A 3-D modular fixture with enhanced localization accuracy and immobilization capability”, *International Journal of Machine Tools & Manufacture,* vol. 48, no. 6, 677–687, 2008.

[11] L. Fan and A. S. Kumar, “Development of robust fixture locating layout for machining workpieces”, *Proc. IMechE.*, vol. 224, no. 12, pp. 1792-1803, 2010.

[12] G. Moroni, S. Petr`o and W. Polini, “Robust design of fixture configuration”, *Procedia CIRP*, vol. 21, pp. 189-194, 2014.

[13] S. A. Choudhuri and E. C. De Meter, “Tolerance Analysis of Machining Fixture Locators”, *Journal of Manufacturing Science and Engineering,* vol. 121, no. 2, pp. 273-281, 1999.

[14] N. Kaya, “Machining fixture locating and clamping position optimization using genetic algorithms”, *Computers in Industry*, vol. 57, no. 2, pp. 112-120, 2006.

[15] A. Armillotta, G. Moroni and W. Polini, “To analytically estimate the 3D position deviation of a holes pattern due to fixturing”, *Procedia CIRP*, vol. 10, pp. 186-193, 2013.

[16] W. Chen, X. Luo, H. Su and F. Wardle, “An integrated system for ultra-precision machine tool design in conceptual and fundamental design stage”, *The International Journal of Advanced Manufacturing Technology*, pp. 1-7, 2015.

[17] G. Qin, W. Zhang and M. Wan, “Analysis and Optimal Design of Fixture Clamping Sequence”, *Transactions of the ASME,* vol. 128, no. 2, pp. 482-493, 2006.

[18] A. Armillotta, G. Moroni, W. Polini and Q. Semeraro, “A Unified Approach to Kinematic and Tolerance Analysis of Locating Fixtures”, *Journal of Computing and Information Science in Engineering*, vol. 10, no.2, pp. 1-11, 2010.

[19] R. A. Marin, M. Placid and P. M. Ferreira, “Analysis of the Influence of Fixture Locator Errors on the Compliance of Work Part Features to Geometric Tolerance Specifications”, *Journal of Manufacturing Science and Engineering*, vol. 125, no.3, pp. 609-616, 2003.

[20] E. Olaiz, J. Zulaika, F. Veiga, M. Puerto and A. Gorrotxategi, “Adaptive fixturing system for the smart and flexible positioning of large volume workpieces in the wind-power sector”, *Procedia CIRP*, vol. 21, pp. 183-188, 2014.

[21] G. H. Qin, W. H. Zhang and M. Wan, “A mathematical approach to analysis and optimal design of a fixture locating scheme”, *Int. J. Adv. Manuf. Technol*., vol. 29, no. 3-4, pp. 349-359, 2006.

[22] A. Raghu and S. N. Melkote, “Modeling of Workpiece Location Error due to Fixture Geometric Error and Fixture-Workpiece Compliance”, *Journal of Manufacturing Science and Engineering*, vol. 127, no. 1, pp. 75-83, 2005.

[23] H. Tohidi and T. AlGeddawy, “Planning of modular fixtures in a robotic assembly system”, *Procedia CIRP*, vol. 41, pp. 252-257, 2016.

[24] Y. Tian, D. Zhang and B. Shirinzadeh, “Dynamic modelling of a flexure-based mechanism for ultra-precision grinding operation”, *Precision Engineering*, vol. 35, no. 4, pp. 554-565, 2011.

[25] C. Liu, “A Systematic Conceptual Design of Modular Fixtures”, *Int. J. Adv. Manuf. Technol.*, vol. 9, no. 4, pp. 217-224, 1994.

[26] J. Kakish, P. Zhang and I. Zeid, “Towards the design and development of a knowledge-based universal modular jigs and fixtures system”, *Journal of Intelligent Manufacturing*, vol. 11, no. 4, pp. 381-401, 2000.

[27] E. G. Hoffman, *Jig and Fixture Design.* Delmar, 2004.

[28] "Calculate magnetic flux density with formula - supermagnete", Supermagnete.de, 2019. [Online]. Available: https://www.supermagnete.de/eng/faq/How-do-you-calculate-the-magnetic-flux-density. [Accessed: 30-Jan- 2019].

[29] S. Chaiprapat and S. Rujikietgumjorn, “Modeling of positional variability of a fixtured workpiece due to locating errors”, *Int J Adv Manuf Technol*, vol. 36, no. 7-8, pp. 724-731, 2008.

[30] P. Blumenthal and A. Raatz, “Adhesive Workpiece Fixturing for Micromachining”, *In: Ratchev S. (eds) Precision Assembly Technologies and Systems. IPAS, IFIP Advances in Information and Communication Technology,* vol. 371, Springer, 2012.

[31] M. H. Raffles, K. Kolluru, D. Axinte and H. Llewellyn-Powell, “Assessment of adhesive fixture system under static and dynamic loading conditions”, *Proc IMechE Part B: J Engineering Manufacture,* vol. 227, no. 2, 267–280, 2012.

[32] S. Kushendarsyah and S. Sathyan, “Orthogonal Microcutting of Thin Workpieces”, *Journal of Manufacturing Science and Engineering,* vol. 135. no. 3, pp. 1-11, 2013.

[33] E. C. De Meter, “Light Activated Adhesive Gripper (LAAG) Workholding Technology and Process”, *Journal of Manufacturing Processes,* vol. 6, no. 2, pp. 201-214, 2004.

[34] E. C. De Meter and J. S. Kumar, “Assessment of photo-activated adhesive workholding (PAW) technology for holding ‘‘hard-to-hold’’ workpieces for

machining”, *Journal of Manufacturing Systems*, vol. 29, no. 1, pp. 19–28, 2010.

[35] Bluephotongrip.com, 2019. [Online]. Available: https://www.bluephoton grip.com/wp-content/uploads/2019/01/Blue-Photon-2019-Product-Catalog.pd f. [Accessed: 30- Jan- 2019].

[36] "Shellac", En.wikipedia.org, 2019. [Online]. Available: https://en.wikipedia. org /wiki/Shellac. [Accessed: 30- Jan- 2019].

[37] J. Lucas, P. Lucas, T. L. Mercier, A. Rollat, and W. Davenport, “*Rare Earths Science, Technology, Production and Use*. Elsevier, 2015.

[38] "Neodymium Pot Mıknatıslar", Miknatisteknik.com, 2019. [Online]. Available: https://www.miknatisteknik.com/miknatis-cesitleri/miknatislar/ne odymium-miknatislar.html. [Accessed: 30- Jan- 2019].

[39] Tdsna.henkel.com, 2019. [Online]. Available: https://tdsna.henkel.com/NA/ UT/HNAUTTDS.nsf/web/36736C9DBAAAB551882571870000D765/$File/ 406-2012NEW-EN.pdf. [Accessed: 30- Jan- 2019].

[40] R. D. Lorenz and L. P. Haines, *Understanding Modern Power Conversion.* Madison: University of Wisconsin, 1995.

[41] Walter 2017 General Catalogue – Milling.

[42] A.Y.C. Nee, K. Whybrew and A. S. Kumar, *Advanced Fixture Design for FMS.* Springer-Verlag, 1995.

[43] J. G. Nee, W. Dufraine, J. W. Evans and M. Hill, *Fundamentals of Tool Design*. Society of Manufacturing Engineers, 2010.

[44] R. Coope, "Modular Fixturing VS. Dedicated Tooling", Stevenseng.com, 2019. [Online]. Available: http://www.stevenseng.com/tech_mod_vs_dedi cated.html. [Accessed: 30- Jan- 2019].

[45] B. Shirinzadeh, “Flexible and automated workholding systems”, *Industrial Robot: An International Journal*, vol. 22, no. 2, pp. 29-34, 1995.

[46] K. L. Johnson, *Contact Mechanics.* Cambridge University Press, 1985.

[47] L. C. Hale, “Principles and Techniques for Designing Precision Machines”, Doctoral Dissertation, MIT, 1999.

[48] Ceratizit.com, 2019. [Online]. Available: https://www.ceratizit.com/uploads/tx_extproduct//files/GD_KT_PRO-0607-0714_SUS_ABS_V1.pdf. [Accessed: 30- Jan- 2019].

[49] "Er-El 2018 Product Catalog", Er-el.com.tr, 2018. [Online]. Available: http://www.er-el.com.tr/katalog/erel2018.pdf. [Accessed: 30- Jan- 2019].

[50] "GrabCAD", 2019. [Online]. Available: https://grabcad.com/. [Accessed: 30- Jan- 2019].

[51] Tdsna.henkel.com, 2019. [Online]. Available: https://tdsna.henkel.com/NA/UT/HNAUTTDS.nsf/web/1263FDE02A9A8717882571870000D79C/$File/480-EN.pdf. [Accessed: 30- Jan- 2019].

[52] L. L. Lacalle and A. Lamikiz, *Machine tools for high performance machining*. London: Springer, 2010.

[53] Y. Altintas, *Manufacturing automation: metal cutting mechanics, machine tool vibrations, and CNC design.* Cambridge University Press, 2012.

[54] M. Akkurt, 2015, *Talaş Kaldırma CNC Takım Tezgahları ve Üretim Otomasyonu Problemleri*. Birsen Yayınevi, 2015.

APPENDICES

A. CUTTING FORCE ESTIMATION

Cutting force estimation is of critical importance to assess the elastic deformations taking place in the fixture (and the workpiece). Not surprisingly, the literature on the estimation of forces/torque in milling operations is vast. In this section, a simplified cutting force model adapted from [41] and [54] is summarized. The model, which is essentially based on specific cutting energy, yields the average machining forces (in tangential and axial direction) during end-milling operations.

Figure A.1 illustrates a generic milling operation with its essential parameters. The tangential force (F_t) and axial force (F_a) are expressed as

$$F_t = z_e b h_m k_c \tag{A.1a}$$

$$F_a = F_t \tan\beta \tag{A.1b}$$

Here, b is the chip width [mm]; h_m is the average chip thickness [mm]; β is the helix angle; k_c is the specific cutting energy [N/mm^2]; z_e refers to the number of flutes engaging into cut:

$$b = \frac{a_p}{\cos\beta} \tag{A.2a}$$

$$z_e = z_n \frac{\varphi}{2\pi} \tag{A.2b}$$

$$h_m = \frac{2 f_z a_e}{\varphi D_c} \tag{A.2c}$$

where z_n is the number of flutes on the cutting tool while f_z denotes the feed-per-tooth [mm/tooth].

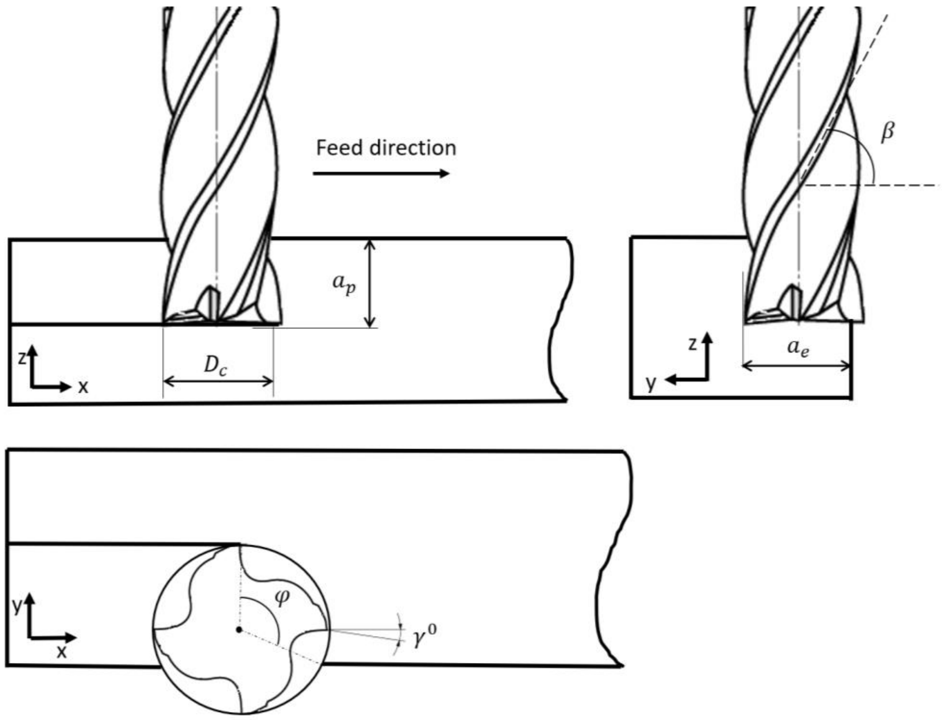

Figure A.1. Basic Parameters of a Generic End-milling Process.

Note that the immersion angle (φ) in Eqns. (A.2b) and (A.2c) takes the following form:

$$\varphi = \cos^{-1}\left(1 - \frac{2a_e}{D_c}\right) \tag{A.3}$$

Similarly, the specific cutting energy respective to a specific cut in Eqn. (A.1a) can be expressed as

$$k_c = k_{c11}(h_m)^{-m_c}(1 - 0.01\gamma^o) \tag{A.4}$$

where k_{c11} is the specific cutting energy for 1 mm of (undeformed) chip thickness and 1 mm of chip width; γ^o is the rake angle in degrees. Notice that the specific cutting energy is highly correlated with the yield strength of the material [41, 54]. Since hardening a material via certain processes (i.e. heat treatment, plastic deformation, aging, alloying, etc.) is known to increase its elastic limit (i.e. pushing the yield strength above that of the annealed state), k_{c11} is often times shown as a function of the material type as well as overall hardness in metal cutting literature. Table A.1 [48] tabulates these constants for some key engineering metals.

Table A.1. Material Comparison Table, $k_{c1.1}$ and m_c values [48]

Germany DIN	Mat. no.	United Kingdom BS	France AFNOR	Sweden SS	USA AISI	Japan JIS	Kc1.1 N/mm²	mc
10 SPb 20	1.0722		10 PbF 2		11 L 08		1350	.20
100 Cr 6	1.2067	BL 3	Y 100 C 6		L 3	SUJ2	1775	.24
105 WCr 6	1.2419		105 WC 13			SKS31	1775	.24
12 CrMo 9 10	1.7380	1501-622 Gr. 31; 45	10 CD 9.10	2218	A 182-F22	SPVA,SCMV4	1675	.24
12 Ni 19	1.5680		Z 18 N 5		2515		2450	.23
13 CrMo 4 4	1.7335	1501-620 Gr. 27	15 CD 3.5	2216	A 182-F11; F12	SPVAF12	1675	.24
14 MoV 6 3	1.7715	1503-660-440					1675	.24
14 Ni 6	1.5622		16 N 6		A 350-LF 5		1675	.24
14 NiCr 10	1.5732		14 NC 11		3415	SNC415(H)	1675	.24
14 NiCr 14	1.5752	655 M 13	12 NC 15		3310; 9314	SNC815(H)	1675	.24
14 NiCrMo 13 4	1.6657						1675	.24
15 Cr 3	1.7015	523 M 15	12 C 3		5015		1675	.24
15 CrMo 5	1.7262		12 CD 4			SCM415(H)	1675	.24
15 Mo 3	1.5415	1501-240	15 D 3	2912	A 204 Gr. A		1675	.24
16 MnCr 5	1.7131	527 M 17	16 MC 5	2511	5115	SCR415	1675	.24
16 Mo 5	1.5423	1503-245-420			4520	SB450M	1675	.24
17 CrNiMo 6	1.6587	820 A 16	18 NCD 6				1675	.24
21 NiCrMo 2	1.6523	805 M 20	20 NCD 2	2506	8620	SNCM220(H)	1725	.24
25 CrMo 4	1.7218	1717 CDS 110	25 CD 4 S	2225	4130	SM420;SCM430	1725	.24
28 Mn 6	1.1170	150 M 28	20 M 5		1330		1500	.22
32 CrMo 12	1.7361	722 M 24	30 CD 12	2240			1775	.24
34 Cr 4	1.7033	530 A 32	32 C 4		5132	SCR430(H)	1725	.24
34 CrMo 4	1.7220	708 A 37	35 CD 4	2234	4135; 4137	SCM432;SCCRM3	1775	.24
34 CrNiMo 6	1.6582	817 M 40	35 NCD 6	2541	4340	SNCM447	1775	.24
35 S 20	1.0726	212 M 36	35 MF 4	1957	1140		1525	.22
36 CrNiMo 4	1.6511	816 M 40	40 NCD 3		9840	SNCM447	1775	.24
36 Mn 5	1.1167						1525	.22
36 NiCr 6	1.5710	640 A 35	35 NC 6		3135	SNC236	1800	.24
38 MnSi 4	1.5120						1800	.24
39 CrMoV 13 9	1.8523	897 M 39					1775	.24
40 Mn 4	1.1157	150 M 36	35 M 5		1039		1525	.22
40 NiCrMo 2 2	1.6546	311-Type 7	40 NCD 2		8740	SNCM240	1775	.24
41 Cr 4	1.7035	530 M 40	42 C 4		5140	SCR440(H)	1775	.24
41 CrAlMo 7	1.8509	905 M 39	40 CAD 6.12	2940	A 355 Cl. A	SACM645	1775	.24
41 CrMo 4	1.7223	708 M 40	42 CD 4 TS	2244	4142; 4140	SCM440	1775	.24
42 Cr 4	1.7045	530 A 40	42 C 4 TS	2245	5140	SCr440	1775	.24
42 CrMo 4	1.7225	708 M 40	42 CD 4	2244	4142; 4140	SCM440(H)	1775	.24
45 WCrV 7	1.2542	BS 1		2710	S 1		1775	.24
50 CrV 4	1.8159	735 A 50	50 CV 4	2230	6150	SUP10	1775	.24
55 Cr 3	1.7176	527 A 60	55 C 3	2253	5155	SUP9(A)	1775	.24
55 NiCrMoV 6	1.2713		55 NCDV 7		L 6	SKH1;SKT4	1775	.24
55 Si 7	1.0904	250 A 53	55 S 7	2085; 2090	9255		1775	.24
58 CrV 4	1.8161						1775	.24
60 SiCr 7	1.0961		60 SC 7		9262		1775	.24
9 SMn 28	1.0715	230 M 07	S 250	1912	1213	SUM22	1350	.21
9 SMn 36	1.0736	240 M 07	S 300		1215		1350	.21
9 SMnPb 28	1.0718		S 250 Pb	1914	12 L 13	SUM22L	1350	.21
9 SMnPb 36	1.0737		S 300 Pb	1926	12 L 14		1350	.21
Al99	3.0205						700	.25
AlCuMg1	3.1325						700	.25
AlMg1	3.3315						700	.25

Table A.1. Material Comparison Table, $k_{c1.1}$ and m_c values [48] (continued 1)

Germany DIN	Mat. no.	United Kingdom BS	France AFNOR	Sweden SS	USA AISI	Japan JIS	Kc1.1 N/mm²	mc
AlMgSi1	3.2315						700	.25
C 105 W1	1.1545		Y1 105	1880	W 110	SK3	1675	.24
C 125 W	1.1663		Y2 120		W 112		1675	.24
C 15	1.0401	080 M 15	AF3 7 C 12; XC 18	1350	1015	S15C	1350	.21
C 22	1.0402	050 A 20	AF 42 C 20	1450	1020	S20C, S22C	1350	.21
C 35	1.0501	060 A 35	AF 55 C 35	1550	1035	S35C	1525	.22
C 45	1.0503	080 M 46	AF 65 C 45	1650	1045	S45C	1525	.22
C 55	1.0535	070 M 55		1655	1055	S55C	1675	.24
C 60	1.0601	080 A 62	CC 55		1060	S60C	1675	.24
Cf 35	1.1183					S35C	1525	.22
Cf 53	1.1213					S50C	1525	.22
Ck 101	1.1274	060 A 96		1870	1095		1675	.24
Ck 15	1.1141	080 M 15	XC 15; XC 18	1370	1015	S15C	1350	.21
Ck 55	1.1203	070 M 55	XC 55		1055	S55C	1675	.24
Ck 60	1.1221	080 A 62	XC 60	1665; 1678	1060	S58C	1675	.24
CoCr20W15Ni	2.4764						3300	.24
CuZn15	2.0240						700	.27
CuZn36Pb3	2.0375						700	.27
E-Cu57	2.0060						700	.27
G-AlSi10Mg	3.2381						700	.25
G-AlSi12	3.2581						700	.25
G-AlSi9Cu3	3.2163						700	.25
G-CuSn5ZnPb	2.1096						700	.27
G-CuZn40Fe	2.0590						700	.27
G-X 120 Mn 12	1.3401	Z 120 M 12	Z 120 M 12		A 128 (A)		3300	.24
G-X 20 Cr 14	1.4027	420 C 29	Z 20 C 13 M			SCS2	1875	.21
G-X 40 NiCrSi 38 18	1.4865	330 C 40					2600	.24
G-X 45 CrSi 9 3	1.4718	401 S 45	Z 45 CS 9		HNV 3		2450	.23
G-X 5 CrNi 13 4	1.4313	425 C 11	Z 5 CN 13.4	2385	CA 6-NM		1875	.21
G-X 5 CrNiMoNb 18 10	1.4581	318 C 17	Z 4 CNDNb 18.12 M				2150	.2
G-X 6 CrNi 18 9	1.4308	304 C 15	Z 6 CN 18.10 M	2333	CF-8		2150	.2
G-X 6 CrNiMo 18 10	1.4408						2150	.2
G-X 7 Cr 13	1.4001						1875	.21
GG-10	.6010		Ft 10 D	01 10-00	A48-20 B	FC100	1150	.2
GG-15	.6015	Grade 150	Ft 15 D	01 15-00	A48-25 B	FC150	1150	.2
GG-20	.6020	Grade 220	Ft 20 D	01 20-00	A48-30 B	FC200	1150	.2
GG-25	.6025	Grade 260	Ft 25 D	01 25-00	A48-40 B	FC250	1250	.24
GG-30	.6030	Grade 300	Ft 30 D	01 30-00	A48-45 B	FC300	1350	.28
GG-35	.6035	Grade 350	Ft 35 D	01 35-00	A48-50 B	FC350	1350	.28
GG-40	.6040	Grade 400	Ft 40 D	01 40-00	A48-60 B	FC400	1350	.28
GGG-35.3	.7033					FCD350	1225	.25
GGG-40	.7040	SNG 420/12	FGS 400-12	0717-02	60-40-18	FCD400	1225	.25
GGG-40.3	.7043	SNG 370/17	FGS 370-17	0717-15		FCD400	1225	.25
GGG-50	.7050	SNG 500/7	FGS 500-7	0727-02	65-45-12	FCD500	1350	.28
GGG-60	.7060	SNG 600/3	FGS 600-3	0732-03	80-55-06	FCD600	1350	.28
GGG-70	.7070	SNG 700/2	FGS 700-2	0737-01	100-70-03	FCD700	1350	.28
GGG-NiCr 20 2	.7660	S-NiCr 20 2	S-NC 20 2		A 439 Type D-2		1350	.28
GGG-NiMn 13 7	.7652	S-NiMn 13 7	S-NM 13 7				1350	.28
GS-Ck 45	1.1191	080 M 46	XC 42	1672	1045	S45C	1525	.22
GTS-35-10	.8135	B 340/12	MN 35-10				1225	.25
GTS-45-06	.8145	P 440/7					1420	.3

Table A.1. Material Comparison Table, $k_{c1.1}$ and m_c values [48] (continued 2)

Germany DIN	Mat. no.	United Kingdom BS	France AFNOR	Sweden SS	USA AISI	Japan JIS	Kc1.1 N/mm²	mc
GTS-55-04	.8155	P 510/4	MP 50-5				1420	.3
GTS-65-02	.8165	P 570/3	MP 60-3				1420	.3
GTS-70-02	.8170	P 690/2	IP 70-2				1420	.3
NiCr20TiAl	2.4631	HR 401; 601	Nimonic 80 A				3300	.24
NiCr22Mo9Nb	2.4856		Inconel 625				3300	.24
NiCu30Al	2.4375		Monel K 500				3300	.24
NiFe25Cr20NbTi	2.4955						3300	.24
S 18-0-1	1.3355	BT 1	Z 80 WCV 18-04-01		T 1		2450	.23
S 18-1-2-5	1.3255	BT 4	Z 80 WKCV 18-05-04-0		T 4		2450	.23
S 2-9-2	1.3348		Z 100 DCWV 09-04-02-	2782	M 7		2450	.23
S 6-5-2	1.3343	BM 2	Z 85 WDCV 06-05-04-0	2722	M 2	SKH9; SKH51	2450	.23
S 6-5-2-5	1.3243		Z 85 WDKCV 06-05-05-	2723		SKH55	2450	.23
TiAl6V4	3.7165	TA 10 bis TA 13	T-A 6 V				2110	.22
X 10 Cr 13	1.4006	410 S 21	Z 12 C 13	2302	410; CA-15	SUS410	1875	.21
X 10 CrNiMoNb 18 12	1.4583				318		2150	.2
X 10 CrNiS 18 9	1.4305	303 S 21	Z 10 CNF 18.09	2346	303		2150	.2
X 100 CrMoV 5 1	1.2363	BA 2	Z 100 CDV 5	2260	A 2		2450	.23
X 12 CrMoS 17	1.4104		Z 10 CF 17	2383	430 F	SUS430F	1875	.21
X 12 CrNi 17 7	1.4310	301 S 21	Z 12 CN 17.07		301		2150	.2
X 12 CrNi 22 12	1.4829					SUS301	1350	.28
X 12 CrNi 25 21	1.4845	310 S24	Z 12 CN 25.20	2361	310 S	SUH310; SUS310S	2150	.2
X 12 CrNiTi 18 9	1.4878	321 S 20	Z 6 CNT 18.12 (B)	2337	321		2150	.2
X 12 NiCrSi 36 16	1.4864	NA 17	Z 12 NCS 37.18		330	SUH330	2600	.24
X 15 CrNiSi 20 12	1.4828	309 S 24	Z 15 CNS 20.12		309	SUH309	1350	.28
X 165 CrMoV 12	1.2601			2310			2450	.23
X 2 CrNiMo 18 13	1.4440						2150	.2
X 2 CrNiMoN 17 13 3	1.4429	316 S 62	Z 2 CND 17.13 Az	2375	316 LN	SUS316LN	2150	.2
X 2 CrNiN 18 10	1.4311	304 S 62	Z 2 CN 18 .10	2371	304 LN	SUS304LN	2150	.2
X 20 CrNi 17 2	1.4057	431 S 29	Z 15 CN 16.02	2321	431	SUS431	1875	.21
X 210 Cr 12	1.2080	BD 3	Z 200 C 12		D 3		2450	.23
X 210 CrW 12	1.2436			2312			2450	.23
X 30 WCrV 9 3	1.2581	BH 21	Z 30 WCV 9		H 21	SKD5	2450	.23
X 40 CrMoV 5 1	1.2344	BH 13	Z 40 CDV 5	2242	H 13	SKD61	2450	.23
X 46 Cr 13	1.4034	420 S 45	Z 40 C 14				1875	.21
X 5 CrNi 18 9	1.4301	304 S 15	Z 6 CN 18.09	2332; 2333	304; 304 H	SUS304	2150	.2
X 5 CrNiMo 17 13 3	1.4436	316 S 16	Z 6 CND 17.12	2343	316	SUS316	2150	.2
X 5 CrNiMo 18 10	1.4401	316 S 16	Z 6 CND 17.11	2347	316	SUS316	2150	.2
X 53 CrMnNiN 21 9	1.4871	349 S 54	Z 52 CMN 21.09		EV 8		1875	.21
X 6 Cr 13	1.4000	403 S 17	Z 6 C 13	2301	403	SUS403	1875	.21
X 6 Cr 17	1.4016	430 S 15	Z 8 C 17	2320	430	SUS430	1875	.21
X 6 CrMo 17	1.4113	434 S 17	Z 8 CD 17.01	2325	434	SUS434	1875	.21
X 6 CrNiMoTi 17 12 2	1.4571	320 S 31	Z 6 CNT 17.12	2350	316 Ti		2150	.2
X 6 CrNiNb 18 10	1.4550	347 S 17	Z 6 CNNb 18.10	2338	347		2150	.2
X 6 CrNiTi 18 10	1.4541	321 S 12	Z 6 CNT 18.10	2337	321		2150	.2
X2 CrNi 18-8	1.4317						2150	.2

B. LOCATING STATUS DETERMINATION

Table B.1. Matlab Script for Determining Locating Status

```
clear,clc
% This M.file determines the constraint status
% of the workpiece according to related configuration.
% # is the number of the part. (1-2-3-4-5-6)
% Please Enter the desired part number
INPUT_#
% Locating vector
A1=(C1-Sp1)/sqrt(sum((Sp1-C1).^2));
A2=(C2-Sp2)/sqrt(sum((Sp2-C2).^2));
A3=(C3-Sp3)/sqrt(sum((Sp3-C3).^2));
A4=(C4-Sp4)/sqrt(sum((Sp4-C4).^2));
A5=(C5-Sp5)/sqrt(sum((Sp5-C5).^2));
A6=(C6-Sp6)/sqrt(sum((Sp6-C6).^2));
% Normal vetor and contact point of each locator.
L=[ A1 Sp1;
    A2 Sp2;
    A3 Sp3;
    A4 Sp4;
    A5 Sp5;
    A6 Sp6];
[m,n]=size(L);
 for i=1:m
    W(i,:)=[L(i,1) L(i,2) L(i,3) L(i,3)*L(i,5)-L(i,2)*L(i,6) ...
      L(i,1)*L(i,6)-L(i,3)*L(i,4)  L(i,2)*L(i,4)-L(i,1)*L(i,5)  ];
    end
W;
CS=rank(W)
% Determination of Constraint Status
if m > 6 & CS == 6
        disp('over constrained')
    elseif CS < 6
        disp('underconstrained')
    elseif m == 6 & CS == 6
        disp('well constrained')
    else
        disp('Please check your inputs!')
end
```

C. ERROR SIMULATION

Table C.1. Error Simulation

```
% Error Metric
clear, clc,close all,
CON=0;t=1;
format short
% FUNCTION SCRIPTS - REPLACE # WITH THE DESIRED PART NUMBER
% INPUT_# / TOOL FORCE AND POINTS_# / HTM / LOCATOR_DEFLECTION /
CONTACT /
% CHECK_COMPRESSION_#
INPUT_1
% TOOL_FORCE_AND_POINTS_#
[ Ftool_magnitude, Ftool_random_p, poc, xyz ] =
TOOL_FORCE_AND_POINTS_1(  );
for nf=1:2  % number of forces
 for np=1:poc    % number of points
        for i=1:13;
        % small perturbations come here
        delta_x=PM(i,1);delta_y=PM(i,2);delta_z=PM(i,3);
        eps_x=PM(i,4);eps_y=PM(i,5);eps_z=PM(i,6);
        limits(i,:)= [delta_x delta_y delta_z eps_x eps_y eps_z];
        % relevant HTM'S for deflection points on locators
        HTM3  = HTM( delta_x,delta_y,delta_z,eps_x,eps_y,eps_z )  ;

    [deflection_S1_1, deflection_S2_1, deflection_S3_1, ...
    deflection_S4_1, deflection_S5_1,
deflection_S6_1,R_1,R_2,R_3,R_4,R_5,R_6] ...
    =
RADIUS_DEFLECTION_01(HTM3,Sp1,C1,Sp2,C2,Sp3,C3,Sp4,C4,Sp5,C5,Sp6,C6,
V_1,V_2,V_3,V_4,V_5,V_6);

        DEFLECTION_1=[deflection_S1_1; deflection_S2_1;
deflection_S3_1; ...
            deflection_S4_1; deflection_S5_1; deflection_S6_1];

        Sf_1=-1*DEFLECTION_1.*Sk;

        Total_Force  = [Sf_1 ; Fm ;Ftool_magnitude(nf,:)];
        Total_Points = [ Sp ; Fp ;Ftool_random_p(np,:)];

        Moment=cross(Total_Points,Total_Force);

        FX_SUM=sum(Total_Force(:,1));
        FY_SUM=sum(Total_Force(:,2));
        FZ_SUM=sum(Total_Force(:,3));
        MX_SUM=sum(Moment(:,1));
        MY_SUM=sum(Moment(:,2));
        MZ_SUM=sum(Moment(:,3));

        B(i,:)=[FX_SUM FY_SUM FZ_SUM MX_SUM MY_SUM MZ_SUM];
        end
```

```
        B;

    P=[13 11 9 7 5 3];
    for ma=1:6;
        for na=1:6;
       A(na,ma)=(B(P(ma),na)-B(P(ma)-1,na))/(PM(P(ma),ma)-PM(P(ma)-
1,ma));
         end
    end
% necessary translation and rotation for this force-moment balance
% B(1,:) is equal to = Force Moment matrix has zero delta and eps
r_d=inv(A)*B(1,:)';

% expected translational & rotational movements
delta_x_2 = r_d(1);   delta_y_2 = r_d(2);   delta_z_2 = r_d(3);
eps_x_2   = r_d(4);   eps_y_2   = r_d(5);   eps_z_2   = r_d(6);

% new HTM's for np * nf
% HTM3_New  = HTM( delta_x,delta_y,delta_z,eps_x,eps_y,eps_z );
HTM3_New  = HTM(
delta_x_2,delta_y_2,delta_z_2,eps_x_2,eps_y_2,eps_z_2 );

% Locator new points
    [deflection_S1_2, deflection_S2_2, deflection_S3_2, ...
    deflection_S4_2, deflection_S5_2,
deflection_S6_2,R_12,R_22,R_32,R_42,R_52,R_62] ...
    =
RADIUS_DEFLECTION_01(HTM3_New,Sp1,C1,Sp2,C2,Sp3,C3,Sp4,C4,Sp5,C5,Sp6
,C6,V_1,V_2,V_3,V_4,V_5,V_6);
% Radius
RAD =
[norm(R_12);norm(R_22);norm(R_32);norm(R_42);norm(R_52);norm(R_62)];

DEFLECTION_2=[deflection_S1_2;deflection_S2_2;deflection_S3_2;deflec
tion_S4_2;...
    deflection_S5_2;deflection_S6_2];

% Deformation at machining point
DEF_AT_TOOL_POINT=[HTM3_New*[Ftool_random_p(np,:) 1]']' -
[Ftool_random_p(np,:) 1];
DEF_AT_TOOL_POINT(4)=[];
% ux^2 + uy^2 + uz^2
% Difference between tool force and without tool force
% !!! IMPORTANT OVERALL ERROR
OVERALL_ERROR(np,nf)=norm(DEF_AT_TOOL_POINT);

% Forces acts on locators
Sf1=deflection_S1_2.*Sk1; Sf2=deflection_S2_2.*Sk2;
Sf3=deflection_S3_2.*Sk3;
Sf4=deflection_S4_2.*Sk4; Sf5=deflection_S5_2.*Sk5;
Sf6=deflection_S6_2.*Sk6;
Sf_2=[Sf1; Sf2; Sf3; Sf4; Sf5; Sf6];

Total_Force_2  = [Sf_2 ; Fm ;Ftool_magnitude(nf,:)];
```

```
Moment_2 = cross(Total_Points,Total_Force_2);
FMY=[Total_Force_2 Moment_2 ];
FMY_balance=sum(FMY);
 end
end
OVERALL_ERROR; % difference between first and second column gives
final error
length(OVERALL_ERROR)
for q= 1:length(OVERALL_ERROR)
ERROR_DIFFERENCE(q,1) = OVERALL_ERROR(q,1) - OVERALL_ERROR(q,2);
end
disp('average error [micron]')
mean(1000*ERROR_DIFFERENCE)
disp('maximum error [micron]')
max(1000*ERROR_DIFFERENCE)
disp('std. deviation [micron]')
std(1000*ERROR_DIFFERENCE)
figure(1)
bar(1000*ERROR_DIFFERENCE);  % micrometer * 1000
xlabel('number of random tool points')
ylabel('Error [\mum]')
grid
figure(2)
hist(ERROR_DIFFERENCE,20)
xlabel('number of error')
ylabel('Error frequency ')
grid
```

D. FUNCTIONS FOR ERROR SIMULATION

Table D.1. Homogeneous Transformation Matrix for 3D

```
function [ HTM3 ] = HTM( delta_x,delta_y,delta_z,eps_x,eps_y,eps_z )
%Homogeneous Transformation matrix
HTM3=[cos(eps_y)*cos(eps_z)     -cos(eps_y)*sin(eps_z)
sin(eps_y)       delta_x;...
  sin(eps_x)*sin(eps_y)*cos(eps_z)+cos(eps_x)*sin(eps_z)   ...
 -sin(eps_x)*sin(eps_y)*sin(eps_z)+cos(eps_x)*cos(eps_z)   ...
 -sin(eps_x)*cos(eps_y)     delta_y;...
 -cos(eps_x)*sin(eps_y)*cos(eps_z)+sin(eps_x)*sin(eps_z)   ...
  cos(eps_x)*sin(eps_y)*sin(eps_z)+sin(eps_x)*cos(eps_z)    ...
  cos(eps_x)*cos(eps_y)   delta_z;
   0      0      0     1     ];
end
```

Table D.2. Computation of Locator Deflection

```
function [deflection_S1, deflection_S2, deflection_S3, ...
    deflection_S4, deflection_S5,
deflection_S6,R_1,R_2,R_3,R_4,R_5,R_6]...
    =
RADIUS_DEFLECTION_01(HTM3,Sp1,C1,Sp2,C2,Sp3,C3,Sp4,C4,Sp5,C5,...
    Sp6,C6,V_1,V_2,V_3,V_4,V_5,V_6)
R_1=[HTM3*[Sp1 1]']' - [C1 1];
R_1(4)=[];
deflection_S1=(10-norm(R_1))*V_1;
R_2=[HTM3*[Sp2 1]']' - [C2 1];
R_2(4)=[];
deflection_S2=(10-norm(R_2))*V_2;
R_3=[HTM3*[Sp3 1]']' - [C3 1];
R_3(4)=[];
deflection_S3=(10-norm(R_3))*V_3;
R_4=[HTM3*[Sp4 1]']' - [C4 1];
R_4(4)=[];
deflection_S4=(10-norm(R_4))*V_4;
R_5=[HTM3*[Sp5 1]']' - [C5 1];
R_5(4)=[];
deflection_S5=(10-norm(R_5))*V_5;
R_6=[HTM3*[Sp6 1]']' - [C6 1];
R_6(4)=[];
deflection_S6=(10-norm(R_6))*V_6;
end
```

E. TOOL FORCE AND POINT GENERATION

Table E.1. Tool Force and Point Generation for Part 1 – Surface A1

```
function [ Ftool_magnitude, Ftool_random_p, poc, xyz ] =
TOOL_FORCE_AND_POINTS_1(  )
% TOOL FORCE AND POINTS 1
Ftool_magnitude = [ -25 -25 -25; 0 0 0 ];
% For loop or  point matrix (j * 3)
    for j =1 :199
      Ftool_random_p(j,:) =  [((60-42)*rand+42)*cos(2*pi*rand)
158.8 ((60-42)*rand+42)*sin(2*pi*rand)+62 ];
        [poc , xyz] =size(Ftool_random_p);
    end
end
```

Table E.2. Tool Force and Point Generation for Part 1 – Surface A2

```
function [ Ftool_magnitude, Ftool_random_p, poc, xyz ] =
TOOL_FORCE_AND_POINTS_1(  )
% TOOL FORCE AND POINTS 1
Ftool_magnitude = [ -25 -25 -25; 0 0 0 ];
    for j =1 :199
      Ftool_random_p(j,:)  = [60*rand-30    260*rand-130    86 ];
        [poc , xyz] =size(Ftool_random_p);
    end
end
```

Table E.3. Tool Force and Point Generation for Part 2 – Surface B1

```
function [ Ftool_magnitude, Ftool_random_p, poc, xyz ] =
TOOL_FORCE_AND_POINTS_2(  )
% TOOL FORCE AND POINTS 2
Ftool_magnitude = [ -15 -15 -15; 0 0 0];
    for j =1 :199
    Ftool_random_p(j,:)  = [(150+130)*rand-130 (90+110)*rand-110
52.5 ];
      [poc , xyz] =size(Ftool_random_p);
    end
end
```

Table E.4. Tool Force and Point Generation for Part 2 – Surface B2

```
function [ Ftool_magnitude, Ftool_random_p, poc, xyz ] =
TOOL_FORCE_AND_POINTS_2(  )
% TOOL FORCE AND POINTS 2
Ftool_magnitude = [ -15 -15 -15; 0 0 0];
    for j =1 :199
        Ftool_random_p(j,:)  = [68.5+10*cos(2*pi*rand()) -
85.7+10*sin(2*pi*rand()) (56.25-36.25)*rand+36.25];
        [poc , xyz] =size(Ftool_random_p);
    end
    Ftool_random_p;
end
```

Table E.5. Tool Force and Point Generation for Part 3 – Surface C1

```
function [ Ftool_magnitude, Ftool_random_p, poc, xyz ] =
TOOL_FORCE_AND_POINTS_3(  )
% TOOL FORCE AND POINTS 3
Ftool_magnitude = [ -40 -40 -40; 0 0 0 ];
    for j =1 :199;
        Ftool_random_p(j,:)  = [(45*rand)*cos(2*pi*rand) 85.4
(90*rand-45)*sin(2*pi*rand)+85 ];
        [poc , xyz] =size(Ftool_random_p);
    end
end
```

Table E.6. Tool Force and Point Generation for Part 3 – Surface C2

```
function [ Ftool_magnitude, Ftool_random_p, poc, xyz ] =
TOOL_FORCE_AND_POINTS_3(  )
% TOOL FORCE AND POINTS 3
Ftool_magnitude = [ -40 -40 -40; 0 0 0 ];
    for j =1 :199;
        Ftool_random_p(j,:)  = [(69-35)*rand+35 -
100+20*cos(2*pi*rand()) 75+20*cos(2*pi*rand())];
        [poc , xyz] =size(Ftool_random_p);
    end
end
```

Table E.7. Tool Force and Point Generation for Part 4 – Surface D1

```
function [ Ftool_magnitude, Ftool_random_p, poc, xyz ] =
TOOL_FORCE_AND_POINTS_4(  )
% TOOL FORCE AND POINTS 4
Ftool_magnitude = [ -25 -25 -25; 0 0 0 ];
for j =1 :199
    Ftool_random_p(j,:)  = [8+85*cos(2*pi*rand) -11+85* sin(2*pi
*rand) 70.0 ];
    [poc , xyz] =size(Ftool_random_p);
 end
end
```

Table E.8. Tool Force and Point Generation for Part 4– Surface D2

```
function [ Ftool_magnitude, Ftool_random_p, poc, xyz ] =
TOOL_FORCE_AND_POINTS_4(  )
% TOOL FORCE AND POINTS 4
Ftool_magnitude = [ -25 -25 -25; 0 0 0 ];
for j =1 :199
    Ftool_random_p(j,:)  = [8+51*cos(2*pi*rand) -11+51*sin(2*pi*
rand) (105-70)*rand+70 ];

    [poc , xyz] =size(Ftool_random_p);
 end
end
```

Table E.9. Tool Force and Point Generation for Part 5– Surface E1

```
function [ Ftool_magnitude, Ftool_random_p, poc, xyz ] =
TOOL_FORCE_AND_POINTS_5(  )
% TOOL FORCE AND POINTS 5
Ftool_magnitude = [ -15 -15 -15; 0 0 0 ];
    for j =1 :199
        RAND_ANG =rand()
        Ftool_random_p(j,:)  = [((29-25)*rand+25)*cos(2*pi*RAND_ANG)
((29-25)*rand+25)*sin(2*pi*RAND_ANG)  186 ];
        [poc , xyz] =size(Ftool_random_p);
    end
end
```

Table E.10. Tool Force and Point Generation for Part 5– Surface E2

```
function [ Ftool_magnitude, Ftool_random_p, poc, xyz ] =
TOOL_FORCE_AND_POINTS_5(  )
% TOOL FORCE AND POINTS 5
Ftool_magnitude = [ -15 -15 -15; 0 0 0 ];
    for j =1 :199
        Ftool_random_p(j,:)  = [180*rand-90 160*rand-80 62 ];
        [poc , xyz] =size(Ftool_random_p);
    end
end
```

Table E.11. Tool Force and Point Generation for Part 6

```
function [ Ftool_magnitude, Ftool_random_p, poc, xyz ] =
TOOL_FORCE_AND_POINTS_6(  )
% TOOL FORCE AND POINTS 6
Ftool_magnitude = [ -15 -15 -15; 0 0 0 ];
    for j =1 :199
      Ftool_random_p(j,:)  = [200*rand-100 160*rand-80 50*rand+50 ];
      [poc , xyz] =size(Ftool_random_p);
    end
end
```

F. INPUT FILES

Table F.1. Input File for Part 1

```
% INPUTS 1
% Springs (Locators)
    %Points (Contacts) [mm]
    Sp1 = [139.47  -22.19  37.54];
    Sp2 = [139.47   22.19  37.54];
    Sp3 = [ -9.0   -81.0   90.0 ];
    Sp4 = [ -9.0    81.0   90.0 ];
    Sp5 = [-24.21  -107.1  91.0 ];
    Sp6 = [-24.21   107.1  91.0 ];

    % Locator Center point
    C1 = [135  -27.0  30.0];
    C2 = [135   27.0  30.0];
    C3 = [-9.0  -81.0  80.0];
    C4 = [-9.0  81.0  80.0];
    C5 = [-30.07 -99.0   91.0];
    C6 = [-30.07  99.0   91.0];

    % LOCATING VECTOR
    V_1=(Sp1-C1)/sqrt(sum((Sp1-C1).^2));
    V_2=(Sp2-C2)/sqrt(sum((Sp2-C2).^2));
    V_3=(Sp3-C3)/sqrt(sum((Sp3-C3).^2));
    V_4=(Sp4-C4)/sqrt(sum((Sp4-C4).^2));
    V_5=(Sp5-C5)/sqrt(sum((Sp5-C5).^2));
    V_6=(Sp6-C6)/sqrt(sum((Sp6-C6).^2));
    Loc_Vector = [V_1;V_2;V_3;V_4;V_5;V_6];

    %Stiffness [N/mm]
    Sk1 = [70000  70000 70000];
    Sk2 = [70000  70000 70000];
    Sk3 = [70000  70000 70000];
    Sk4 = [70000  70000 70000];
    Sk5 = [70000  70000 70000];
    Sk6 = [70000  70000 70000];

    % Points and locator stiffness
    Sk=[Sk1;Sk2;Sk3;Sk4;Sk5;Sk6];
    Sp=[Sp1;Sp2;Sp3;Sp4;Sp5;Sp6];

% External Forces
    % Points [mm]
    Fp1=[65.4 -0.51  74.5];       % Center of gravity
    Fp2=[0  0  90.61];            % Clamping point
    Fp3=[106.6  -71.9  87.6];       % Clamping point
    Fp4=[105.0 75.6  87.6];         % Clamping point
    Fp5=[0 0 0];                  % Clamping point
    Fp6=[0 0 0];                  % Clamping point

    % Magnitudes [Newton]
```

```
    Fm1 = [0  0 -6];      % WEIGHT
    Fm2 = [0 0 -200];       % CLAMP FORCE
    Fm3 = [-50  50 -50];     % CLAMP FORCE
    Fm4 = [-50 -50 -50];    % CLAMP FORCE
    Fm5 = [0 0 0];          % CLAMP FORCE
    Fm6 = [0 0 0];          % CLAMP FORCE

    % Total Points and their magnitudes
    Fp=[Fp1;Fp2;Fp3;Fp4;Fp5;Fp6];
    Fm=[Fm1;Fm2;Fm3;Fm4;Fm5;Fm6];

    % perturbation matrix
PM=      [0         0         0         0         0         0;
          0         0         0         0         0   -0.0002;
          0         0         0         0         0    0.0002;
          0         0         0         0   -0.0002         0;
          0         0         0         0    0.0002         0;
          0         0         0   -0.0002         0         0;
          0         0         0    0.0002         0         0;
          0         0   -0.0100         0         0         0;
          0         0    0.0100         0         0         0;
          0   -0.0100         0         0         0         0;
          0    0.0100         0         0         0         0;
    -0.0100         0         0         0         0         0;
     0.0100         0         0         0         0         0];
```

Table F.2. Input File for Part 2

```
% INPUTS 2
% Springs (Locators)
    %Points (Contacts) [mm]
    Sp1 = [-81.0  63.0  40.0];
    Sp2 = [27.0  45.0  40.0];
    Sp3 = [117.0  -81.0  40.0];
    Sp4 = [ 99.0 -93.0  45.0];
    Sp5 = [ 46.434713222 -85.716818279  45.0  ];
    Sp6 = [-116.201175850 62.925585987 45.0 ];

    % Locator Center point
    C1 = [-81.0  63.0  30.0];
    C2 = [27.0  45.0  30.0];
    C3 = [117.0  -81.0  30.0];
    C4 = [99.0 -103.0  45.0];
    C5 = [37.370982267  -89.941600070   45.0];
    C6 = [-123.695369853   56.304630147  45.0];

    % LOCATING VECTOR
    V_1=(Sp1-C1)/sqrt(sum((Sp1-C1).^2));
    V_2=(Sp2-C2)/sqrt(sum((Sp2-C2).^2));
    V_3=(Sp3-C3)/sqrt(sum((Sp3-C3).^2));
```

```
    V_4=(Sp4-C4)/sqrt(sum((Sp4-C4).^2));
    V_5=(Sp5-C5)/sqrt(sum((Sp5-C5).^2));
    V_6=(Sp6-C6)/sqrt(sum((Sp6-C6).^2));
    Loc_Vector = [V_1;V_2;V_3;V_4;V_5;V_6];

    %Stiffness [N/mm]
    Sk1 = [70000  70000  70000];
    Sk2 = [70000  70000  70000];
    Sk3 = [70000  70000  70000];
    Sk4 = [70000  70000  70000];
    Sk5 = [70000  70000  70000];
    Sk6 = [70000  70000  70000];


    % Points and locator stiffness
    Sk=[Sk1;Sk2;Sk3;Sk4;Sk5;Sk6];
    Sp=[Sp1;Sp2;Sp3;Sp4;Sp5;Sp6];

% External Forces

    % Points [mm]
    Fp1=[39.9 -16.8  46.2]; % Center of gravity
    Fp2=[-14.78  3.21  45.0];          % Clamping point
    Fp3=[80.0  -43.0  51.0];          % Clamping point
    Fp4=[0.3 32.0  51.0];             % Clamping point
    Fp5=[63 -117 45];                   % Clamping point
    Fp6=[0 0 0];                   % Clamping point


    % Magnitudes [Newton]
    Fm1 = [0  0 -10];      % WEIGHT
    Fm2 = [-120 -120 0];       % CLAMP FORCE
    Fm3 = [0 0 -200];      % CLAMP FORCE
    Fm4 = [0 0 -200];      % CLAMP FORCE
    Fm5 = [0 -0 0];         % CLAMP FORCE yeni ekledim
    Fm6 = [0 0 0];         % CLAMP FORCE

    % Total Points and their magnitudes
    Fp=[Fp1;Fp2;Fp3;Fp4;Fp5;Fp6];
    Fm=[Fm1;Fm2;Fm3;Fm4;Fm5;Fm6];

    % perturbation matrix
PM=     [0         0         0         0         0         0;
         0         0         0         0         0   -0.0002;
         0         0         0         0         0    0.0002;
         0         0         0         0   -0.0002         0;
         0         0         0         0    0.0002         0;
         0         0         0   -0.0002         0         0;
         0         0         0    0.0002         0         0;
         0         0   -0.0100         0         0         0;
         0         0    0.0100         0         0         0;
         0   -0.0100         0         0         0         0;
         0    0.0100         0         0         0         0;
   -0.0100         0         0         0         0         0;
```

```
    0.0100         0         0         0         0         0];
```

Table F.3. Input File for Part 3

```
% INPUTS 3
% Springs (Locators)
    %Points (Contacts) [mm]
    Sp1 = [-45.0  -63.0  41.157155095];
    Sp2 = [ -21.892409553  99.0  38.597239082];
    Sp3 = [ 21.892409553  99.0  38.597239082];
    Sp4 = [ 45.0 -63.0  41.157155095];
    Sp5 = [40.713660000 -45.0  54];
    Sp6 = [-9   60.0  45];

    % Locator Center point
    C1 = [-45.0  -63.0  31.157155095];
    C2 = [-27.0  99.0  30];
    C3 = [ 27.0  99.0  30];
    C4 = [45.0 -63.0  31.157155095];
    C5 = [30.713660000 -45.0  54];
    C6 = [-9.0   50.0  45];

    % LOCATING VECTOR
    V_1=(Sp1-C1)/sqrt(sum((Sp1-C1).^2));
    V_2=(Sp2-C2)/sqrt(sum((Sp2-C2).^2));
    V_3=(Sp3-C3)/sqrt(sum((Sp3-C3).^2));
    V_4=(Sp4-C4)/sqrt(sum((Sp4-C4).^2));
    V_5=(Sp5-C5)/sqrt(sum((Sp5-C5).^2));
    V_6=(Sp6-C6)/sqrt(sum((Sp6-C6).^2));
    Loc_Vector = [V_1;V_2;V_3;V_4;V_5;V_6];

    %Stiffness [N/mm]
    Sk1 = [70000 70000  70000];
    Sk2 = [70000 70000  70000];
    Sk3 = [70000 70000  70000];
    Sk4 = [70000 70000  70000];
    Sk5 = [70000 70000  70000];
    Sk6 = [70000 70000  70000];

    % Points and locator stiffness
    Sk=[Sk1;Sk2;Sk3;Sk4;Sk5;Sk6];
    Sp=[Sp1;Sp2;Sp3;Sp4;Sp5;Sp6];

% External Forces

    % Points [mm]
    Fp1=[0.483239142 22.580601860  75.448859633]; % Center of
gravity
    Fp2=[ 0  65.0  114];          % Clamping point
    Fp3=[  9  59.0  99];          % Clamping point
```

```
    Fp4=[39 -9.0  54];              % Clamping point
    Fp5=[0 0 0];                    % Clamping point
    Fp6=[0 0 0];                    % Clamping point

    % Magnitudes [Newton]
    Fm1 = [0  0 -10];        % WEIGHT
    Fm2 = [0 0 -200];        % CLAMP FORCE
    Fm3 = [0 -100 0];        % CLAMP FORCE
    Fm4 = [-100 0 0];        % CLAMP FORCE
    Fm5 = [0 0 0];           % CLAMP FORCE
    Fm6 = [0 0 0];           % CLAMP FORCE

    % Total Points and their magnitudes
    Fp=[Fp1;Fp2;Fp3;Fp4;Fp5;Fp6];
    Fm=[Fm1;Fm2;Fm3;Fm4;Fm5;Fm6];

    % perturbation matrix
PM=      [0          0          0          0          0          0;
          0          0          0          0          0    -0.0002;
          0          0          0          0          0     0.0002;
          0          0          0          0    -0.0002          0;
          0          0          0          0     0.0002          0;
          0          0          0    -0.0002          0          0;
          0          0          0     0.0002          0          0;
          0          0    -0.0100          0          0          0;
          0          0     0.0100          0          0          0;
          0    -0.0100          0          0          0          0;
          0     0.0100          0          0          0          0;
   -0.0100          0          0          0          0          0;
    0.0100          0          0          0          0          0];
```

Table F.4. Input File for Part 4

```
 % INPUT_4
% Springs (Locators)
    %Points (Contacts) [mm]
    Sp1 = [ 72.0 45.0  40.0];
    Sp2 = [-54.0 45.0  40.0];
    Sp3 = [0    -99.0  40.0];
    Sp4 = [ 81.438037166 -74.144902040 54.0];
    Sp5 = [-72.054664457 -51.529018796 54.0];
    Sp6 = [-29.132787791 83.466666667 54 ];

    % Locator Center point
    C1 = [72.0 45.0  30.0];
    C2 = [-54.0 45.0  30.0];
    C3 = [0    -99.0  30.0];
    C4 = [90.0 -79.311408831 54.0];
    C5 = [-81.0 -55.999026854 54.0];
    C6 = [-36.703491560 90 54];
```

```
    % LOCATING VECTOR
    V_1=(Sp1-C1)/sqrt(sum((Sp1-C1).^2));
    V_2=(Sp2-C2)/sqrt(sum((Sp2-C2).^2));
    V_3=(Sp3-C3)/sqrt(sum((Sp3-C3).^2));
    V_4=(Sp4-C4)/sqrt(sum((Sp4-C4).^2));
    V_5=(Sp5-C5)/sqrt(sum((Sp5-C5).^2));
    V_6=(Sp6-C6)/sqrt(sum((Sp6-C6).^2));
    Loc_Vector = [V_1;V_2;V_3;V_4;V_5;V_6];

    %Stiffness [N/mm]
    Sk1 = [70000 70000   70000];
    Sk2 = [70000 70000   70000];
    Sk3 = [70000 70000   70000];
    Sk4 = [70000 70000   70000];
    Sk5 = [70000 70000   70000];
    Sk6 = [70000 70000   70000];

    % Points and locator stiffness
    Sk=[Sk1;Sk2;Sk3;Sk4;Sk5;Sk6];
    Sp=[Sp1;Sp2;Sp3;Sp4;Sp5;Sp6];

% External Forces

    % Points [mm]
    Fp1=[8.99  -2.45  69.40];           % Center of gravity
    Fp2=[ 54.0    27.0   64.0];          % Clamping point
    Fp3=[ -36.0   27.0   64.0];          % Clamping point
    Fp4=[0.0      -63.0   64.0];           % Clamping point
    Fp5=[9.0 110.0 54.0];                  % Clamping point
    Fp6=[106.0 -9.0 54.0];                  % Clamping point

    % Magnitudes [Newton]
    Fm1 = [0   0 -10];      % WEIGHT
    Fm2 = [0 0 -100];       % CLAMP FORCE
    Fm3 = [0 0 -100];       % CLAMP FORCE
    Fm4 = [0 0 -100];       % CLAMP FORCE
    Fm5 = [0 -100 -0];          % CLAMP FORCE
    Fm6 = [-200 0 -0];          % CLAMP FORCE

    % Total Points and their magnitudes
    Fp=[Fp1;Fp2;Fp3;Fp4;Fp5;Fp6];
    Fm=[Fm1;Fm2;Fm3;Fm4;Fm5;Fm6];

    % perturbation matrix
PM=     [0          0          0          0          0          0;
         0          0          0          0          0    -0.0002;
         0          0          0          0          0     0.0002;
         0          0          0          0    -0.0002          0;
         0          0          0          0     0.0002          0;
         0          0          0    -0.0002          0          0;
         0          0          0     0.0002          0          0;
         0          0    -0.0100          0          0          0;
         0          0     0.0100          0          0          0;
```

```
        0    -0.0100         0         0         0         0;
        0     0.0100         0         0         0         0;
  -0.0100          0         0         0         0         0;
   0.0100          0         0         0         0         0];
```

Table F.5. Input File for Part 5

```
 % INPUT_5
% Springs (Locators)
    %Points (Contacts) [mm]
    Sp1 = [-9.0  117.0  40.0];
    Sp2 = [-63.0 -45.0  40.0];
    Sp3 = [63.0  -63.0  40.0];
    Sp4 = [44.651005033   -93.006091730  54.0];
    Sp5 = [-82.313775496 -90.0  54.0];
    Sp6 = [-93.0   72.0  54];

    % Locator Center point
    C1 = [-9.0  117.0  30.0];
    C2 = [-63.0 -45.0  30.0];
    C3 = [63.0  -63.0  30.0];
    C4 = [45.0 -103.0  54.0];
    C5 = [-92.313775496 -90.0  54.0];
    C6 = [-103.0   72.0  54];

    % LOCATING VECTOR
    V_1=(Sp1-C1)/sqrt(sum((Sp1-C1).^2));
    V_2=(Sp2-C2)/sqrt(sum((Sp2-C2).^2));
    V_3=(Sp3-C3)/sqrt(sum((Sp3-C3).^2));
    V_4=(Sp4-C4)/sqrt(sum((Sp4-C4).^2));
    V_5=(Sp5-C5)/sqrt(sum((Sp5-C5).^2));
    V_6=(Sp6-C6)/sqrt(sum((Sp6-C6).^2));
    Loc_Vector = [V_1;V_2;V_3;V_4;V_5;V_6];

    %Stiffness [N/mm]
    Sk1 = [70000 70000 70000];
    Sk2 = [70000 70000 70000];
    Sk3 = [70000 70000 70000];
    Sk4 = [70000 70000 70000];
    Sk5 = [70000 70000 70000];
    Sk6 = [70000 70000 70000];

    % Points and locator stiffness
    Sk=[Sk1;Sk2;Sk3;Sk4;Sk5;Sk6];
    Sp=[Sp1;Sp2;Sp3;Sp4;Sp5;Sp6];

% External Forces
    % Points [mm]
    Fp1=[-8.33 10.74  84.78];       % Center of gravity
    Fp2=[ -9.0    63.0   39.0];     % Clamping point
```

```
Fp3=[ -27.0   -45.0   39.0];     % Clamping point
Fp4=[-27.0   -63.0   39.0];      % Clamping point
Fp5=[18.0 -95.0 45.0];           % Clamping point
Fp6=[66.5 0 41.6];               % Clamping point

% Magnitudes [Newton]
Fm1 = [0  0 -32];        % WEIGHT
Fm2 = [0 0 -100];        % CLAMP FORCE
Fm3 = [0 0 -100];        % CLAMP FORCE
Fm4 = [0 0 -100];        % CLAMP FORCE
Fm5 = [0 -100 0];        % CLAMP FORCE
Fm6 = [-100 0 0];        % CLAMP FORCE

% Total Points and their magnitudes
Fp=[Fp1;Fp2;Fp3;Fp4;Fp5;Fp6];
Fm=[Fm1;Fm2;Fm3;Fm4;Fm5;Fm6];

% perturbation matrix
PM=     [0          0          0          0          0          0;
         0          0          0          0          0    -0.0002;
         0          0          0          0          0     0.0002;
         0          0          0          0    -0.0002          0;
         0          0          0          0     0.0002          0;
         0          0          0    -0.0002          0          0;
         0          0          0     0.0002          0          0;
         0          0    -0.0100          0          0          0;
         0          0     0.0100          0          0          0;
         0    -0.0100          0          0          0          0;
         0     0.0100          0          0          0          0;
   -0.0100          0          0          0          0          0;
    0.0100          0          0          0          0          0];
```

Table F.6. Input File for Part 6

```
% INPUT_6
% Springs (Locators)
    %Points (Contacts) [mm]
    Sp1 = [-54.0  18.0  40.0];
    Sp2 = [ 90.0  54.0  40.0];
    Sp3 = [ 90.0  -18.0  40.0];
    Sp4 = [99.0  -32.0  45.0];
    Sp5 = [-63.0 -32.0  45.0];
    Sp6 = [-72.0   45.0  45];

    % Locator Center point
    C1  = [-54.0  18.0  30.0];
    C2  = [ 90.0  54.0  30.0];
    C3  = [ 90.0  -18.0  30.0];
    C4  = [99.0  -42.0  45.0];
    C5  = [-63.0 -42.0  45.0];
    C6  = [-82.0   45.0  45];

    % LOCATING VECTOR
    V_1=(Sp1-C1)/sqrt(sum((Sp1-C1).^2));
    V_2=(Sp2-C2)/sqrt(sum((Sp2-C2).^2));
    V_3=(Sp3-C3)/sqrt(sum((Sp3-C3).^2));
    V_4=(Sp4-C4)/sqrt(sum((Sp4-C4).^2));
    V_5=(Sp5-C5)/sqrt(sum((Sp5-C5).^2));
    V_6=(Sp6-C6)/sqrt(sum((Sp6-C6).^2));
    Loc_Vector = [V_1;V_2;V_3;V_4;V_5;V_6];

    %Stiffness [N/mm]
    Sk1 = [70000 70000 70000];
    Sk2 = [70000 70000 70000];
    Sk3 = [70000 70000 70000];
    Sk4 = [70000 70000 70000];
    Sk5 = [70000 70000 70000];
    Sk6 = [70000 70000 70000];

    % Points and locator stiffness
    Sk=[Sk1;Sk2;Sk3;Sk4;Sk5;Sk6];
    Sp=[Sp1;Sp2;Sp3;Sp4;Sp5;Sp6];

% External Forces

    % Points [mm]
    Fp1=[15.981708835 17.823168313  53.255416690]; % Center of
gravity
    Fp2=[ 36.0    18.0   40.0];           % Clamping point
    Fp3=[  9.0   -32.0   45.0];           % Clamping point
    Fp4=[-72.0   -18.0   54.0];           % Clamping point
    Fp5=[-18.0    18.0   40.0];           % Clamping point
    Fp6=[0  0  0];                        % Clamping point


    % Magnitudes [Newton]
```

```
    Fm1 = [0  0 -10];           % WEIGHT
    Fm2 = [0 0 -100];           % CLAMP FORCE
    Fm3 = [0 -100 0];           % CLAMP FORCE
    Fm4 = [-100 0 0];           % CLAMP FORCE
    Fm5 = [0 0 -0];           % CLAMP FORCE
    Fm6 = [0 0 0];              % CLAMP FORCE

    % Total Points and their magnitudes
    Fp=[Fp1;Fp2;Fp3;Fp4;Fp5;Fp6];
    Fm=[Fm1;Fm2;Fm3;Fm4;Fm5;Fm6];

    % perturbation matrix
PM=      [0         0         0         0         0         0;
         0         0         0         0         0   -0.0002;
         0         0         0         0         0    0.0002;
         0         0         0         0   -0.0002         0;
         0         0         0         0    0.0002         0;
         0         0         0   -0.0002         0         0;
         0         0         0    0.0002         0         0;
         0         0   -0.0100         0         0         0;
         0         0    0.0100         0         0         0;
         0   -0.0100         0         0         0         0;
         0    0.0100         0         0         0         0;
   -0.0100         0         0         0         0         0;
    0.0100         0         0         0         0         0];
```

G. ISO WORKPIECE MATERIAL GROUPS

A wide variety of materials are used in machining industry. These materials are classified by ISO due to their unique characteristics such as alloying element, hardness, etc. Alloying element of the workpiece material is important for the material whether it is magnetic or nonmagnetic. Besides, the amount of the Fe, Co or Ni has a direct effect in the ferromagnetism of the material. Therefore, nonmagnetic materials must be listed to determine the usage of the method mentioned in section 3.10.2.

ISO P Steel: Iron is the major element in steels, therefore, all of the members of this group have magnetic characteristic.

ISO M Stainless steel: Iron is also major element in stainless steels but iron percentage is not high as ISO P group. Therefore, the method mentioned in Section 3.10.2. is required to apply in case of magnet usage.

ISO K Cast Iron: Major element is Iron. It has a strong magnetic characteristic.

ISO N Non-ferrous materials: These materials are completely nonmagnetic. Aluminum, Magnesium, Copper, Bronze, etc. are the members of this group. Because of their nonmagnetic characteristic gluing method of ferromagnetic material to the workpiece material must be applied in case of magnet usage.

ISO S: Heat resistant superalloys and titanium are the members of this group. Super alloys are magnetic due to their high Nickel content. But Titanium alloys have non-magnetic characteristic.

ISO H Hardened Steel: This group materials have shown both magnetic and nonmagnetic characteristics.

Magnetic characteristics of the materials are shown in Table G.1 according to their ISO material groups.

Table G.1 Magnetic properties of various materials

ISO Group	Material Code	Strongly Magnetic	Weakly magnetic	Non-magnetic
P	D3 (X210Cr12)	x		
P	O2 (90MnCrV8)	x		
P	1020 (C22)	x		
P	1045 (C45)	x		
P	5120 (20MnCr5)		x	
P	D6 (X210CrW12)		x	
P	4140 (42CrMo4)	x		
K	No 35B (GG25)	x		
M	A2 (X100 Cr Mo V 5 1)		x	
N	AL (all types)			x
N	Mg (all types)			x
N	Ti (all types)			x